APPLICATION OF CARBON FIBRE REINFORCED POLYMER LAMINATE FOR STRENGTHENING REINFORCED CONCRETE T- BEAM

MUHAMMAD MUKHLESUR RAHMAN

FACULTY OF ENGINEERING
UNIVERSITY OF MALAYA
KUALA LUMPUR

2012

APPLICATION OF CARBON FIBRE REINFORCED POLYMER LAMINATE FOR STRENGTHENING REINFORCED CONCRETE T- BEAM

MUHAMMAD MUKHLESUR RAHMAN

DISSERTATION SUBMITTED IN FULFILMENT OF THE REQUIREMENTS FOR THE DEGREE OF MASTER OF ENGINEERING SCIENCE

FACULTY OF ENGINEERING
UNIVERSITY OF MALAYA
KUALA LUMPUR

2012

UNIVERSITY OF MALAYA

ORIGINAL LITERARY WORK DECLARATION

Name of the Candidate: **Muhammad Mukhlesur Rahman**

Passport No:

Registration /Metric No: **KGA 090034**

Name of the degree: **Master in Engineering Science.**

Title of Project Paper/Dissertation/Thesis: **APPLICATION OF CARBON FIBRE REINFORCED POLYMER LAMINATE FOR STRENGTHENING REINFORCED CONCRETE T- BEAM.**

Field of study: **Structural Engineering**

I do solemnly and sincerely declare that:

1. I am the sole author/writer of this work;
2. This work is original;
3. Any use of any work in which copy exists was done by way of fair dealing and for permitted purposes and any excerpt or extract from, or reference to or reproduction of any copyright work has been disclosed expressly and sufficiently and the title of the work and its authorship have been acknowledged;
4. I do not have any actual knowledge nor do I ought reasonably to know that the making of this work constitutes an infringement of any copyright work;
5. I hereby assign all and every rights in the copyright to this work to the University of Malaya (UM), who henceforth shall be owner of the copyright of this work and that any reproduction or use in any form or by any means whatsoever is prohibited without the written consent of UM having been first had and obtained;
6. I am fully aware that if in the course of making this work I have infringed any copyright whether intentionally or otherwise, I may be subject to legal action or any other action as may be determined by UM.

Candidate's Signature Date

Subscribed and solemnly declared before,

Witness's Signature Date

Name:

Designation:

ABSTRACT

Most of the researches on strengthening so far had been focused on rectangular reinforced concrete (RC) beams. Researches on strengthening of RC T-beams are rather limited. This study focuses on the application of carbon fibre reinforced polymer (CFRP) laminate for strengthening the tension zone of RC T-beam constrained by the presence of a stump (representative of a column) and the effect of varying the length of the strengthening laminates. Three different orientations of the CFRP laminates were tested to evaluate the best orientation. The behaviour of RC T-beams (with stump) flexurally strengthened both in tension and compression zones were also studied here. In addition, FEM (non-linear finite element analysis) was applied to model the experimental results.

To evaluate the effectiveness of the proposed strengthening method, a total of eight RC T-beams were fabricated and tested. Four of them were cast with a column stump in the midspan to provide constraints for the application of CFRP laminates. The other four beams were cast without any column stump. The following orientations were chosen. Orientation 1 was the full application of CFRP laminate along the centre of beam length assuming no stump was present. Orientation 2 was the full application of CFRP laminate alongside the stump parallel to beam length and Orientation 3 was the application of CFRP laminate around the stump and a continuous strip from the side of the stump to the ends of the beam. The beams were tested using the three point bending test set-up.

The results showed that the load carrying capacities of the tension zone strengthened beams were increased by about 50% compared to un-strengthened beams. The length of the CFRP laminate recommended in the Technical Report 55 did not prevent end peeling but it did increase the load bearing capacity of the RC T-beam. The most

suitable orientation of CFRP laminate determined was Orientation 2. The load carrying capacity had increased by about 70% compared to un-strengthened beam by strengthening both the tension and compression zone. The FEM analyses were in good agreement with the experimental results.

ABSTRAK

Kebanyakan penyelidikan mengenai ‘pengukuhan’ lebih bertumpu kepada rasuk konkrit bertetulang segiempat tepat atau dalam istilah lain ‘rectangular reinforced concrete (RC) beams’. Pada masa yang sama, penyelidikan tentang pengukuhan rasuk konkrit bertetulang T (RC T-beam) adalah amat terhad. Kajian yang dilaksanakan ini berfokus kepada polimer gentian karbon yang diperkuatkan (CFRP) untuk mengukuhkan zon tegangan RC T-beam yang dikekang oleh kehadiran tunggul selain berfokus kepada kesan memvariasikan panjang lamina pengukuh. Tiga orientasi lamina CFRP yang berlainan telah diuji untuk menilai yang mana satu merupakan cara pengukuhan yang terbaik. Selain itu, kesan cara RC T-beam (bertunggul) yang dikukuhkan melalui lenturan di kedua-dua zon tekanan dan mampatan turut dikaji. Dalam pada itu, analisis elemen ‘non-linear finite’ (FEM) telah diaplikasi sebagai model keputusan eksperimen.

Untuk menilai keberkesanan melalui cara-cara yang telah dicadangkan di atas, sejumlah lapan RC T-beam telah direka dan diuji. Empat daripadanya telah ditetapkan mempunyai tunggul di pertengahan rentang untuk memberi kekangan kepada aplikasi lamina CFRP dan empat lagi rasuk tidak mempunyai sebarang tunggul. Berikut merupakan orientasi-orientasi yang telah dipilih: Orientasi 1 merupakan aplikasi penuh lamina CFRP di sepanjang garis pusat panjang rasuk yang dianggap sebagai tiada tunggul; Orientasi 2 pula merupakan aplikasi penuh lamina CFRP di sepanjang tunggul selari dengan panjang rasuk; Orientasi 3 ialah aplikasi penuh lamina CFRP di sekeliling tunggul dan jalur bersambung dari tepi tunggul hingga ke hujung rasuk. Kesemua rasuk diuji di bawah ujian lenturan tiga titik.

Keputusan yang didapati menunjukkan bahawa kapasiti menanggung beban di zon tegangan rasuk pengukuh mengingkat sebanyak 50% berbanding dengan rasuk-rasuk yang tiada pengukuh. Panjang lamina CFRP yang telah disyorkan di dalam Laporan

Teknikal 55 tidak dapat menghindar pengelupasan di hujung (end peeling) tetapi mampu meningkatkan kapasiti menanggung beban RC T-beam. Penentuan orientasi lamina CFRP yang paling sesuai ialah Orientasi 2. Bagi rasuk yang diperkukuh di kedua-dua bahagian tegangan dan mampatan, peningkatan beban tertinggi yang dicatatkan ialah 70% berbanding dengan rasuk yang tidak diperkukuh. Keputusan yang didapati daripada ujikaji yang telah dilakukan adalah setanding dengan keputusan yang diperolehi dari analisis FEM.

ACKNOWLEDGEMENTS

I would like to thank to almighty Allah (SWT) for providing me the opportunity to pursue my studies as well as instilling the patience and perseverance during my research work**.**

I wish to express my sincere thanks and profound appreciation to my supervisor, Prof. Ir. Dr. Mohd Zamin Jumaat for his guidance, encouragement and precious time spent on the fruitful discussion throughout the work, which was extremely valuable in conducting this research work within the stipulated schedule.

I would like to acknowledge the grant (UMRG) provided from the University of Malaya to fulfill the study as well as the research works. My deep appreciation and earnest thanks to all my research colleagues and staffs of Department of Civil Engineering as well as to the non-academic staffs of the Faculty of Engineering and libraries, too for their amiable assistance during my studies.

Finally, I would like to thank the most important people in my life, my parents, brother, sisters and other family members who have provided their endless support and patience throughout the years.

TABLE OF CONTENTS

LIST OF FIGURES

LIST OF TABLES

LIST OF NOTATIONS

AASHTO	American Association for State highway and Transportation Official
CFRP	Carbon fibre reinforced polymer
FEM	Finite element modeling
EB	Externally bonded
FRP	Fibre reinforced polymer
GFRP	Glass fibre reinforced polymer
LVDT	Linear variable displacement transducer
NSM	Near surface mounted
RC	Reinforced concrete
JSCE	Japanese Society of Civil Engineers

CHAPTER 1: INTRODUCTION

1.1 Background

Currently, there is an increased demand for the strengthening or rehabilitation of existing reinforced concrete (RC) bridges and buildings. This is mainly due to the ageing, deterioration, increase in loads, corrosion of steel reinforcement or revision in the design codes and knowledge. Higgins et al. (2007) pointed out that the previous design provisions did not have a comprehensive understanding of the behavior of certain structures. Therefore, design code provisions from pre-1970s would be different from current design codes. In addition, construction materials are changing substantially. The American Association for State Highway and Transportation Officials (AASHTO) bridge design provisions did not consider the use of modern deformed reinforcing bars until 1949, and explicit bond specifications for deformed bars were not announced until 1953 (AASHTO, 2002). The knowledge of proper anchorage was unclear. Therefore, many existing structures designed before 1960s have smaller cross-sectional sizes, smaller dimensions for stirrups, wider spaced reinforcement and decreased requirements for flexural bond stresses. This is why older concrete structures become deficient during their service life and require strengthening and repair. While complete replacement of a deficient/deteriorated structure is a desirable option, strengthening/repair is often the more economical one.

While many methods of strengthening structures are available, strengthening by applying CFRP laminate has become popular. For strengthening purposes, application of CFRP laminate is more advantageous than other materials. Teng et al. (2002) pointed out that, there is increased demand for extensive research work to improve the characteristic behaviour of FRP materials to establish their application acceptability in

RC structures, beams, slabs and columns. In particular, their practical implementations for strengthening civil structures are numerous.

Several researchers (Li et al., 2008; Camata et al., 2007; Toutanji et al., 2006; Bencardino et al., 2002) pointed out that most of the pragmatic works consist mainly of the rectangular beams. Furthermore, the design methodologies as well as guidelines are evolved mainly for the simply supported rectangular beams. Generally, the research works were conducted on RC rectangular sections which are not truly representative for the fact that most RC beams would have a T- Section due to the presence of a top slab.

Although many research studies (Arduini et al., 1997; Nanni, 1995; Chajes et al., 1994; Saadatmanesh et al., 1991) had been conducted on the strengthening and repairing of simply supported RC beams using external plates, there is little reported work on the behavior of strengthened RC-T beams. Especially, works relating to the application of CFRP laminate for strengthening the tension zone of RC T- beams in the presence of column are very few. In addition, there are few difficulties arise due to the presence of columns and other components such as electric and plumbing lines or HVAC ducts. These columns and components hinder the process of applying CFRP laminate in this region using conventional techniques. Another important point is that, the use of thick steel plates for strengthening will raise the floor level, which might be undesirable.

An exhaustive literature review has revealed that, a little amount of research works had been done to address the possibility of strengthening the tension zone of RC T- beam in presence of column using FRP materials .The constraints caused by columns in the application of the strengthening system were not considered in the existing researches.

1.2 Research Objectives

The main objectives of this research program are:

1. To study the behaviour of RC T- beams flexurally strengthened both in the tension and compression zone considering the constraints caused by columns.
2. To identify the most effective orientation of the CFRP laminate for strengthening the tension face of the RC T- beams.
3. To evaluate the effect of CFRP laminate length in the tension zone of the reinforced concrete T-beam.
4. To simulate the structural behaviour of these beams using finite element modeling.

1.3 Research Methodology

An extensive literature review was carried out to identify a suitable methodology for this study. Latest information on strengthening materials, methods of application, problems associated with strengthening techniques, the ways to overcome these problems and information regarding numerical modeling of strengthened beams were taken into consideration. BS EN 1992-1-1:(2004) code was followed for the fabrication of beams. The length effect of CFRP laminate was selected in accordance with Technical Society Report 55 (TR 55). The general methodology of this study can be summarized as follows:

1. A total of eight beams were casted and tested with different arrangements of CFRP to evaluate the most effective orientation for strengthening the tension zone of RC T- beam. A stump was monolithically casted in the middle of the beam to represent a column. Four beams with stump and four beams without stump were tested. The loading was applied in such a way that the flange of the T- beam was in tension. The lengths of CFRP laminate were varied to

investigate the effect of lengths for strengthening the tension zone of RC T-beam.

2. The beams were modeled using a finite element analysis package (LUSAS) .The beams were analyzed based on non-linear structural analysis. The results obtained from this modeling were compared with experimental results. To validate this modeling, existing two well-known research works on strengthening continuous beams are also modeled using this FEM as a case study.
3. From the study conducted, several conclusions and recommendations are comprehended.

1.4 Outline of the Thesis

The research work in this study is composed of six chapters.

Chapter One provides a brief introduction and discusses the objectives and methodology of the research work.

Chapter Two presents a state-of-the-art review of the existing research works as well as identify research gaps related to the current work target. Different failure modes of the strengthened RC beam are introduced in this chapter. Numerical analysis of strengthened beams based on finite element modeling (FEM) is also reviewed in this chapter.

Chapter Three describes the theoretical approaches related to the design of RC T-beams. Description of finite element modeling is also provided in this chapter.

Chapter Four describes the experimental phase.

Chapter Five provides analysis and simulation of test results .Finite element modeling and experimental test results are also compared in this chapter.

Chapter Six includes the conclusions drawn from this research and recommendations.

CHAPTER 2: LITERATURE REVIEW

2.1 Introduction

An exhaustive background information and literature review has been presented to justify the research gaps found for the research work in this thesis. The significance of this research as well as the literature review on numerical models found in existing researches are analyzed briefly in this chapter.

2.2 Strengthening Materials

Different materials are used for strengthening civil structures. These materials are: sprayed concrete, ferrocement, steel plate and fiber reinforced polymer. Initially sprayed concrete was used for strengthening and repairing purposes. After that, ferrocement was used for strengthening and repairing purposes. Romuldi (1987) first introduced the term "ferrocement". Later on Paramasivam et al. (1998) also used ferrocement as strengthening material.

The most commonly used materials for strengthening are steel plates and FRP laminates. Fibre reinforced polymer composites are formed by embedding continuous fibres in a resin matrix that binds the fibres together. Depending on the fibres used, FRP composites are classified into three types:

(a) Glass FRP (GFRP) composites

(b) Carbon FRP (CFRP) composites

(c) Aramid FRP (AFRP) composites

Fibre reinforced polymer materials (FRP) such as: pultruded plates, fabrics and sheets have been widely used as strengthening materials due to their many advantages over other strengthening materials.

2.3 Methods of Strengthening

There are many methods for strengthening, such as: section enlargement, steel plate bonding, and external post tensioning method, epoxy bonded (EB) system, unbounded anchored system and near-surface mounted (NSM) system. General methods for strengthening are summarized in Table 2.1. The basic concept of strengthening is to improve the strength and stiffness of concrete members by adding reinforcement to the concrete surface.

Table 2.1 Methods of strengthening

Methods	Description
(a) Section Enlargement	"Bonded" reinforced concrete is added to an existing structural member in the form of an overlay or a jacket.
(b) Steel plate bonding	Steel plates are glued to the concrete surface by epoxy adhesive to create a composite system and improve flexural strength.
(c) External post tensioning system	Active external forces are applied to the structural member using post-tensioned cables to improve flexural strength.
(d) Epoxy bonded system	FRP composites are bonded to the concrete surface by using epoxy adhesive to improve the flexural strength. FRP material could be in the form of sheets or plates.
(e) Near-surface mounted system	FRP bars or plates are inserted into a groove on the concrete surface and bonded to the concrete using epoxy adhesive.
(f) Unbounded /mechanically fastened system	This method uses a powder-actuated fastener gun to install mechanical fasteners and fender washers through holes in the FRP predrilled into the concrete substrate, "nailing" the FRP in place.

2.3 Various Failure Modes of FRP Strengthened Beams

Failure modes are classified into two types. The first type of failure includes the common failure modes such as concrete crushing and FRP rupture based on complete composite action. The second type of failure is a premature failure without reaching full composite action at failure. The failure modes of FRP strengthened structures with the Epoxy Bonded system are summarized in Figure 2.1 and Table 2.2. Premature failures can significantly limit the enhancement property and the ultimate flexural capacity of the retrofitted beams. Several studies were conducted to identify methods of preventing premature failure with the aim of improving the load capacity and ductility of the RC beams. Researchers (Ceroni, 2010; Jumaat and Alam, 2010; Wang and Hsu, 2009; Alam and Jumaat, 2008; Aram et al., 2008; Ceroni et al., 2008; Xiong et al., 2007; Pham and Al-Mahaidi, 2006; Teng et al., 2003) have studied the usage of end anchorage techniques, such as U-straps, L-shape jackets, and steel clamps to prevent the premature failure of RC beams strengthened with CFRP laminate.

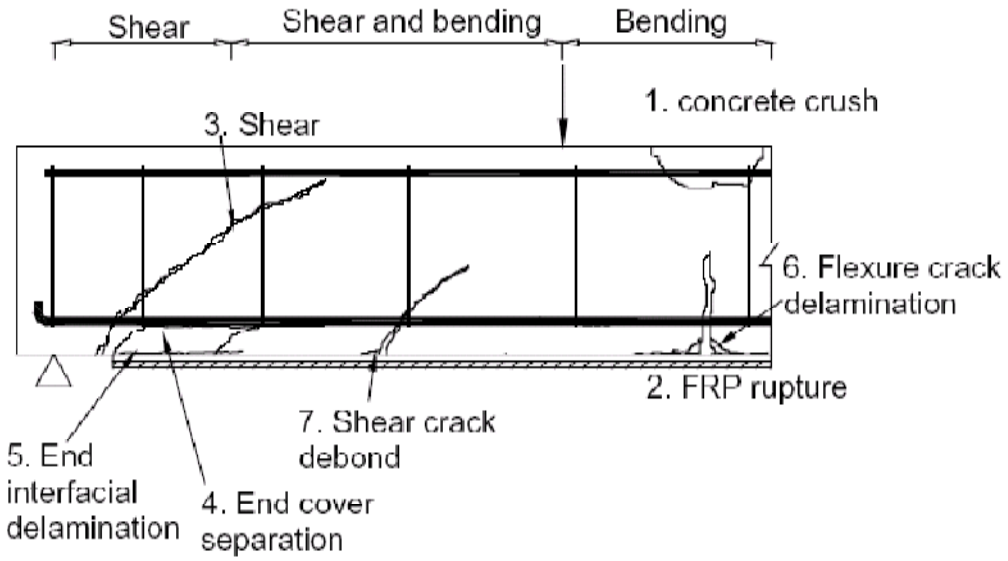

Figure 2.1 Failure modes of EB strengthened beams (Pham and Al-Mahaidi, 2004)

Table 2.2 Description of failure modes (Choi H.T., 2008)

Failure modes		Description
Case I: Full composite action	Concrete Crushing	If premature failures are prevented, the ultimate flexural capacity of the beam is reached when either the FRP composite fails by tensile rupture or the concrete crushes in compression. This is similar to the classical flexural failure modes of RC beams except for the brittle failure of FRP rupture.
	FRP rupture	
Case II: Premature failure	End peeling	Failure of the concrete cover is initiated by the formation of a crack at or near the plate end due to high interfacial shear and normal stresses caused by the abrupt termination of the plate.
	End interfacial delamination	This debonding failure is initiated by high interfacial shear and normal stresses near the end of the plate that exceed the strength of the weakest element (concrete or epoxy).
	Flexural crack induced debonding	Flexural crack induced debonding happens when the concentrated bond stress at the crack location exceeds the shear strength in the weakest layer.
	Shear crack induced debonding	Shear crack induced debonding occurs in the zone where both shear and bending moment are significant. It is caused by the combination of two mechanisms. The first one is similar to that of flexural crack induced debonding. The second is by the vertical movement of the inclined crack.

2.4 Previous Research Works Related to this Topic

Jumaat et al. (2010) pointed out that, although several research studies have been conducted on the strengthening and repair of simply supported reinforced concrete beams using external plates, there are few reported works on the behavior of strengthened T-beams in the presence of column. Furthermore, almost all the available design instructions to strengthen the structures by the external laminates of FRP are demonstrating the simply supported beams (JSCE2001, TR 55, ACI 440R-96). The

literature review revealed that a meager amount of research works had been explored to address the potential of applying CFRP laminate for strengthening the tension zone of RC 'T'– beam in the presence of column .

On the field of strengthening continuous beam, Grace et al. (1999) tested five continuous beams. They found that the use of FRP laminates to strengthen continuous beams is effective for reducing deflections and for increasing their load carrying capacity. They also concluded that beams strengthened with FRP laminates exhibit smaller and better distributed cracks. Later, Grace et al. (2001) investigated the experimental performance of CFRP strips used for flexural strengthening in the hogging region of a full-scale reinforced concrete beam. Grace et al. (2005) also worked on another research where three continuous beams were tested. They noted that CFRP strips were not stressed to their maximum capacity when the beams failed, which led to ductile failures in all the beams. On the other hand, El-Refaie et al. (2003a) examined eleven reinforced concrete (RC) two-span beams strengthened in flexure with external bonded CFRP sheets. In another research, El-Refaie et al. (2003b) tested five reinforced concrete continuous beams strengthened in flexure with external CFRP laminates. They investigated that extending the CFRP sheet length to cover the entire hogging or sagging zones did not prevent peeling failure of the CFRP sheets**.** They also found that, strengthened beams at both sagging and hogging zone produced the highest load capacity**.** Ashour et al. (2004) tested 16 reinforced concrete (RC) continuous beams with different arrangements of internal steel bars and external CFRP laminates. As in previous studies, they observed that increasing the CFRP sheet length in order to cover the entire negative or positive moment zones did not prevent peeling failure of the CFRP laminates. Aiello et al. (2007) compared the behavior between continuous RC beams strengthened with of CFRP sheets at hogging or sagging regions and RC beams strengthened at both sagging and hogging regions. Recently, Maghsoudi and Bengar

(2008) have examined the flexural behavior and moment redistribution of reinforced high strength concrete (RHSC) continuous beams strengthened with CFRP. Finally, Akbarzadeh and Maghsoudi (2010) have conducted an experimental program to study the flexural behavior and moment redistribution of reinforced high strength concrete (RHSC) continuous beams strengthened with CFRP and GFRP sheets.

In all the above cases it is seen that the researches were conducted on RC rectangular sections which are not representative of the fact that most RC beams would have a T-Section due to the presence of top slab. In all the above cases, the restraint caused by the columns in the application of the strengthening system was not considered.

Literature review on strengthening RC beams in the presence of RC slabs (Polies et al**.,** 2010; Smith and Kim, 2009; Anil, 2008) also reveals that the strengthening system is applied in the positive moment region and the restraint caused by the columns in the application of the strengthening system was not considered.

2.5 Numerical Modeling of Flexurally Strengthened RC Beams

Extensive research work on numerical analysis had been carried out over last years to predict the failure mechanisms and interface stresses of strengthened RC beams. The slip effect between concrete and steel plate and the non -linear behavior of concrete, reinforcing bar and steel plate were taken into account for the modeling of RC beams by Adhikary and Mutsuyoshi (2002). Li et al.(2006) carried out the experimental and numerical analysis to predict the load carrying capacity of reinforced concrete beams strengthened with CFRP laminate. Camata et al. (2007) also modeled to describe the failure modes. They found that the numerical and experimental results showed a good agreement on predicting the failure behavior.

2.6 Importance of the Present Study

This paper attempts to address an important practical issue which is not considered in existing conventional strengthening technique in applying the strengthening material i.e. the installation constrains due to the presence of column. This paper presents a straightforward technique of applying CFRP laminate for strengthening the tension zone of RC- T beam considering those constrains due to column. The effect of length of strengthening plate is also studied in this research.The beams are modeled using FEM (LUSAS). Existing two well-known research works on strengthening continuous beams are also modeled using this FEM as case studies, where a good agreement between the test results and results from FEM is observed. Finally, it is concluded that the proposed method is very easy and effective, and for obtaining complete design guideline for strengthening the tension face of RC-T beam, future recommendations are also visualized through this paper.

CHAPTER 3: THEORETICAL AND NUMERICAL APPROACHES

3.1 Introduction

This chapter contains theoretical calculations and numerical approaches of flexurally strengthened RC T- beam. Theoretical calculation for the length effect of strengthening plate is also presented in this chapter. All the detail calculations are shown in Appendix A.

3.2 Design of CFRP Laminate Strengthened Beam

The strengthened beams in this study are designed on the basis of the simplified stress block method in accordance with BS EN 1992-1-1:(2004). The design methods are outlined below. Detail design calculations are shown in Appendix-A.

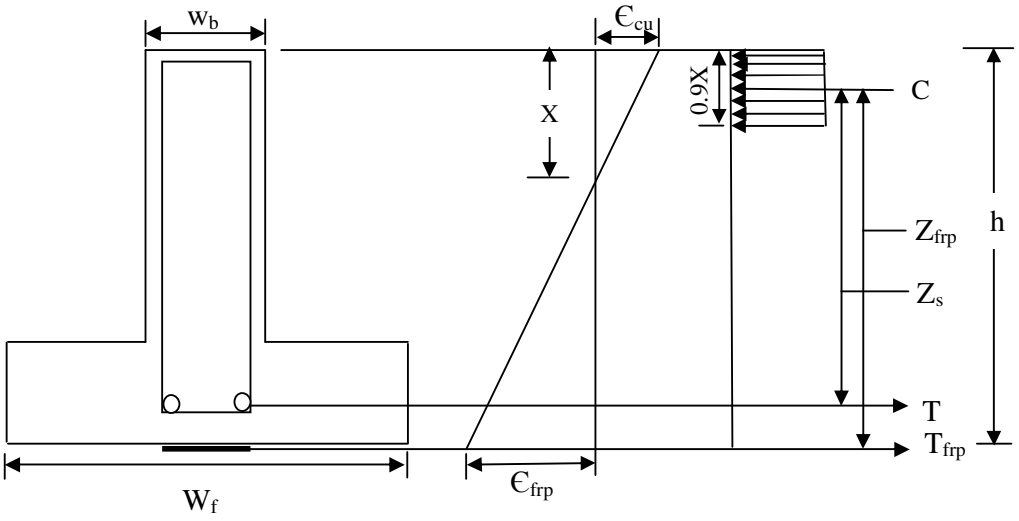

Figure 3.1 Strain and stress block diagram of CFRP laminate strengthened beam

3.2.1 Depth of Neutral Axis

In accordance with BS EN 1992-1-1:(2004), the design strain of concrete is 0.0035. According to Technical Report 55, FRP strain should be less than 0.006 to avoid debonding failure (TR 55).

$$\in_{cu} = 0.0035\ ,\ \in_{frp} = 0.006 \quad \text{----------} \quad (3.1)$$

From the strain diagram (Figure 3.1), we can get the depth of neutral axis 'x'

$$\frac{0.0035}{0.006} = \frac{x}{h-x} \quad \text{----------} \quad (3.2)$$

$$x = 0.368 \times h \quad \text{----------} \quad (3.3)$$

3.2.2 Required Area of CFRP Laminate

According to BS EN 1992-1-1: (2004),

$$C = 0.67 \times f_{cu} \times 0.9x \times b_w \quad \text{----------} \quad (3.4)$$

$$C = 0.603 \times f_{cu} \times x \times b_w \quad \text{----------} \quad (3.5)$$

$$T_{frp} = (0.603 \times f_{cu} \times x \times b_w) - (A_s \times f_y) \quad \text{----------} \quad (3.6)$$

$$A_{frp} = \frac{T_{frp}}{\sigma_{frp}} = \frac{(0.603 \times f_{cu} \times x \times b_w) - (A_s \times f_y)}{E_{frp} \times \in_{frp}} \quad \text{----------} \quad (3.7)$$

3.3 Bar Yield Load of Control Beam

The theoretical bar yield load of the control beam is calculated as followings:

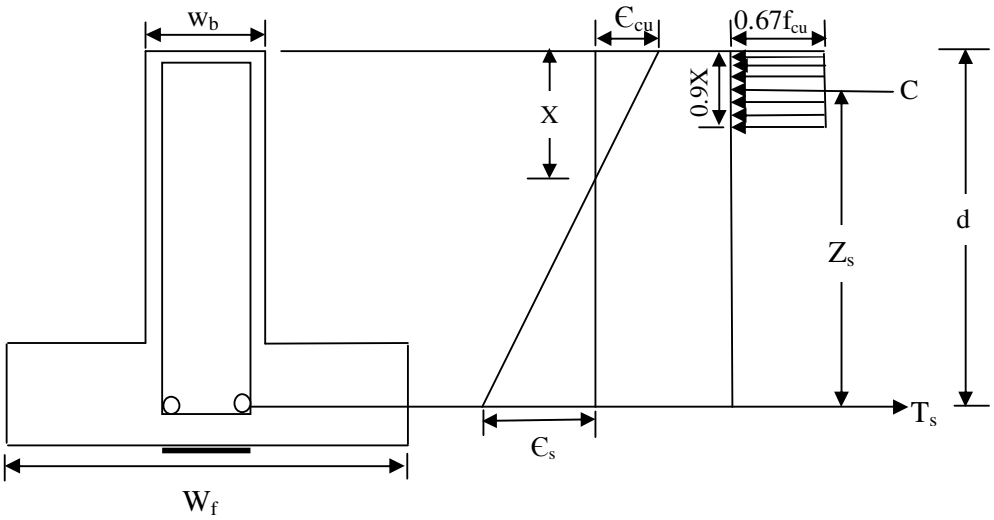

Figure 3.2 Stress block diagram of control beam

Bar yield load of control beam,

$$p_{yield} = \frac{2M_{cy}}{1.5} = \frac{2A_s f_y (d - 0.45x)}{1.5} \text{ ----------(3.8)}$$

Here, A_s is the area of the steel bar, f_y is the yield stress of the steel bar, d is the effective depth of beam and x is the depth of neutral axis.

3.4 Flexural Failure Load of Control Beam

$$p_{failure} = \frac{2M_{ct}}{1.5} = \frac{2A_s f_t (d - 0.45x)}{1.5} \text{ ----------(3.9)}$$

Here f_t is the tensile strength of steel bar

3.5 Bar Yield Load of Strengthened Beam.

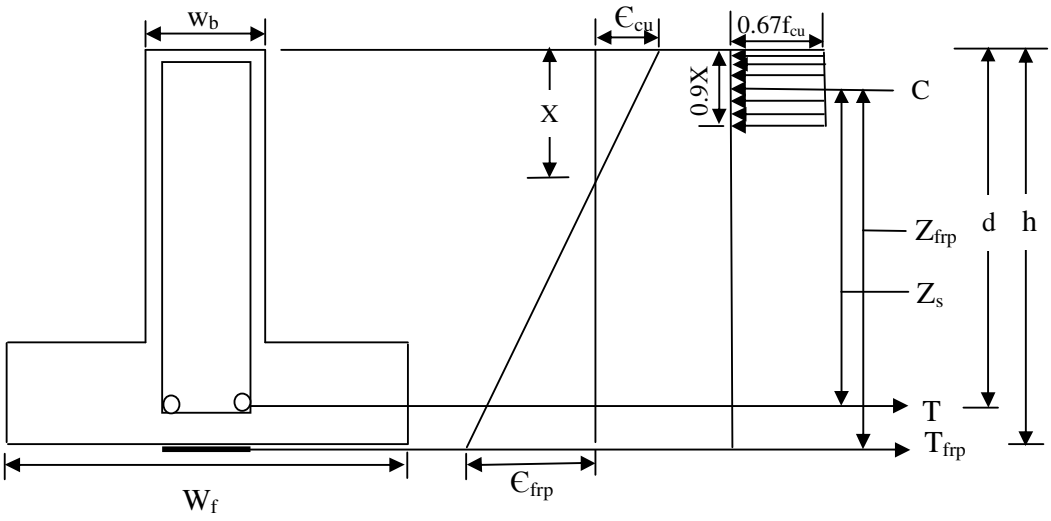

Figure 3.3 Stress block diagram of strengthened beam

Bar yield strain, $\varepsilon_s = \frac{\text{Yield stress}}{\text{Modulus of Elasticity}} = \frac{f_y}{E_s}$ ---------- (3.10)

The strain of CFRP laminate of strengthened beam at bar yield can be obtained by trial and error.

$$x = 0.5d \text{ ----------(3.11)}$$

From the Figure 3.3,

$$\in_{frp}=\frac{\in_s (h-x)}{d-x}=\frac{\in_s (h-.5d)}{d-.5d}=\frac{f_y(h-.5d)}{.5dE_s} \text{----------(3.12)}$$

$$T=T_{frp}+T_s=\frac{f_y(h-.5d)E_{frp}A_{frp}}{.5dE_s}+A_s f_y \text{----------(3.13)}$$

From equ'n (3.5),

$$C=0.603f_{cu}bx=T=\frac{f_y(h-.5d)E_{frp}A_{frp}}{0.5dE_s}+A_s f_y \text{----------(3.14)}$$

$$x=\frac{1}{0.603f_{cu}b}\left(\frac{f_y(h-.5d)E_{frp}A_{frp}}{.5dE_s}+A_s f_y\right) \text{----------(3.15)}$$

The yield load of steel bar,

$$p_{yc}=\frac{2M_{yc}}{1.5}=\frac{2}{1.5}[A_s f_y(d-0.45x)+\frac{f_y(h-x)E_{frp}A_{frp}}{E_s(d-x)}(h-0.45x)] \text{---------(3.16)}$$

Putting the value of 'x', we can get the yield load of steel bar.

3.6 Failure Load of CFRP Laminate Strengthened Beam

From the Figure 3.3,

$$0.603f_{cu}bx=A_s f_t+\frac{0.0035(h-x)}{x}E_{frp}A_{frp} \text{----------(3.17)}$$

$$(0.603f_{cu}b)x^2-(A_s f_t-0.0035A_{frp}E_{frp})x-0.0035A_pE_{frp}h=0 \text{----------(3.18)}$$

$$x=\frac{-m\pm\sqrt{m^2-4nl}}{2l} \text{----------(3.19)}$$

Here,

$$l=0.603f_{cu}b \text{----------(3.20)}$$

$$m=-(A_s f_t-0.0035A_{frp}E_{frp}) \text{----------(3.21)}$$

$$n=-0.0035A_pE_{frp}h \text{----------(3.22)}$$

$$p_{ut} = \frac{2M_{tc}}{1.5} = \frac{2}{1.5}[A_s f_t (d - 0.45x) + A_{frp}\sigma_{frp}(h - 0.45x)] \text{ ---------- (3.23)}$$

3.7 Length Effect of CFRP Laminate

According to TR 55, limiting the longitudinal shear stress between the FRP and the substrate to 0.8 N/mm^2 can prevent end–plate separation. In this research, the longitudinal shear stress is calculated according to two theories. One is according to elastic theory and another one is based on Smith and Teng (2001).

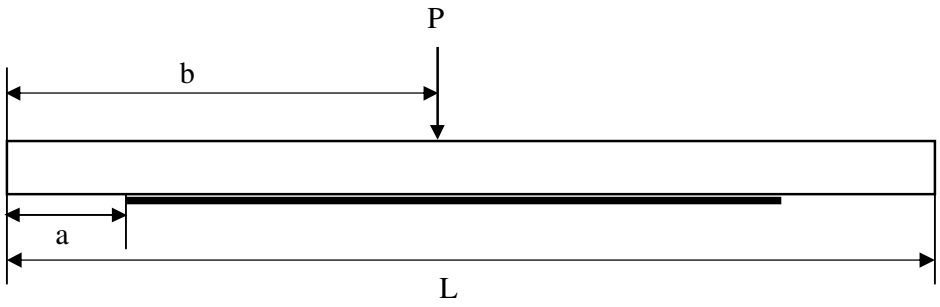

Figure 3.4 Strengthened beam (Smith and Teng, 2001)

According to Smith and Teng (2001), Interfacial shear stress $\tau(x)$ is calculated by,

For a<b,

$$\tau(x) = \frac{m_2}{\lambda} Pa\left(1 - \frac{b}{L}\right)e^{-\lambda x} + m_1 P\left(1 - \frac{b}{L}\right) - m_1 PCosh(\lambda x)e^{-k} \text{ ----- (3.24)}$$

Where,

$$m_1 = \frac{G_a}{t_a}.\frac{1}{\lambda^2}\left(\frac{y_1 + y_2}{E_1 I_1 + E_2 I_{2_1}}\right) \text{ ----------(3.25)}$$

$$m_2 = \frac{G_a}{t_a}.\frac{y_1}{E_1 I_1} \text{ ---------- (3.26)}$$

$$k = \lambda(b - a) \text{ ---------- (3.27)}$$

$$\lambda^2 = \frac{G_a b_2}{t_a}\left(\frac{(y_1 + y_2)(y_1 + y_2 + t_a)}{E_1 I_1 + E_2 I_{2_1}} + \frac{1}{E_1 A_1} + \frac{1}{E_2 A_2}\right) \text{ ---------- (3.28)}$$

According to elastic theory, interfacial shear stress at the adhesive level is calculated by the following equation (Ashour et al. 2004),

$$\tau = \frac{V n_f t_f y_f}{I_c} \quad \text{----------(3.29)}$$

Where,

V=shear force calculated at beam failure,

t_f= thickness of CFRP Laminate,

y_f=depth of neutral axis from the centroid of CFRP laminate.

I_c=transformed second moment of inertia of the cracked reinforced concrete cross section with external CFRP laminates in terms of concrete.

The detail calculation is presented in appendix –A

3.8 Numerical Modeling

In an actual case, indeed, the flange portion of RC-T beam in the beam column intersection remains in tension. The modeling is done in such a way that flanges of T beams are in tension to represent the pragmatic condition. It is done by applying the load on inverted 'T' beam. Three point bending was applied, where the supports are representing the points of inflection of a continuous beam as well as the bending moment is zero.

A finite element program (LUSAS) is employed to build the model of strengthened and unstrengthened beam. The superposition of nodal degrees of freedom assumes that the concrete and reinforcement are perfectly bonded. It is assumed that the self-weight of the beam is negligible compare to the applied load and that the effects of any shear reinforcement can be ignored. In addition, the surface elements of CFRP are right away accompanied by the surface of the concrete and maintain a complete bonding between strengthening plate and the concrete surface is assumed to avert the failure due to

premature debonding (Li et al., 2006).The concrete as well as CFRP section is represented by plane stress (QPM8) elements, and the reinforcement bars are represented by bar (BAR3) elements. A nonlinear concrete cracking material model (cracking model 94) is applied to the plane stress elements and a von Mises plastic material is applied to the reinforcement bars. Units of N,mm,t,s,C are used throughout. The material properties used in this modeling is shown in Table 3.1

Table 3.1 Material properties used for FEM

Concrete			**Steel bar**			**Strengthening plate**	
f'_c (MPa)	E_c (MPa)	Poisson ratio	f_y (MPa)	E_s (MPa)	Poisson ratio	E_p (MPa)	Poisson ratio
37	30000	0.2	560	200000	0.3	165000	0.4

3.8.1 Meshing and Loading Pattern

Reinforcing bars were meshed using a line mesh with two dimensional structural bar elements. Concrete and strengthening plates were meshed using quadrilateral plane stress elements. In all cases quadratic interpolations were used and default meshing divisions were selected. The detailed of meshing and loading pattern is shown in Figures 3.5 to 3.7.

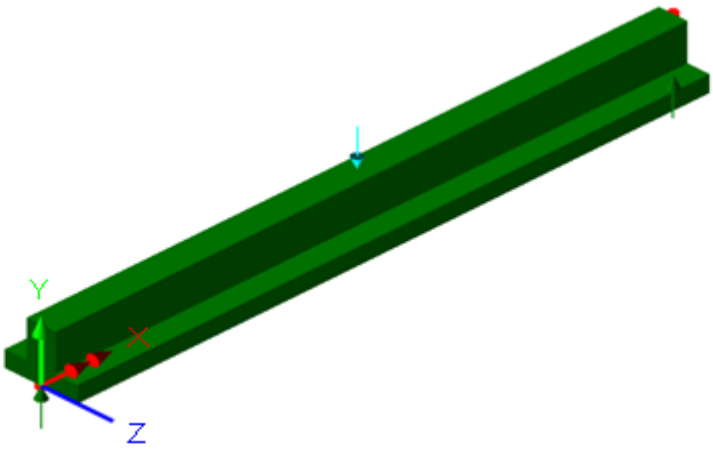

Figure 3.5 Loading pattern of beams

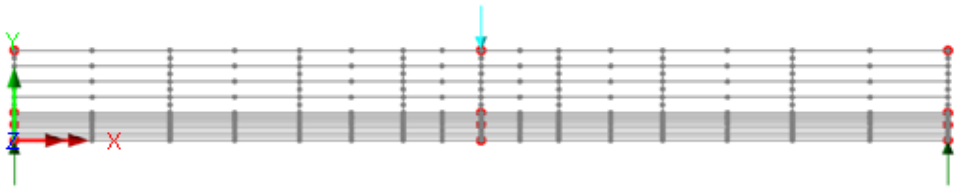

Figure 3.6 Meshing of control beam

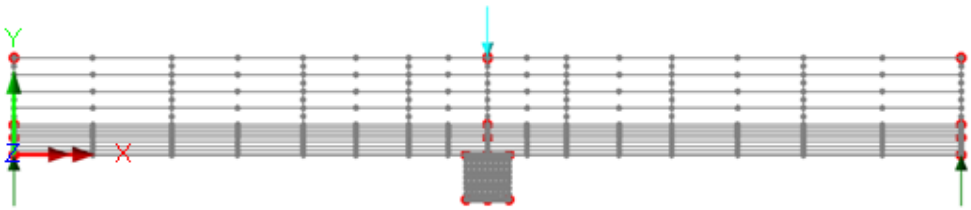

Figure 3.7 Meshing of strengthened beam

3.8.2 Case Study

To validate the proposed model, a total of eight continuous beams are modeled based on previous research works by EI-Refaie et al. (2003b) and Akbarzadeh and Maghsoudi (2010). Akbarzadeh and Maghsoudi (2010) considered high strength concrete while EI-Refaie et al. (2003b) considered normal strength concrete in their research works. Both high strength and normal strength concrete can be modeled by using LUSAS. The results obtained from the computation over the modeling are compared with their experimental results. The details of the beams and meshing of these beams are shown in Figures 3.8 to 3.9. The material properties used by these researchers are shown in Table 3.2 and Table 3.3.

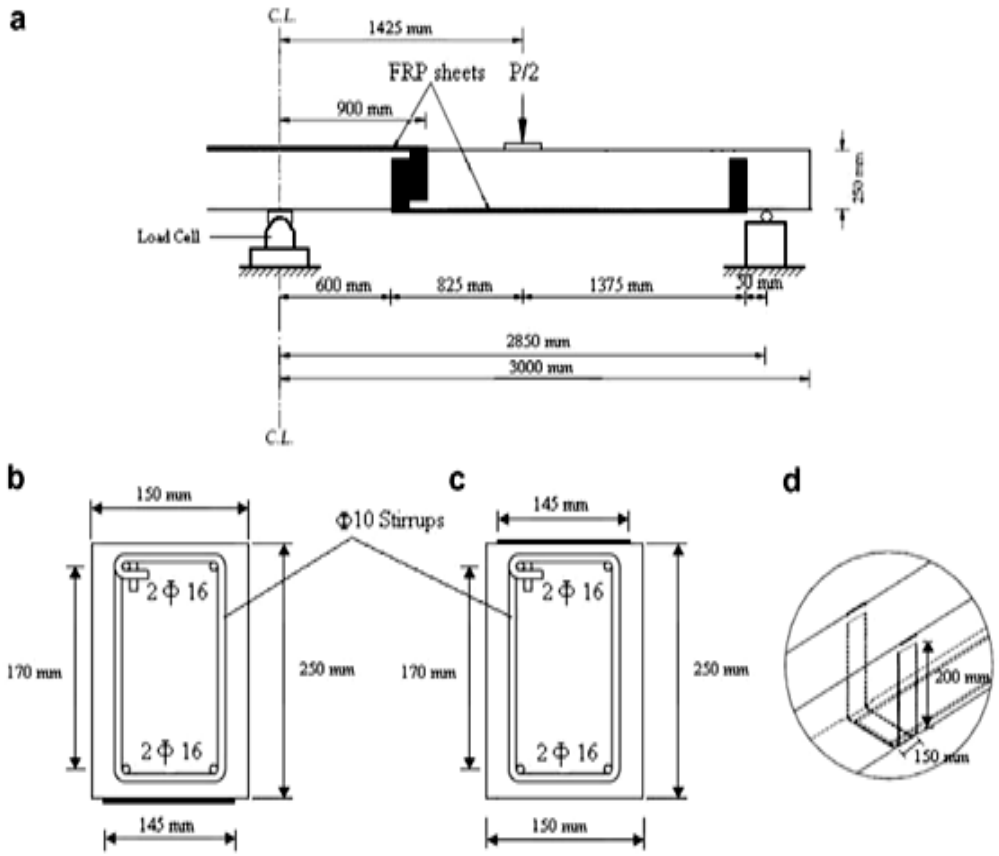

Figure 3.8 Details of beams tested by Akbarzadeh and Maghsoudi, (2010)

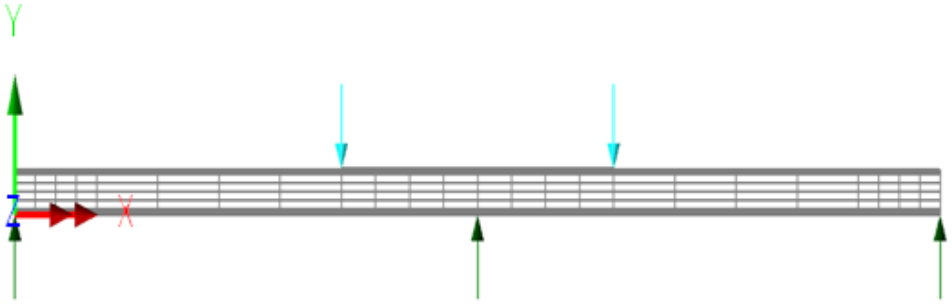

Figure 3.9 Meshing and loading pattern of beam tested by EI-Refaie et al. (2003b)

Table 3.2 Material properties of the beam tested by Akbarzadeh and Maghsoudi (2010).

Beam no	f'_c (MPa)	f_y (MPa)	Positive moment zone		Negative moment zone		Thickness of each layer (mm)	Width of CFRP (mm)	Young's Modulus of FRP E_f (MPa)
			No. of layers	CFRP length (mm)	No. of layers	CFRP length (mm)			
CB	74.2	412.5	-	2200	-	1800	0.11	145	242000
SC1	74.6		1		1				
SC2	74.1		2		2				
SC3	74.4		3		3				

Table 3.3 Material properties of the beam tested by EI-Refaie et al., (2003b)

Beam no	f'_c (MPa)	f_y (MPa)	Positive moment zone		Negative moment zone		Thickness of each layer (mm)	Width of CFRP (mm)	Young's Modulus of FRP E_f (MPa)
			No. of layers	CFRP length (mm)	No. of layers	CFRP length (mm)			
E1	24.0	520	-	-	-	-	1.2	100	150000
E2	43.6		-	-	1	2500			
E3	47.8		1	3500	-	-			
E4	46.1		1	3500	1	2500			

CHAPTER 4: EXPERIMENTAL PROGRAM

4.1 Introduction

An experimental program has been developed to verify the effectiveness of the proposed strengthening technique. Section 4.2 demonstrates the whole test matrix of the experimental program. The specimen fabrication and strengthening procedure are described in section 4.3 and 4.4. Properties of materials used in these experiments are reported in section 4.5. The description of the test setup and instrumentations are described in section 4.6 and 4.7.

4.2 Test Matrix

A total of eight; 3300mm long, 325mm deep, 380mm x 100mm flange, T-shaped RC beams are fabricated for this experimental endeavor. The beams are divided into three groups according to the objectives of this research. The concrete strength of beams B0, B1, B2 and B3 are higher than that of beams B4, B5, B6 and B7. Beams B0, B1, B2and B3 are studied for selecting the best orientation option of CFRP laminate among three orientations (orientation 1, orientation 2 and orientation 3 as shown in Figure 4.5, Figure 4.6 and Figure 4.7 respectively). Beams B4, B5, and B7 are selected for studying the effect of applying CFRP laminate on both the tension and compression faces of T – beam. The purpose of strengthening the compression zone is to improve the strength of the beams up to certain level of strength. Beams B2, B6 and B7 are selected for studying the effect of varying the length of CFRP laminate in the tension face of RC T-beam. The calculation for selecting the length of CFRP laminate is described in Chapter 3.Four of these beams have column stump to represent the column. The stump of height 150mm and cross section 150 x 150 mm was cast in the middle of the flange to represent the intersection of the beam with a column. The objective of casting this

stump is to provide restraints in the application of the strengthening system at the mid-section of the beam. The orientations for different arrangements of CFRP laminates are shown in Figures 4.5 to 4.7. In actual field situation, the flange portion of RC-T beam in the beam column intersection remains in tension. The test setup is arranged in such a way that the flanges of T beams are in tension to represent the actual field condition. It is done by applying the load on inverted T beam. Three point bending is applied, where the supports represents the points of inflection of a continuous beam where the bending moment is zero. The detailed test matrix is shown in Table 4.1

Table 4.1 Test matrix

Beam name	**Concrete strength (MPa)**	**CFRP laminate**			
		Size (mm)	**Length (mm)**	**Applying zone**	**CFRP orientation**
B 0	37	Not applicable			
B 1	39	100 × 1.4	3000	Tension zone	Orientation 1
B 2	40	100 × 1.4	3000	Tension zone	Orientation 2
B 3	42	100 × 1.4	All four sides of stump	Tension zone	Orientation 3
B 4	26	100 × 1.4	3000	Compression zone	-
B5	26	Not applicable			
B 6	26	100 × 1.4	3000, 2500	Tension + compression zone	Orientation 2
B 7	26	100 × 1.4	3000	Tension + compression zone	Orientation 2

4.3 Fabrication of RC-T Beams

The shape and dimensions of the RC-T beams are shown in Figure 4.1. Also, the construction procedure for the RC-T beam is shown in Figure 4.2. The strain gauges attached on to the reinforcing steel bars are coated with wax to provide protection from damage during concrete casting (Figure 4.2a). All of the steel cages are placed inside wooden formwork (Figure 4.2b). Desired clear cover is maintained with the help of previously made concrete blocks. Ready-mixed concrete has been used with a specified concrete compressive strength. Four beams are casted with a compressive strength of 26 MPa and other four beams are casted with 37 MPa. After casting the concrete, the beams were moist cured for seven days, followed by 21 days of curing in air. A total of 8 cylinders, 8 prisms, 16 cubes were made for the concrete strength test.

4.4 Strengthening of RC-T Beams Using CFRP Laminate

4.4.1 General

Strengthening requires a careful observation in each stage of preparing the beam. After 28 days of curing, the beams are strengthened with CFRP laminate. 1.4 mm x 100 mm CFRP laminate (SikaCarboDur S1014/180) has been used for all the strengthened beams. The step by step methods for strengthening the beams are described in the following sub-sections.

4.4.2 Surface Preparation

Preparation of a test surface requires some attention in following the works to perform to assure the impeccable surface for the test. Oil, dirt and other foreign particles removed from the surface in order to expose the texture of aggregate with the help of a diamond cutter (Figure 4.3a).The dust particles were removed by high pressure air jet

(Figure 4.3c). Colma cleaner is used to remove the carbon dust from the bonding face of CFRP laminate.

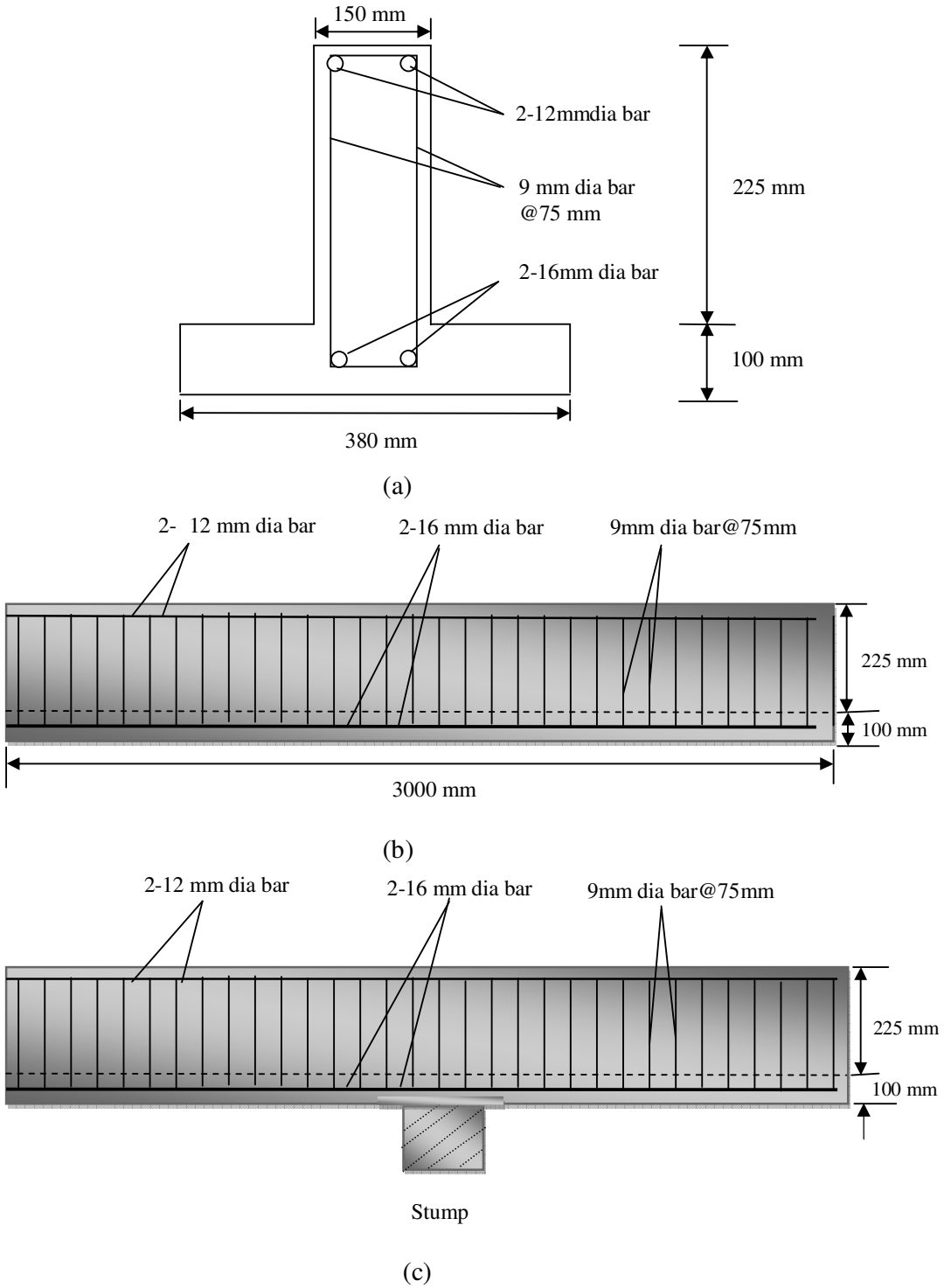

Figure 4.1 Beam geometry and reinforcement details: (a) cross section, (b) longitudinal section without stump, (c) longitudinal section with stump.

(a) Strain gage installed

(b) Wooden forms and cages

(c) Casted beams

Figure 4.2 Construction of RC-T beams

(a) Diamond cutter is being used

(b) Air jetting

(c) Prepared surface

Figure 4.3 Preparation of surface

4.4.3 Placing of CFRP Laminate to Beam Specimens

CFRP laminate was bonded to concrete surface by using Sikadur-30 as a bonding agent. The components of Sikadur-30 (component A and Component B) were mixed properly prior to applying these adhesive to the surfaces of concrete and CFRP laminate. The process of mixing the adhesive and applying it to the surfaces are shown in Figure 4.4. The well –mixed adhesive is pasted to the bonding surface of concrete up to 2-3 mm thickness. The adhesive is applied to the bonding face of CFRP laminate with a special dome shaped spatula (Figure 4.4b). SikaCarboDur Rubber Roller has been used to press the CFRP laminate until the adhesive is forced out on both sides of the laminate (Figure 4.4c).

4.4.4 Different Orientations of CFRP for Strengthening RC-T Beams

The orientations of CFRP laminate for strengthening the RC- T beams are shown in Figures 4.5 to 4.7. Beams having stump, the orientations are of two kinds as shown in Figures 4.6 to 4.7. For beams without stump, strengthening plates are applied in the middle of flanges according to the Figure 4.5.

4.5 Material Properties

The materials used in this experiment are concrete, steel bar and CFRP laminate. In this section their engineering properties are reported.

4.5.1 Concrete

Ready mixed concrete has been used for this research. Concrete compression testing has been carried out at 7^{th}day, 28^{th}day and the day of testing. Three cubes are tested each time and the average strength is calculated. The average compressive strength is 26 MPa for beams B4, B5, B6 and B7. Concrete compressive strength for beams B0, B1, B2 and

B3 varied between 37- 42 MPa. The flexural tensile strength of concrete is estimated using the equation of, $f = 0.53\sqrt{fc'}$ (kg/cm^2).

(a) Mixing of adhesive

(b) Placing of adhesive on CFRP laminate

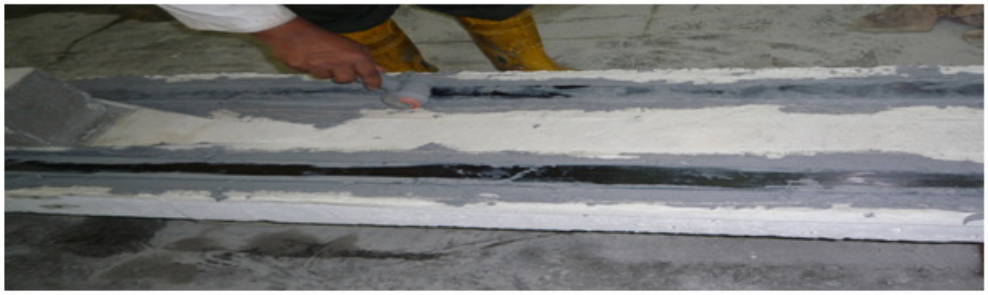

(c) Pressing CFRP with the help of Rubber Roller

Figure 4.4 Installation of CFRP laminate

4.5.2 Steel Reinforcement

Four deformed bars of 16 mm diameter are tested based on ASTM A615/A6156M-09b.The diameter was calculated according to $d=12.736\sqrt{w}$, (w in kg/m).The ultimate strain at rupture is calculated by measuring the final elongation between two points marked on the bar. The average yield strength and ultimate strength were 560 MPa and 645 MPa respectively. Modulus of elasticity of the bar is 200 GPa.

Figure 4.5 CFRP orientation 1

.

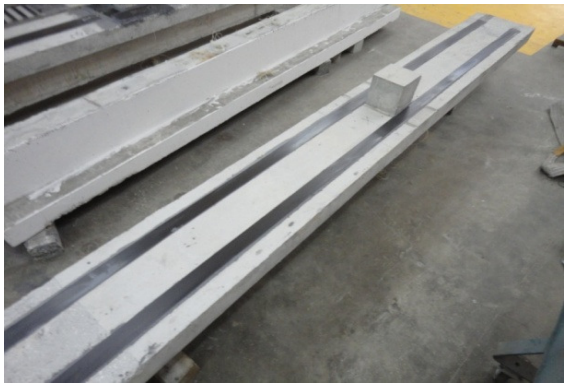

Figure 4.6 CFRP orientation 2

Figure 4.7 CFRP orientation 3

4.5.3 CFRP Laminate

CFRP laminates of type SikaCarboDur S1014/180; (1.4mm x 100 mm) has been used. The maximum design and ultimate strain of CFRP laminates are 0.85% and 1.7% according to the manufacturer's guideline. In this research the design strain of CFRP has been described in Chapter 3 and Appendix A. The tensile strength is 2800MPa. Modulus of elasticity is 165 GPa.

4.6 Instrumentation

4.6.1 Demec Points

To make the cracks clearly visible, beams are painted with white plastic paints. After painting, demec points are installed at the surface of the concrete beam to measure the strain and the neutral axis of the concrete section. The horizontal distance between two consecutive demec points is 200mm. The demec points are installed to the prepared surface by special adhesive (Araldite). After setting the demec points, the beams were instrumented according to the following procedure:

4.6.2 Electrical Resistance Strain Gauges

Strain gages (30 mm) are attached to main reinforcing bars, CFRP laminates and on to the concrete surface to measure their strain (Figure 4.8).The reinforcing bars are smoothed by grinding machine, CFRP laminates are cleaned with acetone and concrete surface are also smoothed before fixing strain gauges. All strain gauges were connected with data logger to record the strain values during the test.

4.6.3 Linear Variable Displacement Transducer (LVDT)

LVDT (50mm capacity) has been used to measure the mid-span deflection of the beam (Figure 4.9). The LVDT was connected to Data Logger to record the readings during test.

4.6.4 Data Logger

Data Logger TDS-530, manufactured by Tokyo Sokki Kenkyujo Co, Ltd. has been employed to record data from various connections. The strain gages were connected as '1G 3W120Ω' and LVDT was connected as '4 GAGE' to Data logger. The readings from strain gages were recorded as 'με' while the readings from LVDT were recorded as 'mm'. Ten second intervals were selected to record the data at every 10 seconds. The data recorded by data logger was collected by CF card of TYPE 1 memory card.

4.6.5 Demec Gauge

Strains at the sides of the beams were measured from the demec points using digital extensometer (Figure 4.10).

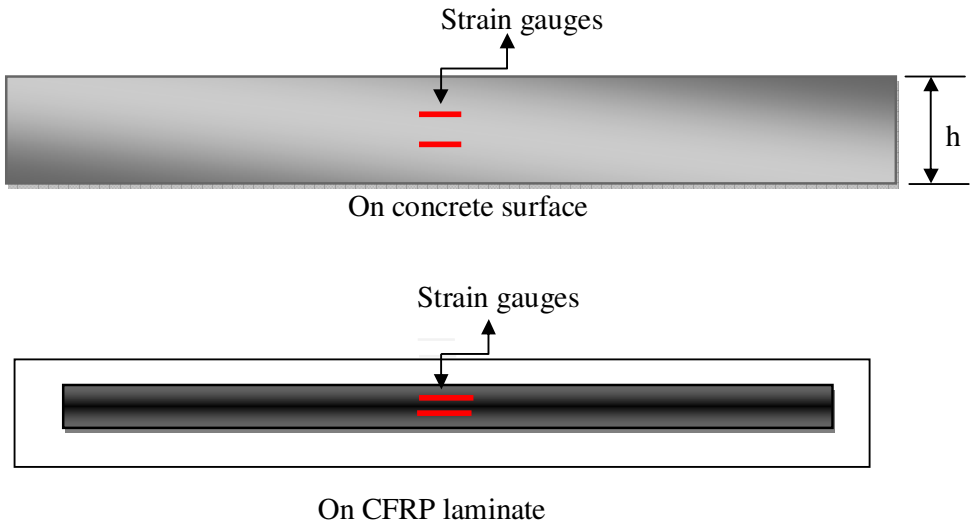

Figure 4.8 Positions of strain gauges

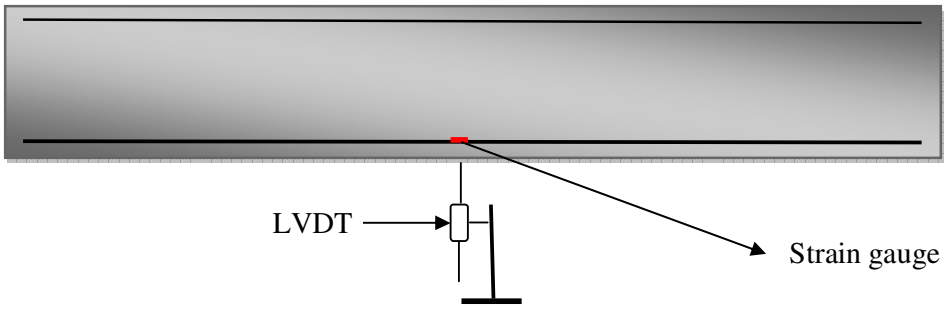

Figure 4.9 Position of LVDT

Figure 4.10 Digital extensometer

4.6.6 Dino-lite Digital Microscope

The crack width of the beams during test was measured with this instrument. By this measuring device, the crack width can be measured up to 0.001 mm. During test, when crack happens, we need just to place the instrument on the cracking line to take the picture of cracking line. From this photo, the crack width is measured with accuracy up to 0.001mm (Figure 4.11).

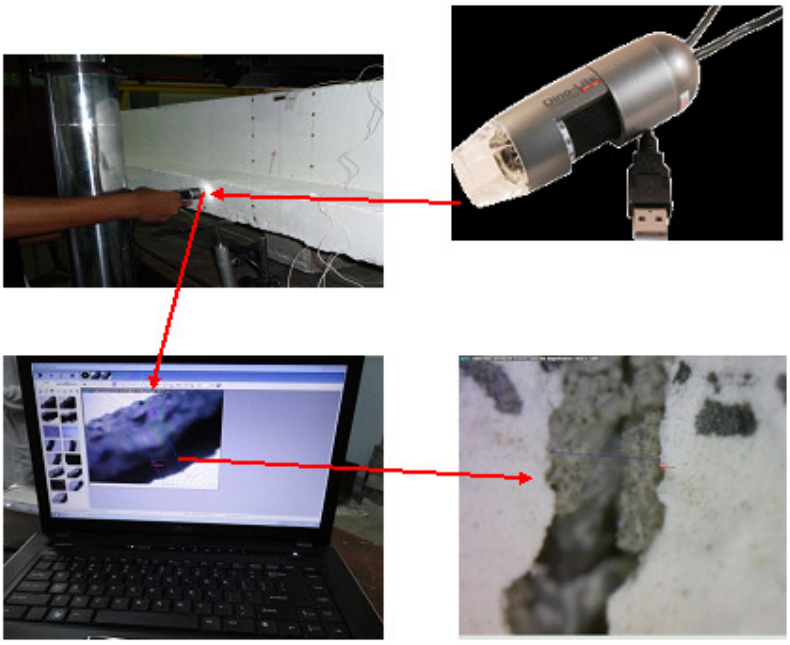

Figure 4.11 Measuring crack width by using Dino-lite

4.7 Test Set Up and Testing Procedure

In actual field situation the flange portion of RC-T beam in the beam column intersection remains in tension. The test setup had been arranged in such a way that the flanges of T beams are in tension to represent the actual field condition. It was done by applying the load on inverted T beam. Three point bending was applied, where the supports represented the points of inflection of a continuous beam where the bending moment is zero. The position of the load as well as the setting of the machine is shown in Figure 4.12. After the beam has been lifted and positioned on the supports, the LVDT was placed and after that all the strain gages as well as the LVDT were connected to data logger properly (Figure 4.12). The load was applied with the help of INSTRON SATEC Testing Machine. This machine can apply up to 600 kN load and this machine can be controlled automatically by computer. The loading rate was controlled by Blue Hill software. The loading rate was controlled by 6 kN /min up to 70 kN for beam B0,

B1, B2 and B3. The same loading rate was applied up to 60 kN for beam B4, B5, B6 and B7. After that deflection control was selected as 2 mm/min. At every 10 kN the loading was hold for 2 minutes so that the manual readings from demec and manual readings of deflection can easily be taken. All other readings were recorded by Data Logger at every 10 second. The cracking width was measured with the help of 'Dino-lite'.

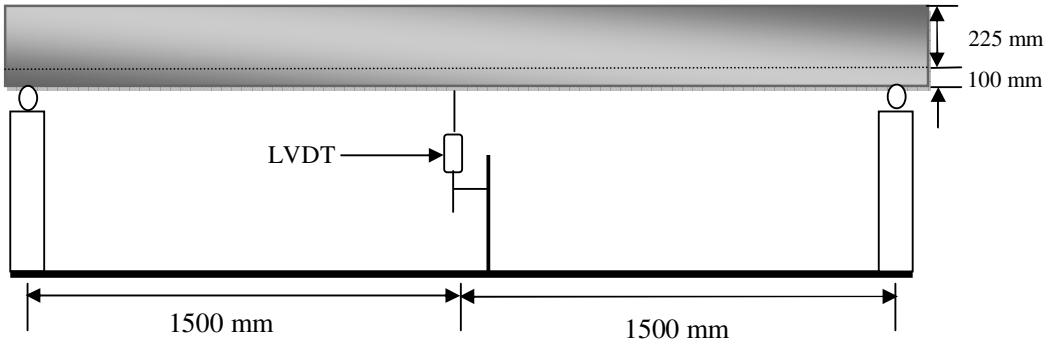

Figure 4.12 Test setup

CHAPTER 5: RESULTS AND DISCUSSIONS

5.1 Introduction

The data obtained from this experiment are discussed into six subsequent sections. The first section (section 5.2) presents the experimental results of all the tested specimens. The second section (section 5.3) describes the effect of different orientations of CFRP laminate for strengthening the tension zone of RC-T beam considering the restraint caused by columns in the application of CFRP laminate. Effects of strengthening both the tension and compression zone of RC-T beams are described in the section 5.4, while the effect of varying CFRP length is described in section 5.5. The data are presented in terms of strength, deformation, failure characteristics and cracking pattern. Finally, (section 5.6) results obtained from finite element analysis (FEM) are compared with experimental results.

5.2 Experimental Results

5.2.1 Failure Load and Failure Mode of all Beams

Summary of the experimental result including failure load, yield load, 1st cracking load is shown in Table 5.1.The strengthened beams showed higher failure load compared to that of control beams. The failure loads of beam B1, B2 and B7 are found very close to each other. The failure modes of all beams are shown in Figures 5.1 to 5.7. Beams B0, B4, and B5 depicted flexural failure, beams B1, B2, B6 and B7 showed end peeling while beam B3 showed debonding failure.

5.2.2 Deflection

The internal bars of control beam yielded at 63 kN. The mid span deflection of all the beams at this load is shown in Table 5.1, where it is seen that the control beam showed

more deflection as compared to the strengthened beams because, the control beam had the lower stiffness than that of strengthened beams.

5.2.3 Strain Distribution

The strain of steel bar and concrete at 63 kN of all the tested beams are shown in Table 5.1. It is seen that the strain of steel bar and concrete of control beam had the highest strain compared to that of strengthened beams.

5.2.4 Cracking

The 1st cracking loads of all the beams are shown in Table 5.1. Strengthened beams showed the higher cracking load than that of control beams. The crack width at 63 kN of all the beams are also shown in Table 5.1 where, more crack width of control beams than that of strengthened beams are observed.

5.3 Performance of Different Orientation of CFRP Laminate

5.3.1 Introduction

In this section, four beams are presented. The cross section and length of CFRP of all the strengthened beams in this section are same but the orientations of CFRP laminates are different. The control beam (B0) is without column stump and is not strengthened. Second beam (B1) is also without column stump and strengthened in the tension zone only (Figure 4.5).The third beam (B2) is with column stump and the orientation of CFRP laminate is shown in Figure 4.6.The fourth beam (B3) is also with column stump but the orientation of CFRP laminate (as shown in Figure 4.7) is different from that of third beam. The performances of these beams are described in the following sections. The beams studied in this section are shown in Table 5.2.

Failure Modes

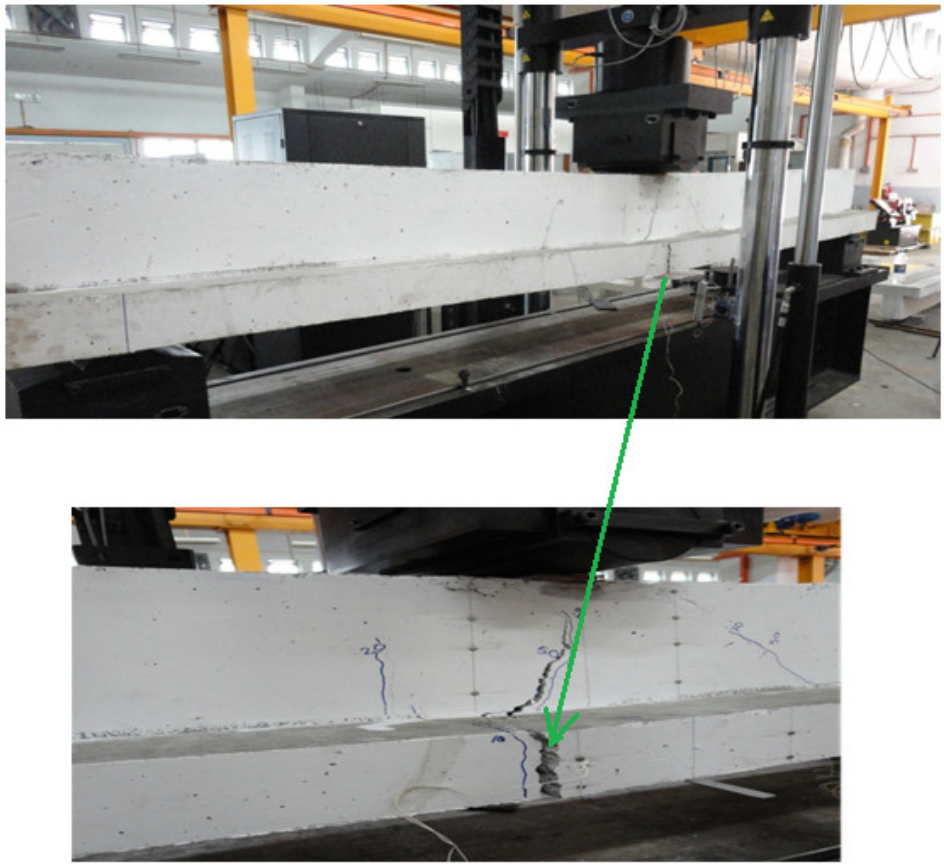

Figure 5.1 Failure mode of beam B0

Figure 5.2 Failure mode of beam B1

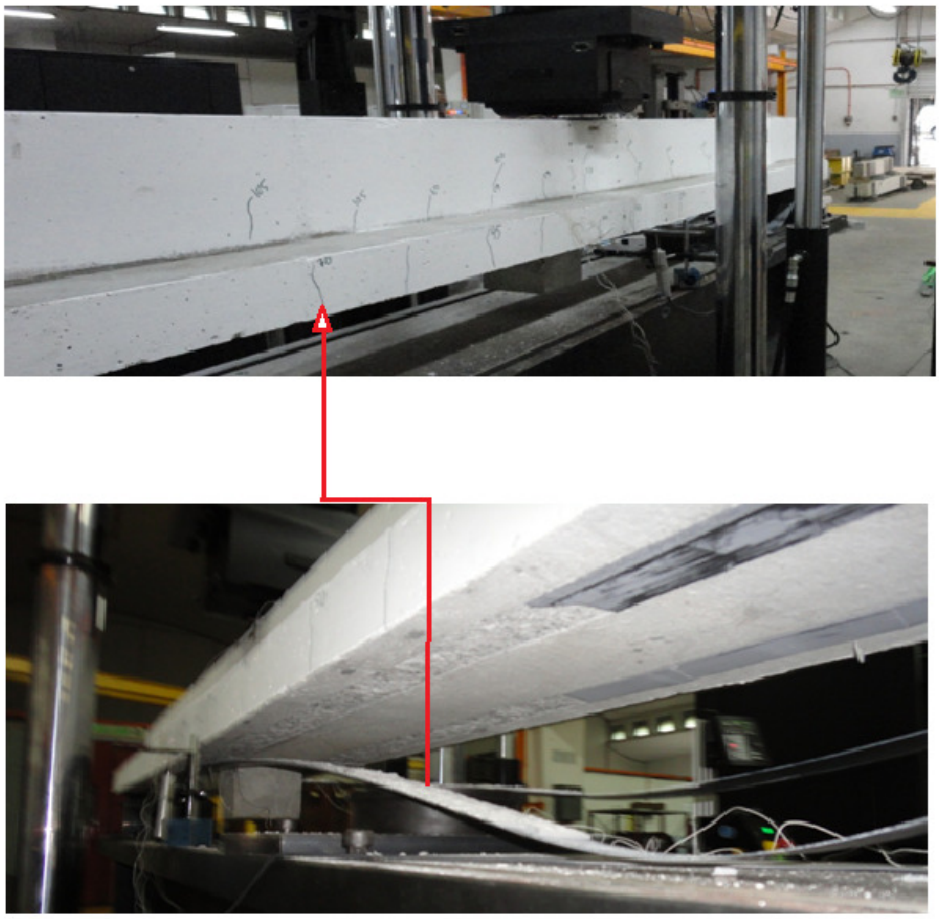

Figure 5.3 Failure mode of beam B2

Figure 5.4 Failure mode of beam B3

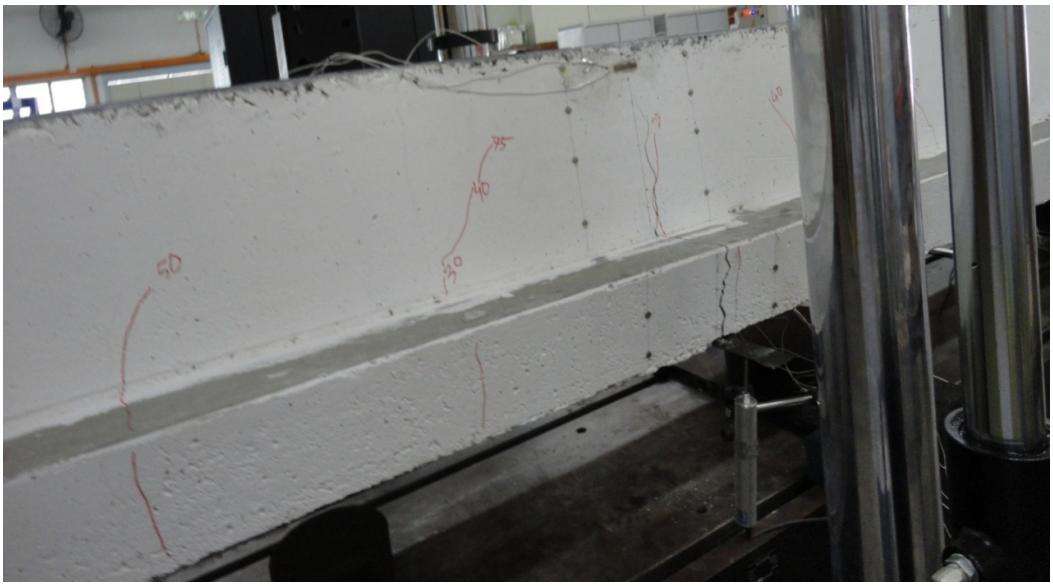

Figure 5.5 Failure mode of beam B4

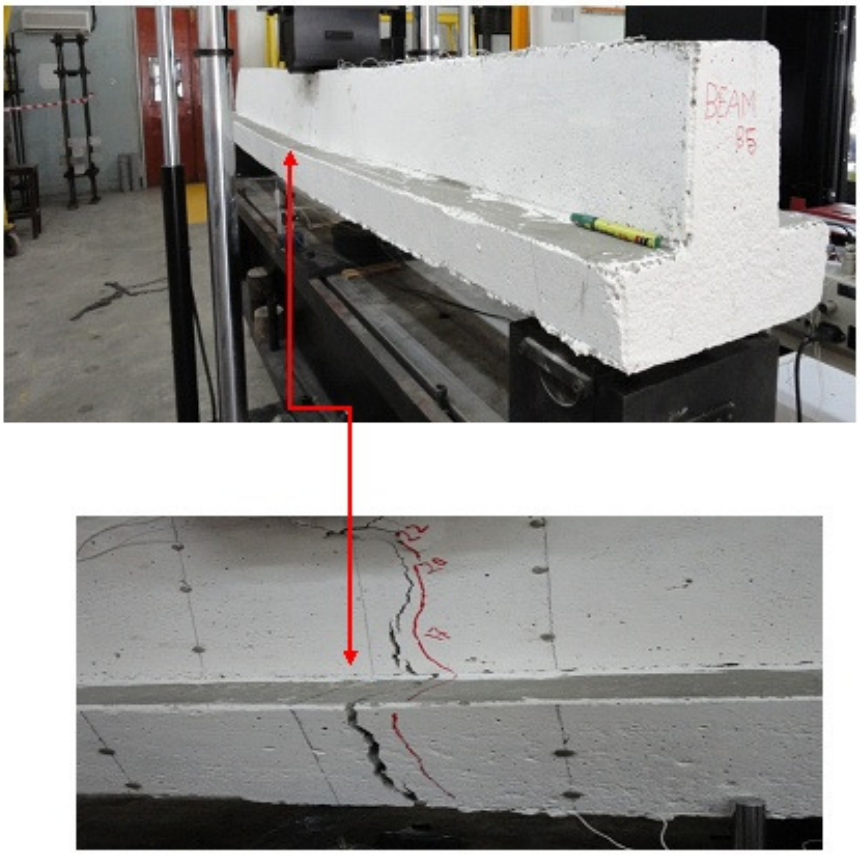

Figure 5.6 Failure mode of beam B5

Figure 5.7 Failure mode of beam B6

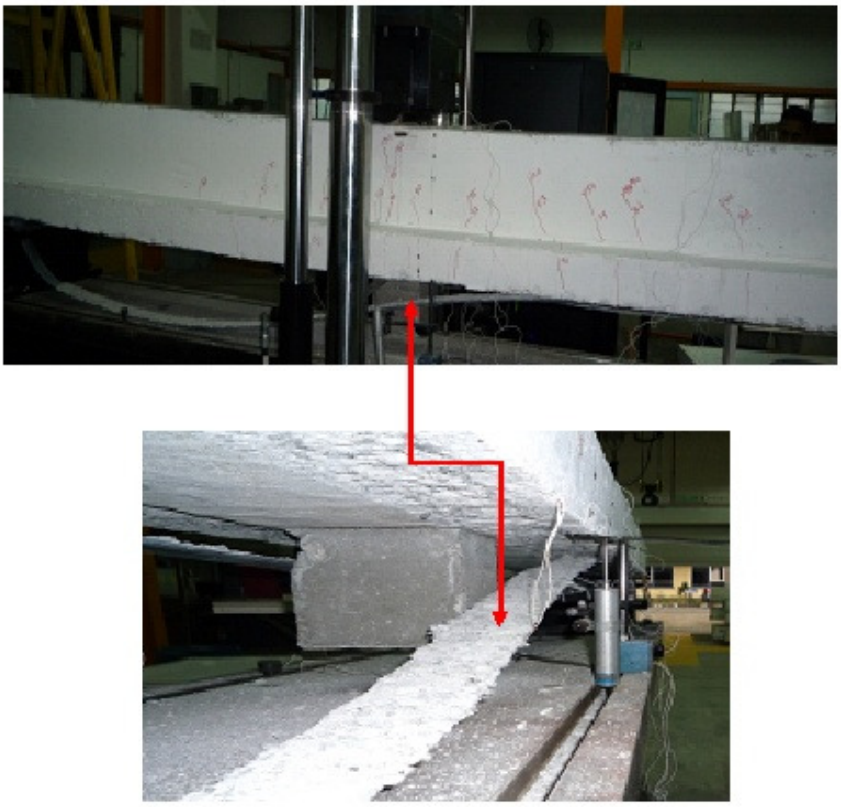

Figure 5.8 Failure mode of beam B7

Table 5.1 Test result

Beam name	1st crack load (kN)	1st crack load increase over control beam (%)	Failure load (kN)	Failure load increase over control beam (%)	Strain (micro) at 63 kN load			Concrete Compressive Strain (με) at failure	Mid-span deflection (mm) at 63 kN load	Crack width(mm) at 63 kN load	Mode of failure
					Steel bar strain (με)	Plate strain (με)	Concrete Compressive Strain (με)				
B0	19	-	76	-	4000	-	1600	2715	12	2.86	Flexure
B1	28	47	124	63	2000	2450	679	2478	9	0.6	End peeling
B2	21	16	116	54	2000	2200	787	2142	9	0.615	End peeling
B3	28	47	90	18	2200	731	940	2100	9	0.889	De bonding
B4	15	-	76	10	2867	-	970	1850	12	-	Flexure
B5	17	-	69	-	3289	-	2452	3389	14	1.305	Flexure
B6	24	41	104	51	1341	2143	933	1300	7	0.7	End peeling
B7	26	53	120	74	1776	2175	624	2056	9	0.21	End peeling

5.3.2 Failure Load

The failure loads of all the beams are presented in Table 5.1. From the table it is seen that, the control beam has the lowest failure load (76 kN) compared to that of strengthened beam. The beam B1 showed the highest failure load (124 kN).The beam B2 had the failure load of 116 kN whereas the beam B3 had the failure load of only 90 kN.The beam B1 showed the highest failure load because in this case the CFRP laminate is placed in the center of the beam (longitudinally) i.e. the eccentricity is zero and the column stump is absent in this case. For the case of beam B2, though the area and length of CFRP laminate is same, there is some eccentricity of CFRP laminate and the restraint caused by the column stump is considered in this case which may led to exhibit a little bit less failure load than that of beam B1. But, still the failure load is high enough compared to control beam and the difference in failure load between B1 and B2 is very small. In the case of beam B3 the failure load is only 90 kN. In this case, the

CFRP are connected to all four sides of the column stump and due to stress concentration at the end of one of the CFRP connection led to the premature failure of the beam. From this discussion it is clear that the CFRP orientation 2 (Figure 4.6) is very effective, efficient and easy, and this orientation has overcome the constraint caused by the column in applying the CFRP laminate.

5.3.3 Failure Mode

The control beam (B0) failed in the traditional flexure mode, because the beam was designed as under reinforced condition (Figure 5.1).The beams B1 and B2 exhibited 'end peeling' while beam B3 exhibited premature failure (Figures 5.2 to 5.4). In the case of B3, due to high stress concentration, the debonding occurred at the end of one of the CFRP connections which led to premature failure without reaching the full capacity. In the case of beam B2 and B3, as there is no end anchors provided, the failure initiated from the end of the strengthening plate and gradually it moved horizontally towards the center of the beam.

Table 5.2 Different orientations of CFRP laminate

Beam name	**Concrete strength (MPa)**	**CFRP laminate**			
		Size (mm)	**Length**	**Applying zone**	**CFRP orientation**
B 0	37	not applicable			
B 1	39	100 × 1.4	3000 mm	Tension zone	Orientation 1
B 2	40	100 × 1.4	3000 mm	Tension zone	Orientation 2
B 3	42	100 × 1.4	All four sides of stump	Tension zone	Orientation 3

5.3.4 Deflection

The load – deflection behavior of the beams B0, B1, B2, B3 are shown in Figure 5.9. Linear increment of deflection was shown by all the beams before failure. The strengthened beams (B1, B2, B3) exhibited lower deflection than that of control beam because of having higher stiffness compared to control beam. It is also seen that the deflection at failure load of control beam is more than that of strengthened beams. The reason is that, the strengthened beams failed by plate debonding with brittle failure mode without any warning, whereas the control beam failed by flexure with ductile failure mode. The same deflection of the beam B1 and B2 at failure load is noticed.

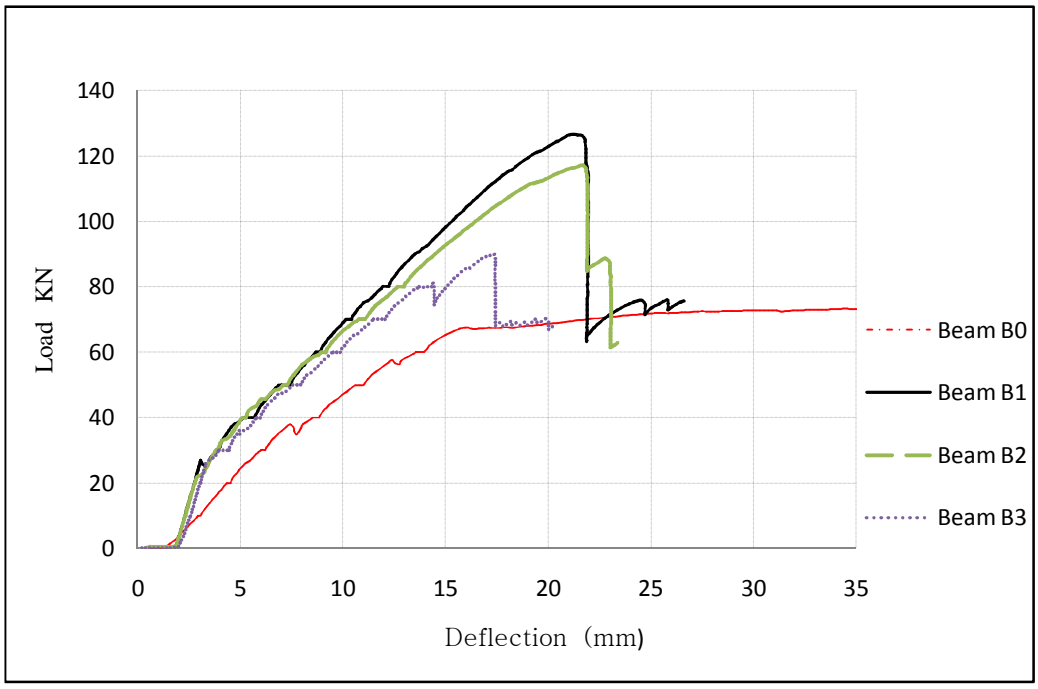

Figure 5.9 Load versus mid span Deflection

5.3.5 Strain Characteristics

5.3.5.1 Bar Strain

The bar strains of the beams B0, B1, B2 and B3 at different loadings are shown in Figure 5.10. It is seen that the bar strain of the control beam is more than that of others.

The strain characteristics of the beam B1 and B2 are identical. From the figure it is noticed that there is a sudden strain increasing rate of beams at 15-25 kN loadings .This is due to the occurrence of 1st crack in the beams. Due to crack, the concrete released stresses to steel. Since it is a sudden release of stress, it acted as an impact stress on the steel bar which led to sudden jump in the strain of the steel bar.

The theoretical yield load of control beam is 70.8 kN but in experiment this load is found 63 kN and the bar strain at this load is 0.004. At the same load (63 kN) the bar strain in beam B1, B2 and B3 are 0.0019, 0.0019 and 0.0023respectively. This variation in bar strain is due to the difference of the stiffness of the beams. The theoretical yield load of strengthened beam is 99 kN. For beams B1, B2, B3 the yield load was found 102,102 and 80 kN respectively and the bar strain at this load is 0.004, 0.004 and 0.004 respectively. It is found that, the theoretical yield load and the experimental yield load of the beam B1 and B2 are identical.

5.3.5.2 Concrete Compressive Strain

Figure 5.11 shows the load versus concrete compressive strain at the top of the beam. It is seen that the strain of the control beam is more than that of strengthened beam. It is noticed that no beam has concrete compressive strain more than 0.0035, which indicate that the beams did not failed by concrete crushing. Pattern of strain changes with loading of the beams B1 and B2 are almost identical.

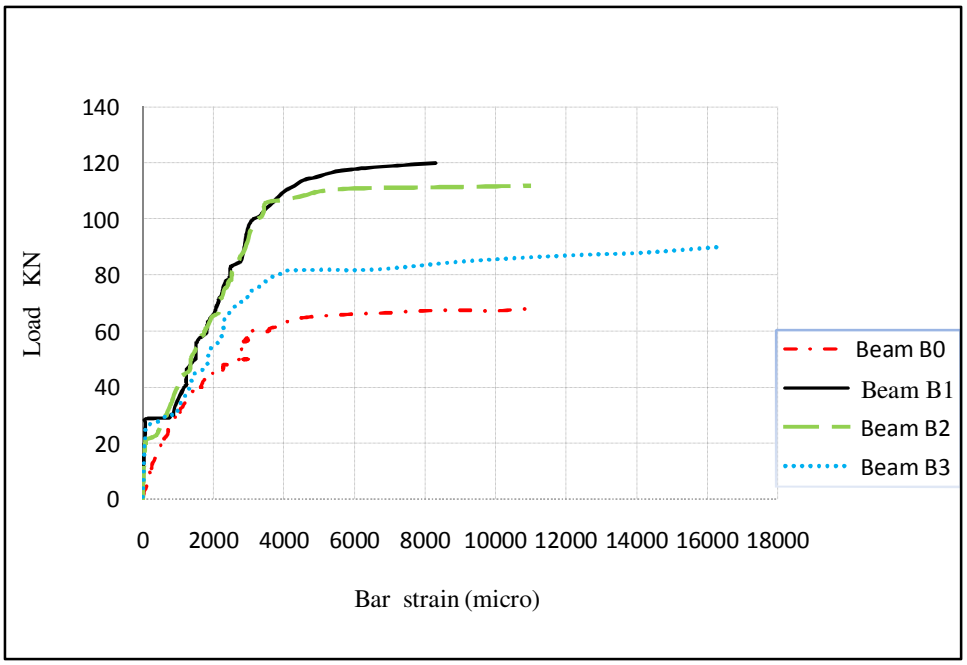

Figure 5.10 Load versus bar strain

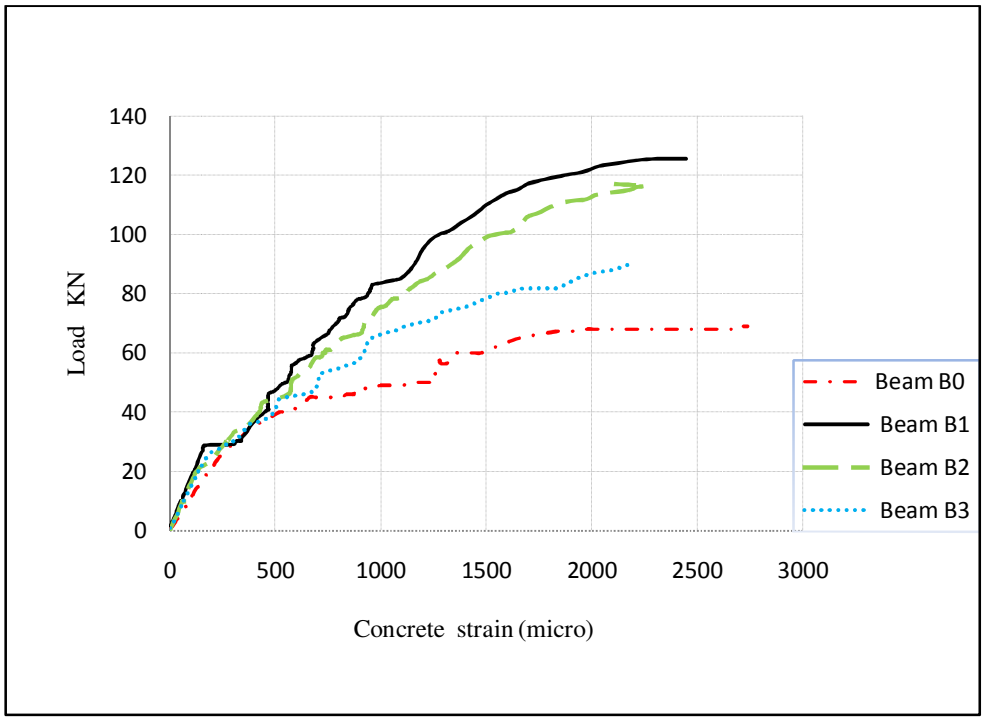

Figure 5.11 Load versus Concrete strain

5.3.5.3 Strain Variation on Beam Depth

The strain variation over the depth of beam up to failure load is shown in Appendix B. The strain was taken from demec points. It is seen that the strain of the beam B0 is higher than that of strengthened beams due to the variation in the stiffness. It is also noticed that, the strain variation characteristics of beam B1 and B2 are almost identical.

5.3.5.4 Strain Characteristics of CFRP Laminate

The CFRP laminate strain of strengthened beams is shown in Figure 5.12. From the figure it is seen that, CFRP laminate don't have definite yield point due to their elastic property. It is also seen that, The CFRP strain of beams B1 and B2 have the same characteristics. Due to premature debonding failure, the strain of CFRP of beam B3 is very less.

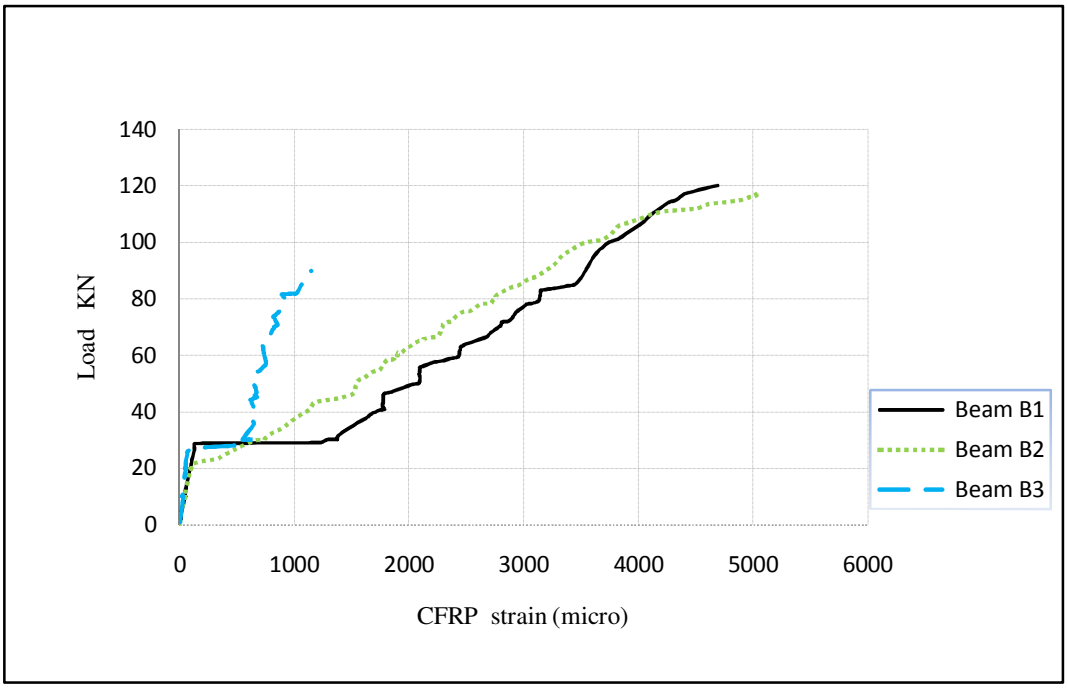

Figure 5.12 Load versus CFRP strain

5.3.5.5 Cracking Pattern

The 1st cracking loads of all the beams are shown in Table5.1.The control beam depicts the lower 1st cracking load than that of strengthened beams. Beams B1, B2 and B3 showed the 1st cracking loads which are very close. It was due to similar material properties of concrete and strengthening laminate. The crack widths at 63 kN load of all the beams are shown in Table 5.1. The strengthened beam had shown the lower crack width than that of control beam.

5.4 Strengthening Both the Tension and Compression Zone

5.4.1 Introduction

Three beams studied in this section are shown in Table 5.3. Beam B5 is a control beam.The second one (B4) is without stump and strengthened in the compression zone only, while the third one (B7) is with stump and this beam is strengthened both in the tension and compression zone. In the case of beam B7, the orientation of CFRP laminate is made the same as in the case of beam B2 i.e. orientation 2 (Figure 4.6).The concrete strength of the beam in this section is relatively lower than that of the beams in the section 5.2.The concrete strength of the beams in section 5.2 is 37 MPa while the concrete strength of the beams in this section is only 26 MPa. The purpose of strengthening the compression zone is to improve the strength of the beams up to the same level of strength as in the beams in section 5.2. All the beams, strengthened in the compression zone, have the same dimension of CFRP laminate (1.4 mm x 100mm) and the length of CFRP laminate for all of these beams are provided up to full span of the beam. The performances of these beams are presented in the following sections.

Table 5.3 Properties of beam and strengthening plate

Beam name	Concrete strength (MPa)	CFRP laminate			
		Size(mm)	Length (mm)	Applying zone	CFRP orientation
B 4	26	100 x1.4	3000	Compression zone	Not applicable
B 5	26	Not applicable			
B 7	26	100 x1.4	3000	Tension + compression zone	Orientation 2

5.4.2 Failure Load

The failure load of control beam (B5) is 69 kN and for beam (B4) and (B7) this load is 76 kN and 120 kN respectively. The failure load of all the beams are described in Table 5.1, in which we can see that all the strengthened beams have higher failure load in comparison to their control beam. The failure load of beam B4 is 76 kN which is similar to the failure load of the control beam (B0) of section 5.2.The beam (B4) is strengthened in the compression zone only. So, it can be ascertained that the beams having lower concrete compressive strength can be improved up to desired strength by strengthening in the compression zone. The failure load of beam (B7) is 120 kN and the failure load of beam (B2) in the section 5.2 is 116 kN. This alteration of failure load between these two beams is very less in extent which indicates that the beams having lower concrete compressive strength and strengthened both in the compression and tension zone behave similarly in terms of failure load as in the case of beams having higher concrete compressive strength and strengthened in the tension zone only.

5.4.3 Failure Mode

The control beam (B5) failed in the traditional flexure mode as the beam was designed as under reinforced condition (Figure 5.6).The failure mode of the beam (B4) is

identical to the failure mode of the control beam (B0) in section 5.2. The failure mode of the beam B7 is also identical to the failure mode of the beam B2 in section 5.2.This similarity in the failure mode also indicate that the beams having lower concrete compressive strength and strengthened both in the compression and tension zone behave similarly in terms of failure mode as in the case of beams having higher concrete compressive strength and strengthened in the tension zone only.

5.4.4 Deflection

The load deflection behavior of the beams B5, B4, B7 is shown in Figure 5.13. A linear increment of deflection is shown by all the beams before failure. The strengthened beams (B4, B7) exhibited lower deflection than that of control beam because of having higher stiffness in compare to control beam. It is also seen that the deflection at failure load of control beam is more than that of strengthened beam. The reason is that, the beams strengthened both in the tension and compression zone, failed by plate debonding in the tension zone with brittle failure mode without any warning ,whereas, the control beam failed by flexure with ductile failure mode. The deflection at failure load of the beam B7 and the beam B2 in section 5.2 is identical. This similarity in the deflection indicates that the beams having lower concrete compressive strength and strengthened both in the compression and tension zone behave similarly in terms of deflection as in the case of beams having higher concrete compressive strength and strengthened in the tension zone only. The same kind of similarity is also shown by the beam B4 and B0.

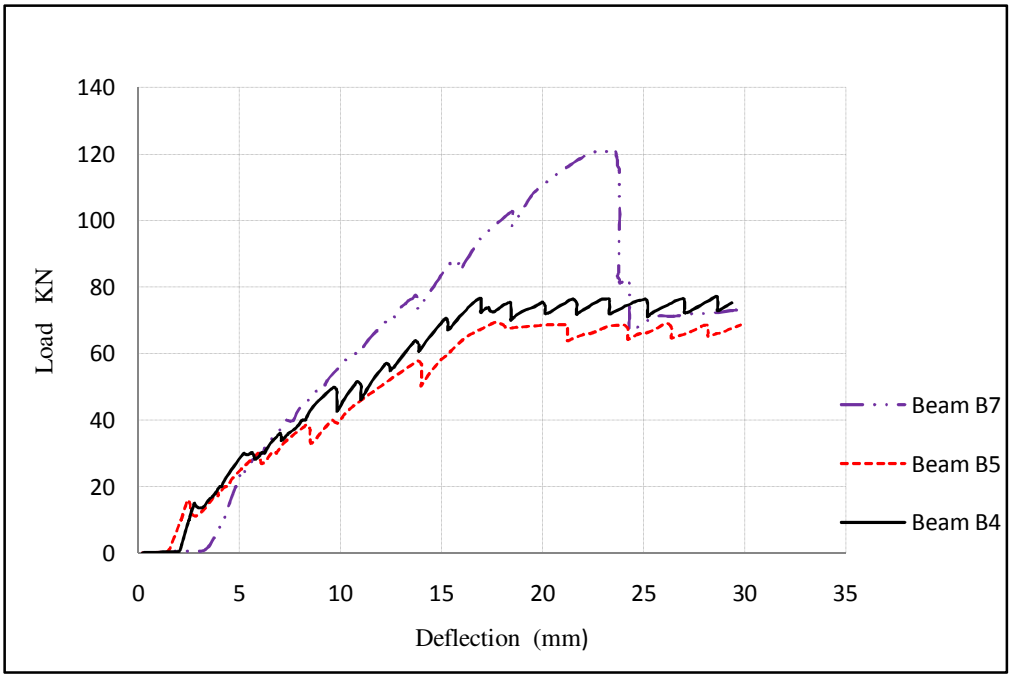

Figure 5.13 Load versus mid span Deflection

5.4.5 Strain Characteristics

5.4.5.1 Bar Strain

The bar strains of the beams B4, B5 and B7 at different loadings are shown in Figure 5.14. It is seen that the bar strain of the control beam is more than that of others. It is noticed that there is a sudden strain increasing rate of beams at 15-25 kN loadings .This is due to the occurrence of 1st crack in the beam. Due to crack, concrete released stresses to steel. Since it is a sudden release of stress, it acted as an impact stress on the steel bar which led to sudden jump in the strain of the steel bar. The similarity in the strain characteristics of the bar between the beams of B4 and B0 is observed. The same kind of similarity is also observed between the beam B7 and B3.

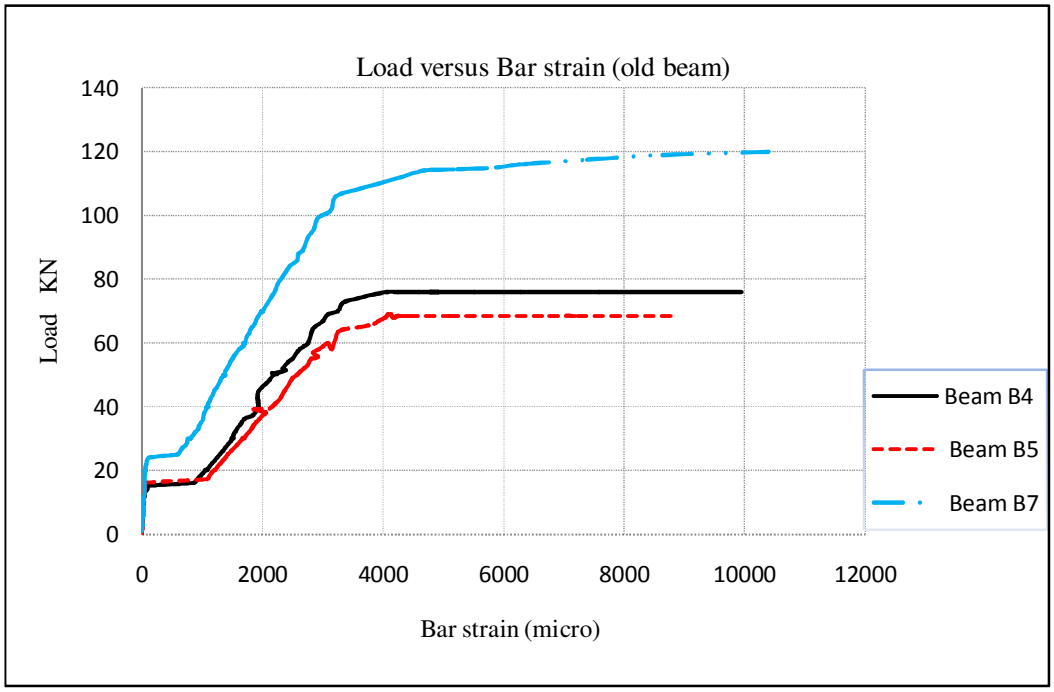

Figure 5.14 Load versus bar strain

5.4.5.2 Concrete Compressive Strain

Figure 5.15 shows the load versus concrete compressive strain at the top of the beam. It is seen that the strain of the control beam is more than that of strengthened beam. It is noticed that no beam has the concrete compressive strain more than 0.0035, which indicate that the beams did not fail by concrete crushing.

5.4.5.3 Strain Variation on Beam Depth

The strain variation over the depth of beam up to failure load is shown in Appendix B. Strain was taken from demec points. It is seen that the strain of the beam B5 is higher than that of strengthened beams due to the variation in the stiffness.

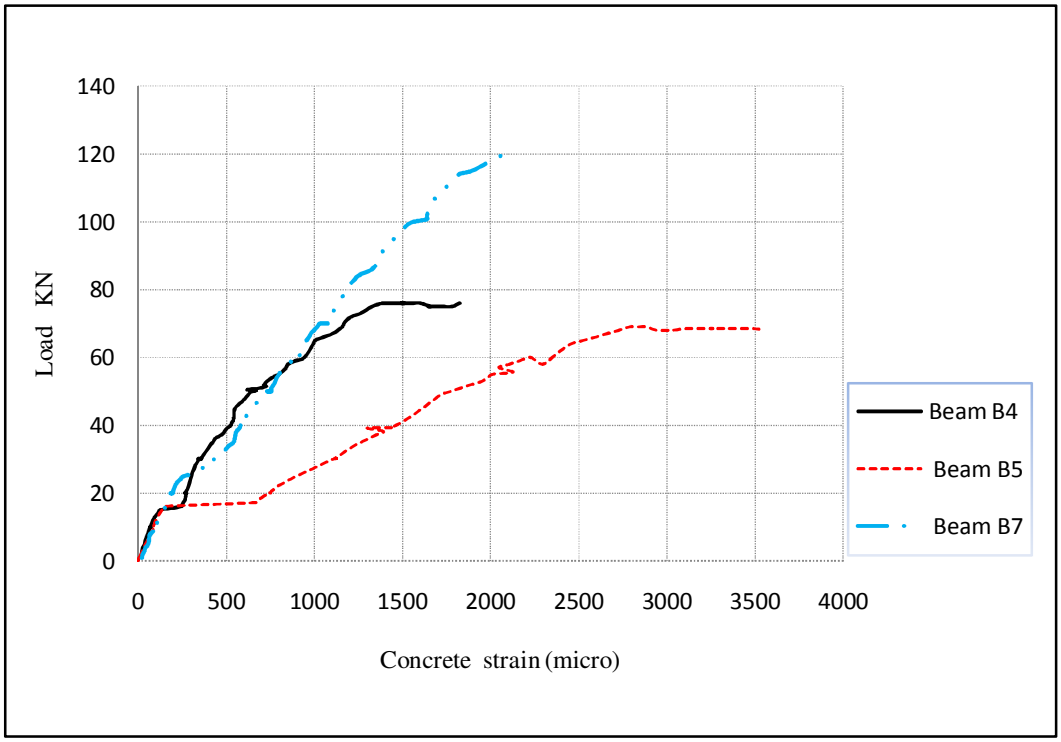

Figure 5.15 Load versus Concrete strain

5.4.5.4 Strain Characteristics of CFRP Laminate

The CFRP laminate strains of all strengthened beams of this section are shown in Figure 5.16 - 5.17. From the figure it is seen that, CFRP laminate did not have definite yield point due to their elastic property. It is also seen that, The CFRP strain of beam B7 and B2 have the same characteristics. The strain in the compression CFRP of the beam B4 is more than that of B7.

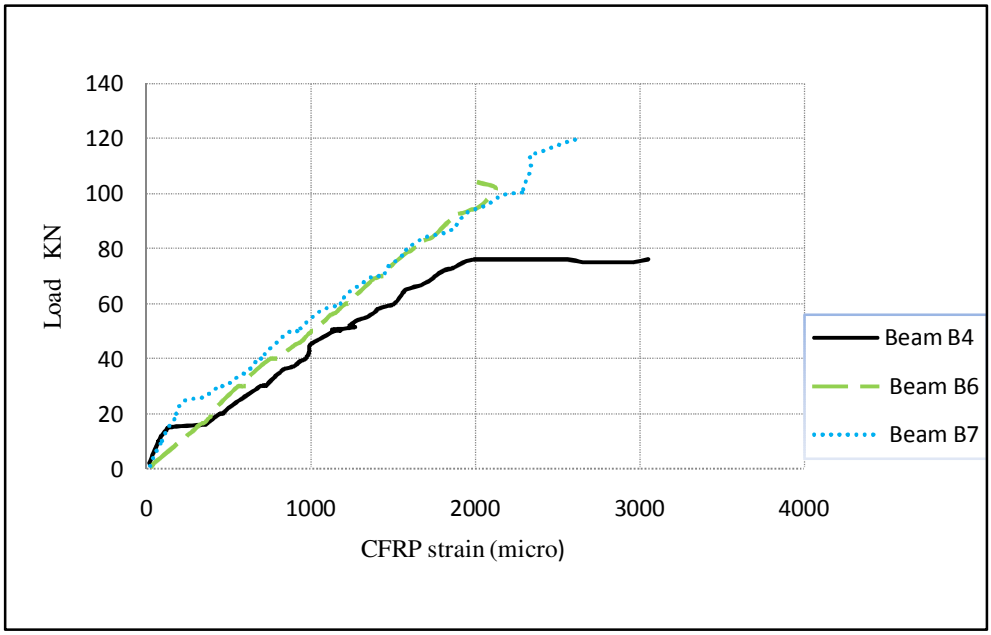

Figure 5.16 Load versus compression CFRP strain

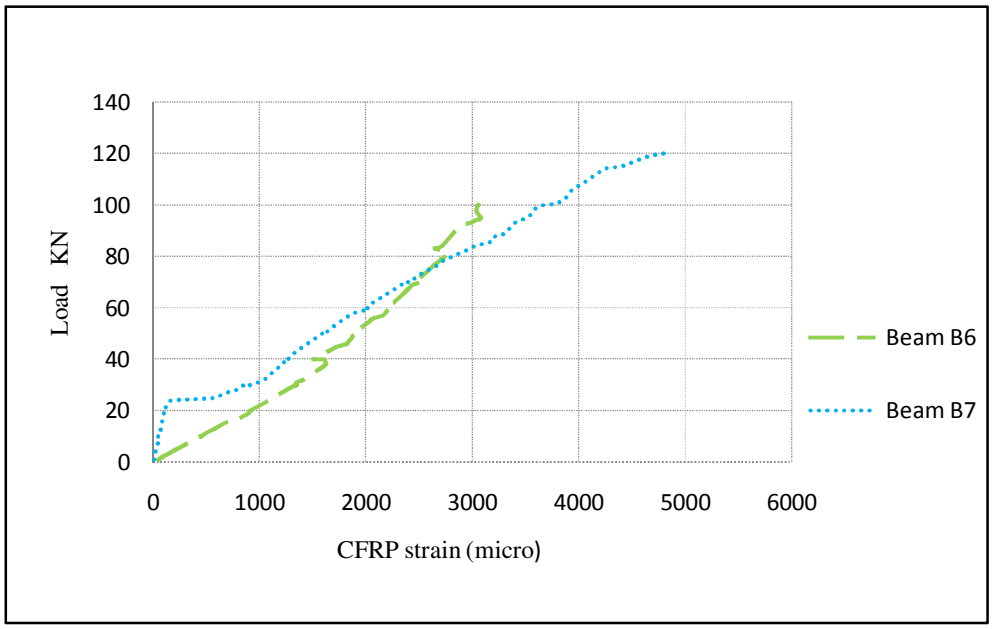

Figure 5.17 Load versus tension CFRP strain

5.5 Effect of CFRP Length in the Tension Zone

5.5.1 Introduction

In this section three beams are presented as shown in Table 5.4. Beam B5 is control and without stump. The other two beams (B6, B7) are with stump and strengthened both in the tension and compression zones with the same orientation of CFRP laminate (orientation2, Figure 4.6) .For the beam B6 and B7, the length of CFRP in the compression zone is provided up to full span while the length of CFRP in the tension zone are varied. According to Technical Report 55, to avoid end peeling, strengthening plate should be extended up to the length where the interfacial shear stress should be ≤0.8 MPa. For the beam B6, the CFRP length is provided up to the length where the shear stress is 0.8MPa.This length is calculated as 2500 mm. Detail calculation is shown in appendix A. On the other hand, the length of CFRP in the tension zone of the beam B7 is provided up to the full span. The performances of these beams are presented in the following sections.

Table 5.4 Properties of beams and CFRP laminates

Beam name	**Concrete strength (MPa)**	**CFRP laminate**			
		Size (mm)	**Length**	**Applying zone**	**CFRP orientation**
B5	26	Not applicable			
B6	26	100×1.4	Compression zone 3000 mm, Tension zone 2500mm	Tension + compression zone	Orientation 2
B7	26	100×1.4	3000 mm	Tension + compression zone	Orientation 2

5.5.2 Failure Mode and Failure Load

The failure load of the beams B5, B6 and B7 are 69 kN, 104 kN and 120 kN respectively. Beam B5 depicted a conventional flexural mode (Figure 5.6) while beam B6 and B7 showed end peeling (Figure 5.7 - 5.8) but the difference in the failure load is remarkable. It is seen that, providing the length of CFRP up to a point where the longitudinal shear stress is 0.8 MPa could not prevent end peeling, even providing the length up to full span of the beam could not prevent end peeling.

5.5.3 Strain Characteristics

5.5.3.1 Bar Strain

The bar strains of the beams B5, B6 and B7 at different loadings are shown in Figure 5.18. It is seen that the bar strain of the control beam is more than that of others. From the figure it is noticed that there is a sudden strain increasing rate of beams at 15-25 kN loadings .This is due to the occurrence of 1st crack in the beam. Due to crack, concrete released stresses to steel. Since it is a sudden release of stress, it acted as an impact stress on the steel bar which led to sudden jump in the strain of the steel bar. It is seen that at failure the bar strain of the beam B7 is more than that of beam B6.

5.5.3.2 Concrete Compressive Strain

Figure 5.19 shows the load versus concrete compressive strain at the top of the beams B5, B6 and B7.It is seen that the strain of the control beam is more than that of strengthened beam. It is noticed that no beam has concrete compressive strain more than 0.0035, which indicates that the beams did not failed by concrete crushing.

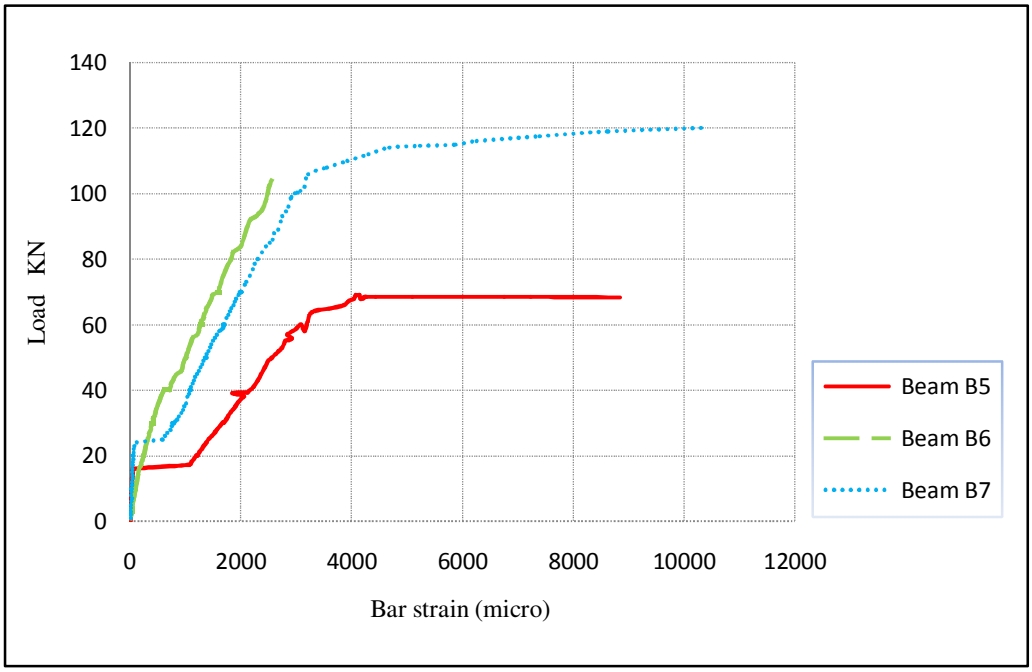

Figure 5.18 Load versus bar strain

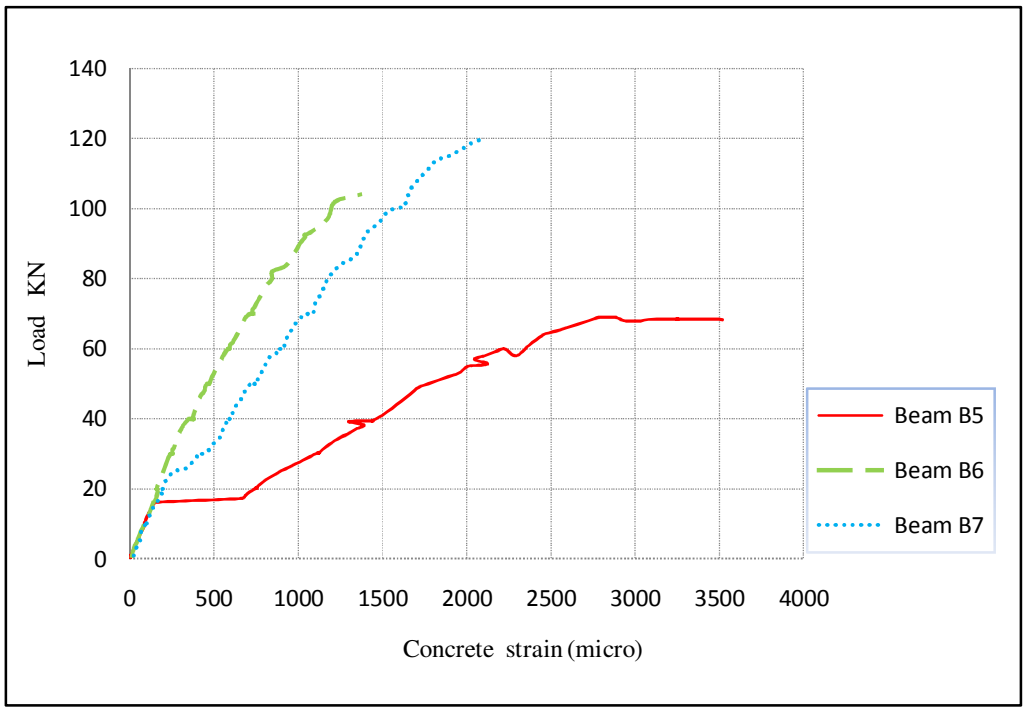

Figure 5.19 Load versus Concrete strain

5.5.3.3 Strain Characteristics of CFRP Laminate

The CFRP laminate strains of beams B6 and B7 are shown in Figure 5.20 - 5.21. From the figures it is found that, CFRP laminate did not have definite yield point and the CFRP strain of beam B7 and B6 have the same characteristics both in tension and compression zone.

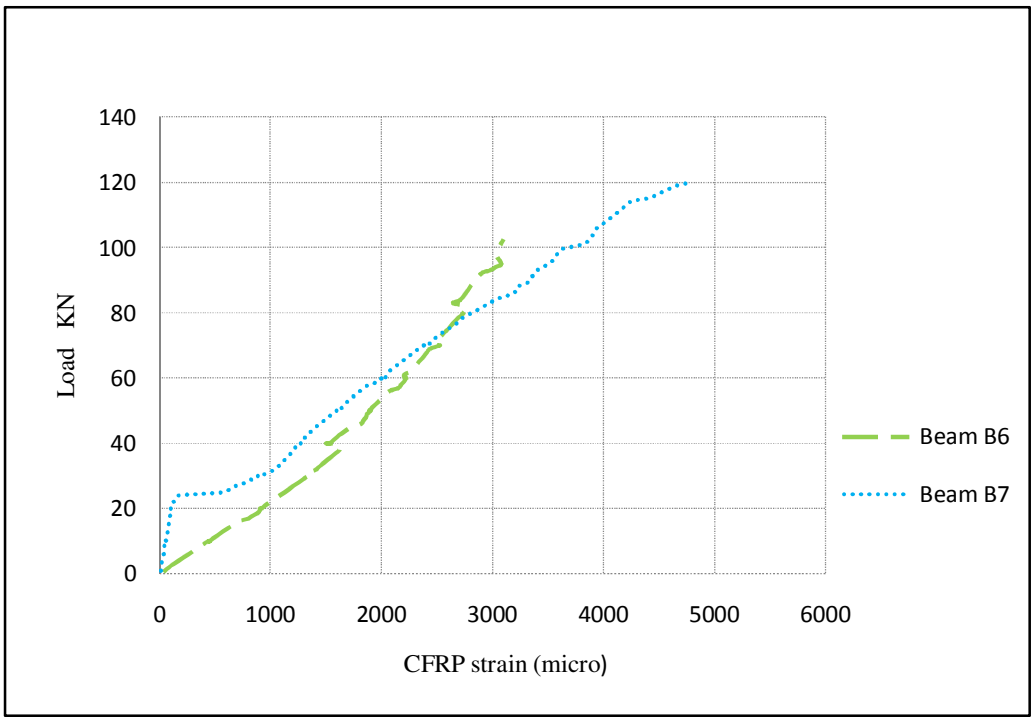

Figure 5.20 Load versus tension CFRP strain

5.5.3.4 Deflection

The load – deflection behavior of the beams B5, B6, B7 are shown in Figure 5.22. A linear increment of deflection is shown by the beam before failure. The strengthened beams (B6, B7) exhibited lower deflection than that of control beam because of having higher stiffness with compared to control beam. It is also seen that the deflection at failure load of control beam is more than that of strengthened beams. The reason is that, the beams strengthened both in the tension and compression zone, failed by plate debonding in the tension zone with brittle failure mode without any warning ,whereas,

the control beam failed by flexure with ductile failure mode. It is also observed that the deflection of the beam B7 is more than that of B6 at failure.

5.6 Results from FEM

The load – deflection behavior of control and strengthened beams are shown in Figure 5.25 and Figure 5.26 respectively. A comparison between FEM result and experimental result of each beam is shown in Table 5.5. From the table we can find that a good agreement exists between the numerical and experimental results in terms of 1st cracking load and failure load. For the case of beam B3, as there are many boundary conditions exists, the FEM result could not be determined. A comparison between FEM and experimental results in terms of Load vs. Deflection is also shown in Figures 5.27-5.28.The same FEM is used to compare the experimental results of the beams tested by EI-Refaie et al. (2003b) and Akbarzadeh and Maghsoudi (2010).The results are shown in Table 5.6. From the results we can say that the finite element models of studied beams can handle all nonlinearities, loading and boundary conditions. The commercial finite element code LUSAS is found to be suitable for the present study. The detail descriptions of the FEM result regarding these beams are presented in Appendix D.

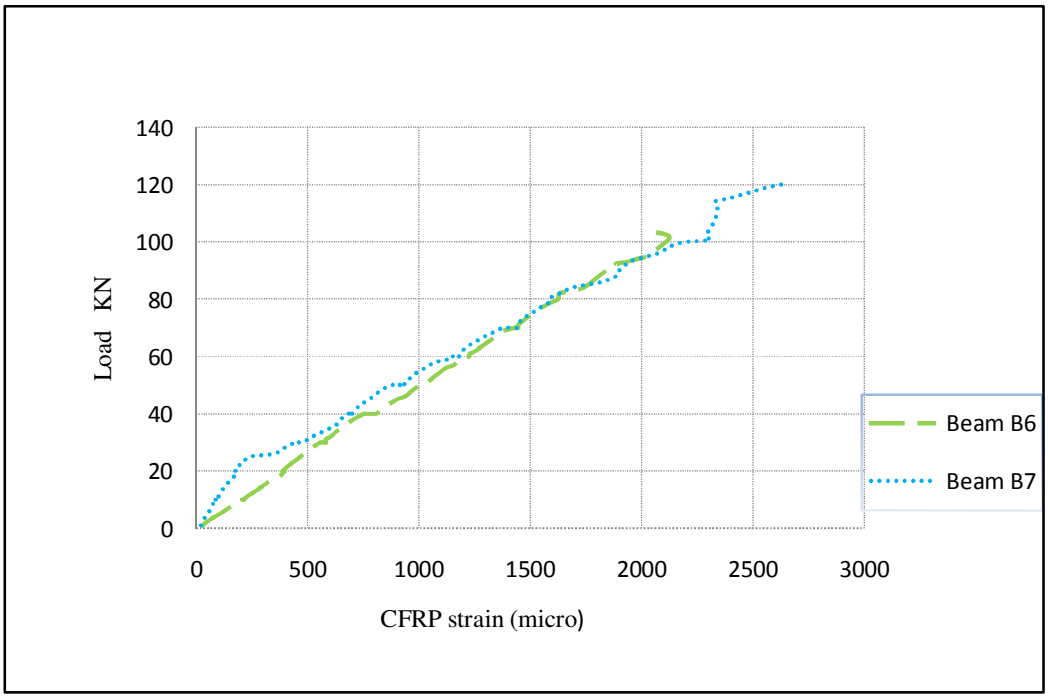

Figure 5.21 Load versus compression CFRP strain

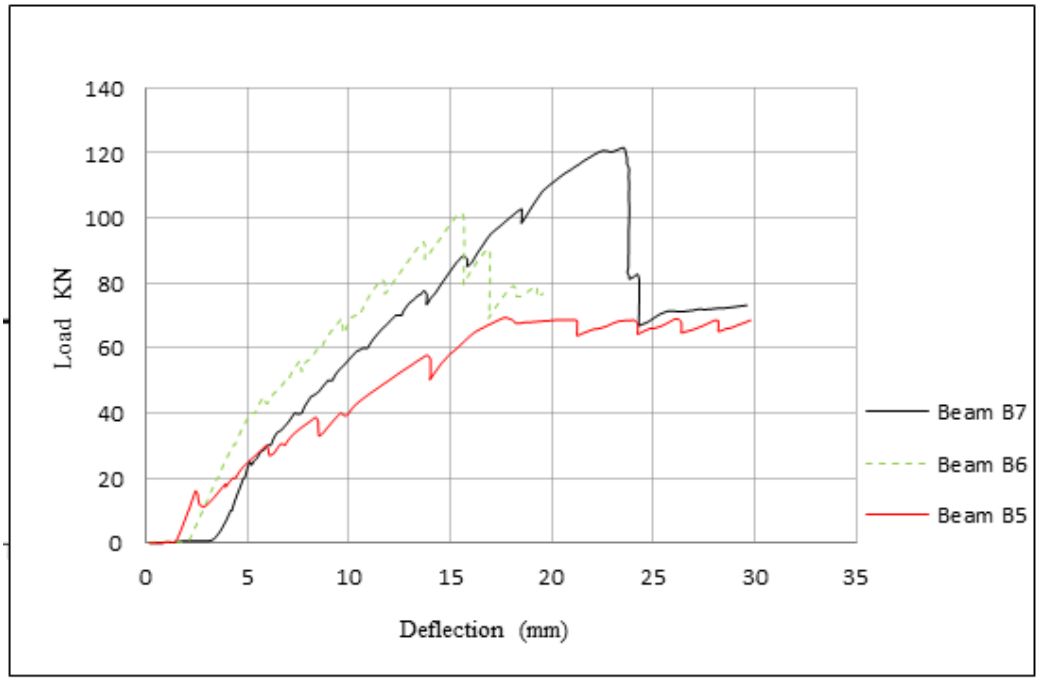

Figure 5.22 Load versus mid span deflection

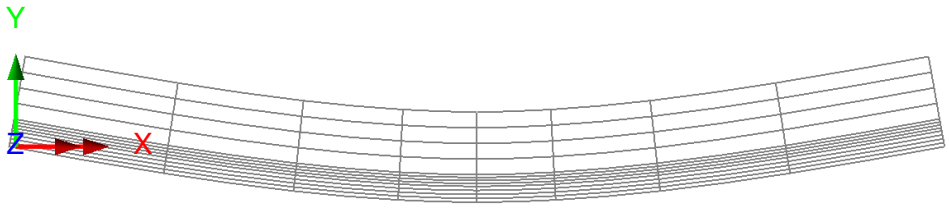

Figure 5.23 Deformed mesh of control beam

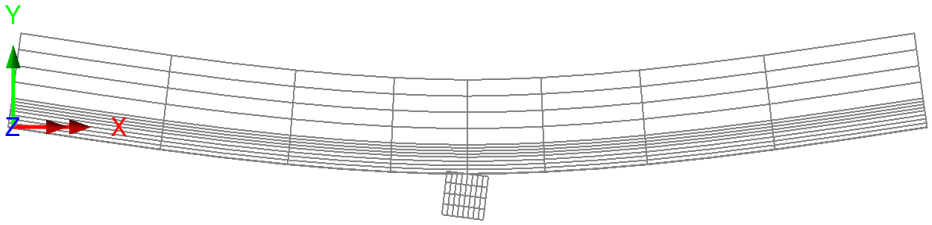

Figure 5.24 Deformed mesh of strengthened beam with stump

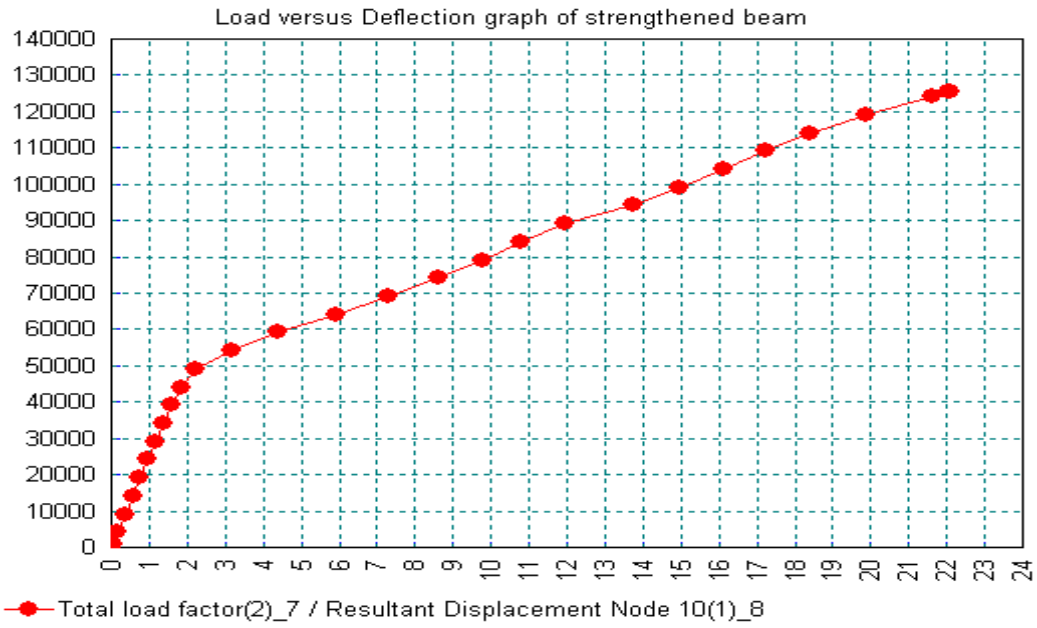

Figure 5.25 Load versus deflection graph of beam B1

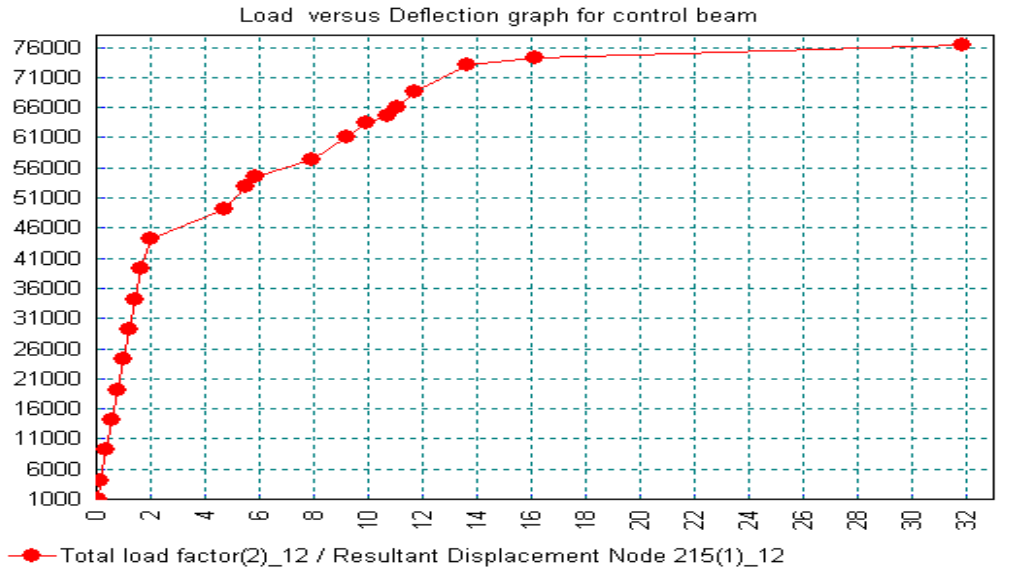

Figure 5.26 Load versus deflection graph of bean B0

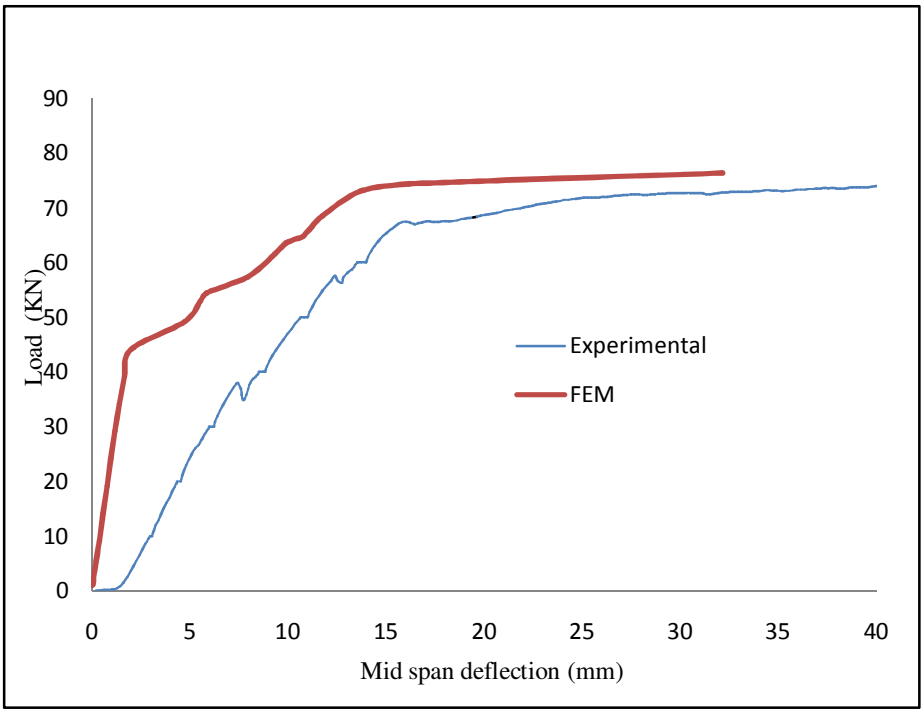

Figure 5.27 Load vs deflection of beam B1

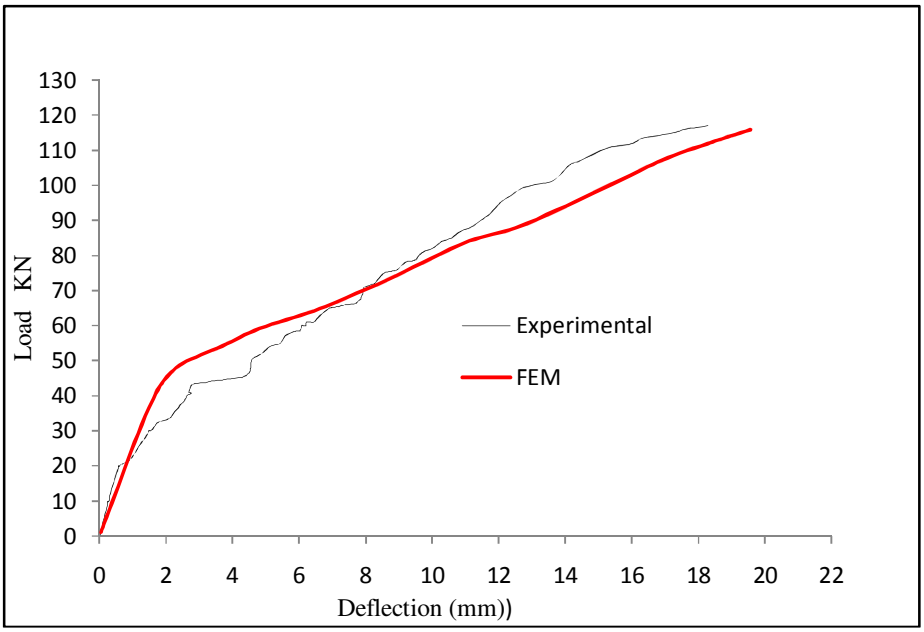

Figure 5.28 Load vs Deflection of Beam B2

Table 5.5 Comparison between Experimental and FEM result

Beam no	Experimental		FEM	
	1st cracking load (kN)	Failure load (kN)	1st cracking load (kN)	Failure load (kN)
B0	19	76	17	77
B1	28	124	24	126
B2	21	116	21	116
B3	28	90	26	-
B4	15	76	12	80
B5	17	69	11	68
B6	24	104	22	110
B7	26	120	21	123

Table 5.6 Comparison between experimental results and FEM results (case study)

Beam no	Ultimate load	
	FEM (kN)	Experimental (kN)
CB	163	162
SC1	185	190.6
SC2	220	219.3
SC3	250	259.3
E1	132	129.67
E2	162	178.67
E3	183	207.06
E4	205	231.42

CHAPTER 6: CONCLUSIONS AND RECOMMENDATIONS

6.1 Conclusions

The following outcomes were concluded from this study:

i. Of the three orientations considered for strengthening of RC T-beams, Orientation 1 showed 38% higher strength and Orientation 2 showed 29% higher strength as compared to Orientation 3. Orientation 1 and Orientation 2 showed similar deflection and strain characteristics for concrete, steel bar & CFRP laminate. In Orientation 2, the restraint offered to the application of CFRP laminate due to the presence of column stump did not affect the strength of the beam significantly. The load carrying capacity was increased by about 50% over un-strengthened beam.

ii. The recommended length for CFRP laminate specified in the Technical Report 55 seemed to be unsuitable for RC T-beams as end peeling was not prevented.

iii. About 70 % load carrying capacity was increased over un-strengthened beam by strengthening both the tension and compression zone. Therefore, CFRP strengthening at both compression and tension zone is able to increase strength significantly.

iv. The un-strengthened beam revealed the conventional flexural failure mode while end peeling of the CFRP laminate was the dominant mode of failure for all the strengthened beams tested.

v. All strengthened beams had shown higher cracking and failure loads, less deflections, smaller crack widths and lower strain characteristics compared to that of un-strengthened control beams.

vi. A good agreement was observed between the numerical and experimental results in terms of bar yield load, ultimate failure load, mid span deflection, bar strain, concrete strain and plate strain of all the beams.

vii. The finite element models for the studied beams seemed to be able to model all nonlinearities, loading and boundary conditions satisfactorily.

6.2 Recommendations

The following recommendations are presented in order to develop and improve current findings:

i. The strengthened beams failed by end peeling. Providing end anchors may prevent this type of failure and can further improve the strength of beam. So, the implementation of end anchors along with designing their appropriate dimensions are strongly recommended for further research for strengthening such kind of beams.

ii. The beams were tested under static loading condition only. More research is needed to determine the effect of repeated loading on strengthened beams.

iii. The experiments were conducted only for flexure. The combined effect of strengthening both for flexure and shear can be of further interest.

iv. Mechanical fastened system, Near Surface Mounted (NSM) method of strengthening of such types of beams may be of particular interest.

REFERENCES

AASHTO (2002), "Standard Specification for Highway Bridges", *American Association of State Highway and Transportation Officials*, 17th ed, Washington, D.C. USA.

ACI 440R- 96 (1996), "State-of-the-art report on fiber reinforced plastic reinforcement for Concrete structures", *American Concrete Institute.*

Adhikary B.B. and Mutsuyoshi H.(2002), "Numerical simulation of steel –plate strengthened concrete beam by a non-linear finite element method model", *Construction and Building Materials*, vol.16, pp.291-301.

Aiello M.A., Valente L. and Rizzo A. (2007),"Moment redistribution in continuous reinforced concrete beams strengthened with carbon-fiber-reinforced polymer laminates" , *Mechanics of Composite Materials*, vol. 43(5), pp. 453–466.

Akbarzadeh, H. and Maghsoudi A.A. (2010), "Experimental and analytical investigation of reinforced high strength concrete continuous beams strengthened with fiber reinforced polymer", *Materials and Design,* vol. 31, pp.1130–1147.

Alam M.A. and Jumaat M.Z. (2008), " Behavior of U and L shaped end anchored steel plate strengthened reinforced concrete beams", *European Journal of Scientific Research*, vol. 22, pp. 184-96.

Anil O. (2008),"Strengthening of RC T-section beams with low strength concrete using CFRP composites subjected to cyclic load", *Construction and Building Materials*, vol. 22(12), pp**.** 2355-2368.

Aram M.R., Czaderski C. And Motavalli M. (2008), "Debonding failure modes of flexural FRP-strengthened RC beams", *Composites Part B: Engineering*, vol. 39, pp. 826-41.

Arduini M. and Nanni A. (1997), "Behaviour of precracked RC beams strengthened with carbon FRP sheets", *Journal of Composites for Construction*, vol.1(2), pp.63–70.

Ashour A.F., El-Refaie S.A. and Garrity S.W. (2004), "Flexural strengthening of RC continuous beams using CFRP laminates", *Cement and Concrete Compostes*,vol.26, pp.765–775.

Bencardino F., Spadea G. and Swamy N.(2002), "Strength and ductility of reinforced concrete beams externally reinforced with carbon fiber fabric", *ACI Structural Journal*, vol. 99(2), pp.163–171.

BS EN 1992-1-1: (2004), "Design of concrete structures. General rules and rules for buildings."

Camata G., Spacone E. and Zarnic R. (2007), "Experimental and nonlinear finite element studies of RC beams strengthened with FRP plates", *Composites: Part B*, vol. 38, pp.277–288.

Ceroni F. (2010), "Experimental performances of RC beams strengthened with FRP materials", *Construction and Building Materials*, vol. 24, pp. 1547-59.

Ceroni F., Pecce M., matthys S. and Taerwe L. (2008), "Debonding strength andanchorage devices for reinforced concrete elements strengthened with FRP sheets", *Composites: Part B*, vol.39, pp.429-441.

Chajes M.J., Thomson T., Finch W. W. and Januszka T. (1994), "Flexural Strengthening of Concrete Beams Using Externally Bonded Composite Materials", *Construction and Building Materials*, Vol. 8, No. 3, pp. 191-201.

Choi H.T. (2008), "Flexural Behaviour of Partially Bonded CFRP Strengthened Concrete T-Beams", PhD thesis, University of Waterloo, Civil and Environmental Engineering, Waterloo, Ontario, Canada.

El-Refaie S.A., Ashour A.F. and Garrity S.W.(2003a), "Sagging and hogging strengthening of continuous reinforced concrete beams using carbon fiber-reinforced polymer sheets", *ACI Structural Journal*, vol.100(4), pp.446–453.

El-Refaie S.A., Ashour A.F. and Garrity S.W. (2003b), "CFRP strengthened continuous concrete beams", *Proceedings of the ICE - Structures and Buildings*, Vol. 156, Issue 4. pp. 395 – 404.

Grace (2001), "Strengthening of Negative Moment Region of RC Beams using CFRP Strips", *ACI Structural Journal*, Vol. 98, No. 3.

Grace N.F., Soliman A.K., Sayed G.A. and Saleh K.R. (1999), "Strengthening of continuous beams using fiber reinforced polymer laminates". *Fourth International Symposium on Fiber Reinforced Polymer Reinforcement for Reinforced Concrete Structures*, American Concrete Institute,SP-188, pp.647-657.

Grace N.F., Wael R. and Abdel-Sayed A. (2005), "Innovative Triaxailly Braided Ductile FRP Fabric for Strengthening Structures", *7th International Symposium on Fiber Reinforce Polymer for Reinforced Concrete Structures (FRPRCS-7)*, American Concrete Institute.

Higgins C., Potisuk T., Robelo M.J., Farrow W.C., McAuliffe T.K. and Nicholas B.S. (2007), "Test of RC Deck Girders with 1950s Vintage Details", *Jurnal of Bridge Engineering*, vol. 12(5) ,pp.621-631.

JSCE (2001), "Recommendations for the upgrading of concrete structures with use of continuous fiber sheets", *Materials and Structures*, Japanese Society of Civil Engineers.

Jumaat M.Z. and Alam M.A. (2010), "Experimental and numerical analysis of end anchored steel plate and CFRP laminate flexurally strengthened r. c. Beams", *International Journal of the Physical Sciences*, vol. 5, pp.132-44.

Jumaat M.Z., Rahman M.M. and Alam M.A. (2010), "Flexural strengthening of RC continuous T beam using CFRP laminate: A review", *International Journal of the Physical Science*s, vol. 5(6), pp 619-625.

Li L., Guo Y. and Liu F. (2008), "Test analysis for FRC beams strengthened with externally bonded FRP sheets", *Construction and Building Materials*, vol. 22, pp. 315–323.

Li L.J., Guo Y.C., Liu F., Bungey J.H. (2006) , "An experimental and numerical study of the effect of thickness and length of CFRP on performance of repaired reinforced concrete beams",*Construction and Building Materials*, vol. 20, pp.901-909.

Maghsoudi A.A. and Bengar H.A. (2008), "Moment redistribution and ductility of RHSC continuous beams strengthened with CFRP", *Turkish Journal of Engineering and Environmental Science*, vol. 33 pp. 45-59.

Nanni A. (1995), "Concrete Repair with Externally Bonded FRP Reinforcement", *Concrete International*, vol. 17(6) , pp. 22-26.

Paramasivam p., Lim C.T.E. and Ong K.C.G. (1998), "Strengthening of RC beams with ferrocement laminates", *Cement and Concrete Composites*, vol.20, pp.53-65.

Pham H. and Al-Mahaidi R. (2006), "Prediction models for debonding failure loads of carbon fiber reinforced polymer retrofitted reinforced concrete beams*", Journal of Composites for Construction*, vol. 10(1), pp. 48–59.

Pham H. and Al-Mahaidi R. (2004), "Assessment of Available Prediction Models for the Strength of FRP Retrofitted RC Beams", *Composite Structures*, vol. 66, pp.601-610.

Polies W**.**, Ghrib F**.** and Khaled S. (2010), "Rehabilitation of interior reinforced concrete slab-column connections using CFRP sheets", *Construction and Building Materials*, vol. 24(7), pp. 1272-1285.

Romualdi, J.P. (1987), Ferrocement for infrastructure rehabilitation, *Concrete International: design and construction*, vol.9, no.9, pp.24-28.

Saadathmanesh H. and Ehsani M.R. (1991), "R.C. Beams Strengthened with FRP Plates I: Experimental Study", *Journal of Structural Engineering*, vol.117, No. 11, pp. 3417-3433.

Smith S.T. and Kim S.J. (2009)**,** "Strengthening of one-way spanning RC slabs with cutouts using FRP composites*", Construction and Building Materials*, vol. 23(4), pp. 1578-1590.

Smith S.T. and Teng J.G. (2001), "Interfacial stresses in plated beams", *Engineering Structures*, vol.23, pp.857-871.

Technical Society Report No. 55 (2000), "Design guidance for strengthening concrete structures using fibre composite materials", *Concrete Society*.

Teng J.G., Chen J.F., Smith S.T. and Lam L. (2002), "FRP strengthened RC structures", Wiley, NewYork.

Teng J.G., Smith T.S. ,Yao J. and Chen J.F. (2003), "Intermediate crack-induced debonding in RC beams and slabs". *Construction and Building Materials*, vol.17, pp. 447-62.

Toutanji H., Zhao L. and Zhang Y. (2006), "Flexural behavior of reinforced concrete beams externally strengthened with CFRP sheets bonded with an inorganic matrix", *Engineering Structure*, vol.28,pp. 557–566.

Wang Y.C. and Hsu K. (2009), "Design recommendations for the strengthening of reinforced concrete beams with externally bonded composite plates", *Composite Structures*, vol.88, pp. 323-32.

Xiong G.J., Jiang X., Liu J.W. and Chen L. (2007), "A Way for Preventing Tension Delamination of Concrete Cover in Midspan of FRP Strengthened Beams", *Construction and Building Materials*, vol. 21, pp. 402-408.

APPENDIX A

A.1 Data Required for Design of Beam

The strengthened beams are designed in accordance with simplified stress block methods of BS EN 1992-1-1:(2004).The design procedures are described below:

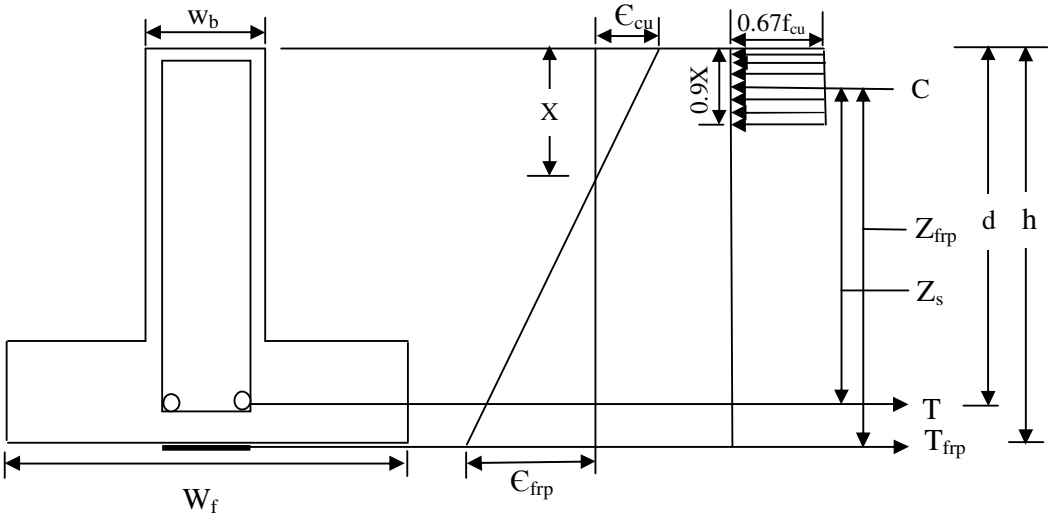

Figure A.1 Stress block diagram of strengthened beam

Strain of CFRP laminate = ϵ_{frp}

Depth of the beam, h = 325 mm

Effective depth of the beam, d = 268 mm

Width of the web, w_b = 150 mm

Width of the flange, w_f = 380 mm

Span length = 3000 mm

Moment arm of the steel bar, Z_s= (d - 0.9x/2)

Moment arm of the CFRP laminate, Z_{frp}= (h - 0.9x/2)

Cross sectional area of steel bar, A_s= 401.92 mm^2

Cross sectional area of CFRP plate = A_{frp}

Yield strength of steel bar, f_y= 560 MPa

Modulus of elasticity of CFRP laminate, E_{frp}=165 GPa

Tensile strength of steel bar, f_t = 645 MPa

A.2 Design of CFRP Laminate Strengthened Beam

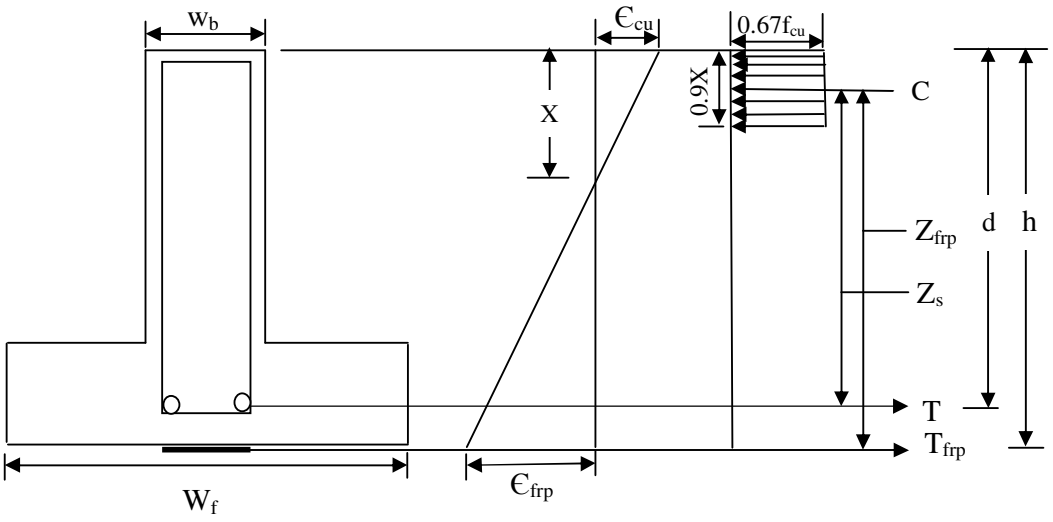

Figure A.2 Stress block diagram of strengthened beam

A.2.1 Depth of Neutral Axis

In accordance with BS EN 1992-1-1 :(2004), the design strain of concrete is 0 .0035

According to Technical Report 55 (TR 55), the FRP strain should be less than 0.006 to avoid debonding failure.

From the Figure A. 2,

$$\frac{0.0035}{0.006} = \frac{x}{h - x} \quad \text{----------} \quad (A.1)$$

$$x = 0.368 \times h$$

$$x = 0.368 \times 325 = 119.6 mm$$

A.2.2 Required Area of CFRP Laminate

$$C = 0.67 \times f_{cu} \times 0.9x \times b_w \quad \text{----------} \quad (A.2)$$

$$C = 0.603 \times f_{cu} \times x \times b_w \quad ----------(A.3)$$

$$T_s + T_{frp} = C \quad ----------(A.4)$$

$$T_{frp} = C - T_s \quad ----------(A.5)$$

$$T_s = A_s \times f_y \quad ----------(A.6)$$

$$\therefore T_{frp} = (0.603 \times f_{cu} \times x \times b_w) - (A_s \times f_y) \quad ----------(A.7)$$

$$E_{frp} = \frac{\sigma_{frp}}{\in_{frp}} \quad ----------(A.8)$$

$$\sigma_{frp} = E_{frp} \times \in_{frp} \quad ----------(A.9)$$

$$A_{frp} = \frac{T_{frp}}{\sigma_{frp}} = \frac{(0.603 \times f_{cu} \times x \times b_w) - (A_s \times f_y)}{E_{frp} \times \in_{frp}} \quad ----------(A.10)$$

$$A_{frp} = \frac{(0.603 \times f_{cu} \times x \times b_w) - (A_s \times f_y)}{E_{frp} \times \in_{frp}} \quad ----------(A.12)$$

$$A_{frp} = \frac{(0.603 \times 35 \times 119.6 \times 150) - 401.92 \times 560}{165000 \times 0.006} = 155.09 mm^2$$

As 140 mm^2 (100 mm x 1.4 mm) is the maximum size available in the market, we can use (100 mm x 1.4 mm) size CFRP laminate.

A.3 Calculation of Bar Yield Load of Control Beam

The theoretical bar yield load of the control beam is calculated as followings:

From the Figure A. 3,

$$T_s = C = 0.67 f_{cu} (0.9xb) = A_s f_y \quad ----------(A.13)$$

Depth of neutral axis,

$$x = \frac{A_s f_y}{0.603 f_{cu} b} \quad ----------(A.14)$$

$$= \frac{401.92 \times 560}{0.603 \times 35 \times 150} = 71.09 mm$$

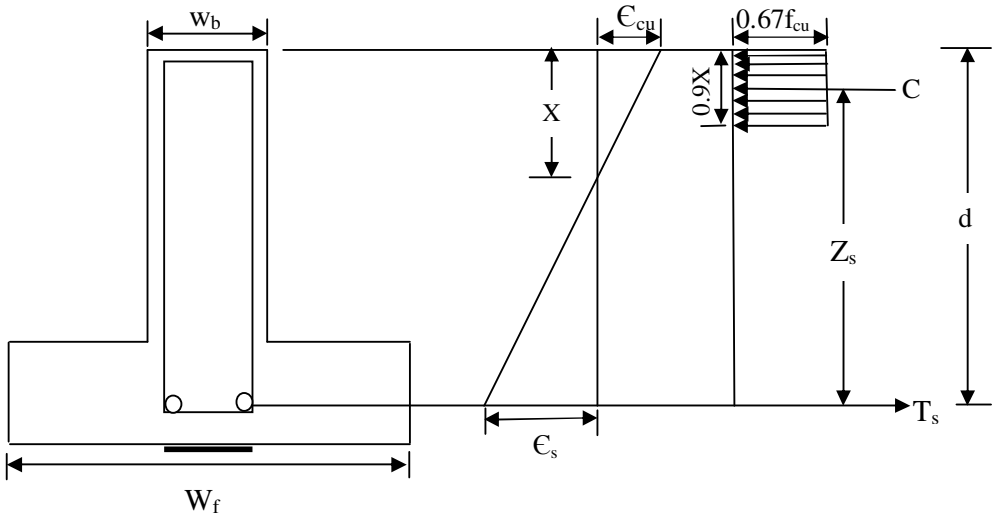

Figure A.3 Stress block diagram of control beam

$$M_{cy} = T_s(d - 0.45x) = A_s f_y (d - 0.45x) \text{ ---------- } (A.15)$$

Bar yield load of control beam,

$$p_{yield} = \frac{2M_{cy}}{1.5} = \frac{2A_s f_y (d - 0.45x)}{1.5} \text{ ---------- } (A.16)$$

$$p_{yield} = \frac{2 \times 401.92 \times 560(268 - 0.45 \times 71.09)}{1.5 \times 1000} = 70.8KN$$

A.4 Flexural Failure Load of Control Beam

From the Figure A.3

$$T_s = C = 0.67 f_{cu}(0.9xb) = A_s f_t \text{ ---------- } (A.17)$$

$$x = \frac{A_s f_t}{0.603 f_{cu} b} \text{ ---------- } (A.18)$$

$$= \frac{401.92 \times 645}{0.603 \times 35 \times 150} = 81.88mm$$

$$M_{ct} = T_s(d - 0.45x) = A_s f_t (d - 0.45x) \text{ ---------- } (A.19)$$

$$p_{failure} = \frac{2M_{ct}}{1.5} = \frac{2A_s f_t (d - 0.45x)}{1.5} \text{ ---------- } (A.20)$$

$$p_{failure} = \frac{2 \times 401.92 \times 645(268 - 0.45 \times 81.88)}{1.5 \times 1000} = 79.80\,KN$$

A.5 Bar Yield Load of Strengthened Beam

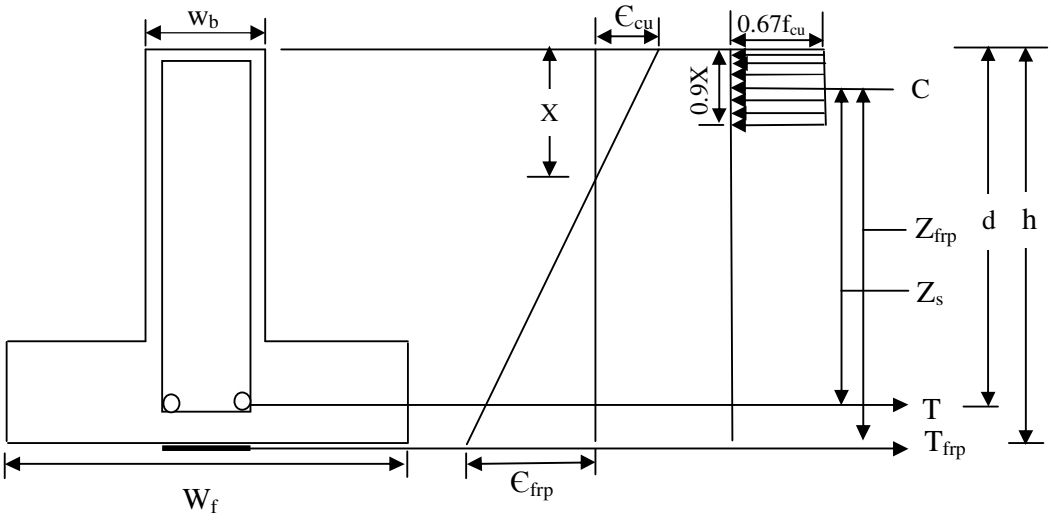

Figure A.4 Stress block diagram of strengthened beam

Bar yield strain , $\varepsilon_s = \frac{Yield stress}{Modulus of Elasticity} = \frac{f_y}{E_s}$

The CFRP laminate strain of strengthened beam at bar yield can be obtained by trial and error.

Assume, x= 0.5d = 0.5 × 268 =134 mm

From the Figure A.4,

$$\in_{frp} = \frac{\in_s (h-x)}{d-x} = \frac{\in_s (h-.5d)}{d-.5d} = \frac{f_y (h-.5d)}{.5dE_s} \quad \text{----------(A.21)}$$

$$T = T_{frp} + T_s = \frac{f_y (h-.5d) E_{frp} A_{frp}}{.5dE_s} + A_s f_y \quad \text{----------(A.22)}$$

$$\sigma_{frp} = \in_{frp} E_{frp} = \frac{f_y (h-.5d) E_{frp}}{.5dE_s} \quad \text{----------(A.23)}$$

$$T_{frp} = \sigma_{frp} A_{frp} = \frac{f_y (h - .5d) E_{frp} A_{frp}}{.5 d E_s} \text{ ----------(A.24)}$$

$$C = 0.603 f_{cu} b x = T = \frac{f_y (h - .5d) E_{frp} A_{frp}}{.5 d E_s} + A_s f_y \text{ ----------(A.25)}$$

$$x = \frac{1}{0.603 f_{cu} b} [\frac{f_y (h - .5d) E_{frp} A_{frp}}{.5 d E_s} + A_s f_y] \text{ ----------(A.26)}$$

$$= \frac{1}{0.603 \times 35 \times 150} [\frac{560 \times (325 - 134) \times 165000 \times 140}{134 \times 200000} + 401.92 \times 560]$$

= 100.21 mm

Moment at yield of internal bar

$$M_{yc} = T_s Z_s + T_{frp} Z_{frp} \text{ ----------(A.27)}$$

$$= A_s f_y (d - 0.45x) + \frac{f_y (h - x) E_{frp} A_{frp}}{E_s (d - x)} (h - 0.45x) \text{ ----------(A.28)}$$

$$= \frac{2}{1.5} [401.92 \times 560 \times (268 - 0.45 \times 100) + \frac{560 \times (325 - 100) \times 165 \times 140}{200 \times (268 - 100)} (325 - 0.45 \times 100)$$

= 99.26 kN

A.6 Failure Load of Strengthened Beam

$$\in_{frp} = \frac{0.0035(h - x)}{x} \text{ ----------(A.29)}$$

$$\sigma_{frp} = \in_{frp} E_{frp} = \frac{0.0035(h - x)}{x} E_{frp} \text{ ----------(A.30)}$$

$$T_s = A_s f_t \text{ ----------(A.31)}$$

$$T_{frp} = \sigma_{frp} A_{frp} \text{ ----------(A.32)}$$

$$T = T_{frp} + T_s = \sigma_{frp} A_{frp} + A_s f_t \text{ ----------(A.33)}$$

$$C = 0.603 f_{cu} b x = T = \sigma_{frp} A_{frp} + A_s f_t \text{ ----------(A.34)}$$

$$0.603 f_{cu} bx = A_s f_t + \frac{0.0035(h-x)}{x} E_{frp} A_{frp} \text{ ---------- } (A.35)$$

$$(0.603 f_{cu} b)x^2 - (A_s f_t)x = 0.0035(h-x)E_{frp} A_{frp} \text{ ---------- } (A.36)$$

$$(0.603 f_{cu} b)x^2 - (A_s f_t - 0.0035 A_{frp} E_{frp})x - 0.0035 A_p E_{frp} h = 0 \text{ ---------- } (A.37)$$

$$x = \frac{-m \pm \sqrt{m^2 - 4nl}}{2l} \text{ ---------- } (A.38)$$

$$l = 0.603 f_{cu} b = 0.603 \times 35 \times 150 = 3165.75$$

$$m = -(A_s f_t - 0.0035 A_{frp} E_{frp}) = -(401.92 \times 645 - 0.0035 \times 140 \times 165000) = -178388.4$$

$$n = -0.0035 A_p E_{frp} h = -0.0035 \times 140 \times 165000 \times 325 = -26276250$$

$$x = \frac{1783884 \pm \sqrt{(-1783884)^2 - 4 \times (-26276250) \times 3165.75}}{2 \times 3165.75}$$

X = 123.53

And,

$$M_{tc} = T_s Z_s + T_p Z_{frp} = A_s f_t (d - 0.45x) + A_{frp} \sigma_{frp} (h - 0.45x) \text{ ---------- } (A.39)$$

CFRP laminate strain,

$$\in_{frp} = \frac{0.0035(h-x)}{x} = \frac{0.0035 \times (325 - 123.53)}{123.53} = 0.0057 \text{ ---------- } (A.40)$$

$$p_{ut} = \frac{2M_{tc}}{1.5} = \frac{2}{1.5}[A_s f_t (d - 0.45x) + A_{frp} \sigma_{frp} (h - 0.45x)] \text{ ---------- } (A.41)$$

Putting the value of x,

$$= \frac{2}{1.5 \times 1000}[401.92 \times 645(268 - 0.45 \times 123.53) + 140 \times 165000 \times 0.0057 \times (325 - 0.45 \times 123.53)]$$

= 120.00 kN

A .7 Length Effect

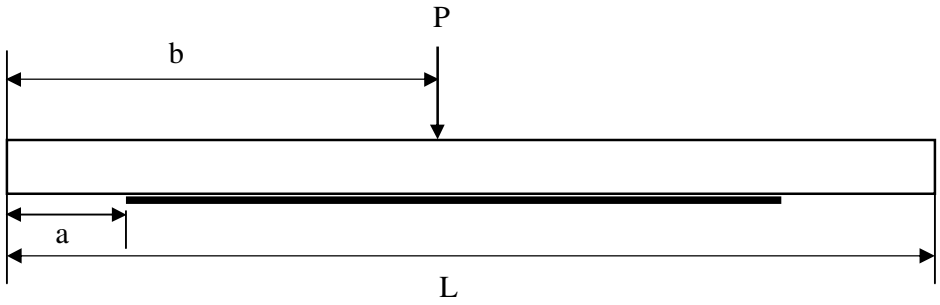

Figure A.5 Strengthened beam (Smith and Teng 2001)

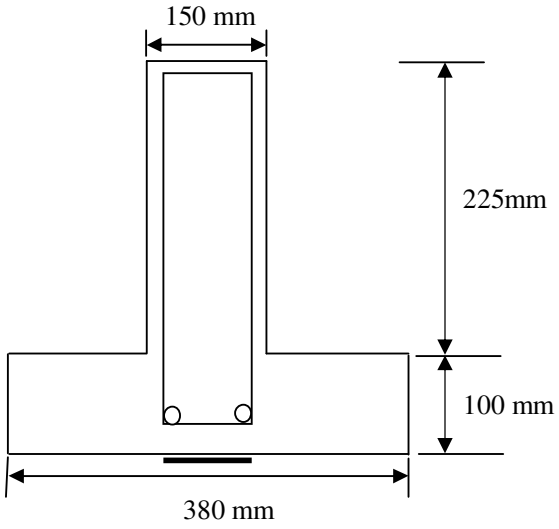

Figure A.6 Cross section

According to Smith and Teng, Interfecial shear stress$\tau(x)$ is calculated by,

For a<b,

$$\tau(x) = \frac{m_2}{\lambda} Pa\left(1 - \frac{b}{L}\right) e^{-\lambda x} + m_1 P\left(1 - \frac{b}{L}\right) - m_1 PCosh(\lambda x) e^{-k} - - - -(\text{A. 42})$$

E=Elastic Modulus,

G_a=Shear Modulus of adhesive,

b_2=width of the plate,

A=cross sectional area,

I=second moment of area,

Subscript 1 &2 denotes beam and laminate respectively.

y_1=distance from bottom of the beam to centroid of beam,

y_2=distance from top of the plate to centroid of laminate,

and,

b=1500

p=127 kN

L=3000 mm

E_1=30000MPa

E_2=165000MPa

G_a=5000 MPa

t_a=2 mm

$$centroid\ f\ rom\ bottom\ = \frac{150\times225\times212.5+380\times100\times50}{150\times225+380\times100}=126.43mm$$

$$I_1=(\frac{150\times225^3}{12}+150\times225\times212.5^2\ )+(\ \frac{380\times100^3}{12}+380\times100\times50^2\ )$$

$$=1793072917mm^4$$

$$I_2=\frac{100\times1.4^3}{12}+140\times0.7^2=91.46mm^4$$

$$E_1I_1=30000\times1793072917=5.3792\times10^{13}$$

$$E_2I_2=165000\times91.46=15090900$$

$$E_1A_1=30000\times(150\times225+380\times100)=2152500000$$

$$E_2A_2=165000\times140=23100000$$

$$y_1=126.43mm,$$

$$y_2=0.7\,mm$$

$$\lambda^2=\frac{5000\times100}{2}\{\frac{(126.43+0.7)(126.43+.7+.2)}{5.3792\times10^{13}+15090900}+\frac{1}{2152500000}+\frac{1}{23100000}\}$$

$$\lambda^2 = 0.01101495$$

$$\lambda = 0.1049$$

$$m_1 = \frac{5000}{2} \times \frac{1}{0.01101495} \left(\frac{126.43 + 0.7}{5.3792 \times 10^{13} + 15090900} \right) = 5.3639 \times 10^{-7}$$

$$k = 0.1049(1500\text{-}0) = 223.5$$

$$e^{-k} = 8.61 \times 10^{-98}$$

(If the laminate is provided up to full span), at the end of the plate , a=0

$$\tau(x) = \frac{m_2}{\lambda} Pa\left(1 - \frac{b}{L}\right) e^{-\lambda x} + m_1 P\left(1 - \frac{b}{L}\right) - m_1 PCosh(\lambda x) e^{-k} - - - -(\text{A. 43})$$

$= 0.034$MPA at the end of plate.

At a = 50,

$$\tau(x) = \frac{m_2}{\lambda} Pa\left(1 - \frac{b}{L}\right) e^{-\lambda x} + m_1 P\left(1 - \frac{b}{L}\right) - m_1 PCosh(\lambda x) e^{-k} - - - -(\text{A. 44})$$

= 0.2118 MPa

At a = 250 mm,

$$\tau(x) = \frac{m_2}{\lambda} Pa\left(1 - \frac{b}{L}\right) e^{-\lambda x} + m_1 P\left(1 - \frac{b}{L}\right) - m_1 PCosh(\lambda x) e^{-k} - - - -(\text{A. 45})$$

=0.79 MPa = 0.8 MPa

So, the length of CFRP laminate will be = (3000-250×2) mm = 2500 mm

Based on Elastic Theory,

Interfacial shear stress at the adhesive level is calculated by the following equation (Ashour et al., 2004),

$$\tau = \frac{Vn_f t_f y_f}{I_c} - (A.46)$$

Where,

V=shear force calculated at beam failure,

$n_f = E_f/E_c$

t_f= thickness of CFRP laminate,

y_f=depth of neutral axis from the centroid of CFRP laminate.

I_c=transformed second moment of inertia of the cracked reinforced concrete cross section with external CFRP laminates in terms of concrete.

Here,

$$n_f = \frac{E_f}{E_c} = \frac{165000}{30000} = 5.5$$

$$t_f = 1.4mm$$

$$I_c = \frac{150\times225^3}{12} + 150\times225\times212.5^2 + \frac{380\times100^3}{12} + 380\times100\times50^2 + \frac{550\times1.4^3}{12} + 770\times0.7^2 + \frac{380\times7^3}{12} + 2673\times60^2$$

$$= 1.802\times10^9 mm^4$$

$$A_{fc} = 5.5\times140 = 770, t_f = 1.4mm$$

$$A_{sc} = 6.6\times401 = 2673mm^2$$

$$\tau = \frac{127\times1000\times5.5\times1.4\times189.7}{1.802\times10^9} = 0.102MPa \le 0.8MPa$$

APPENDIX B

Strain Variation over the Depth of the Beam

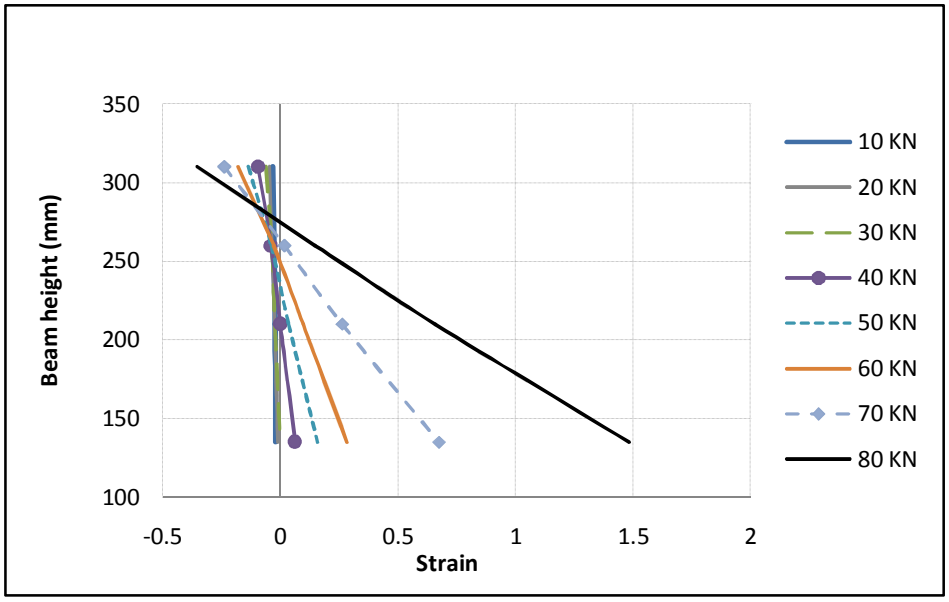

Figure B.1 Strain variation of beam B 0

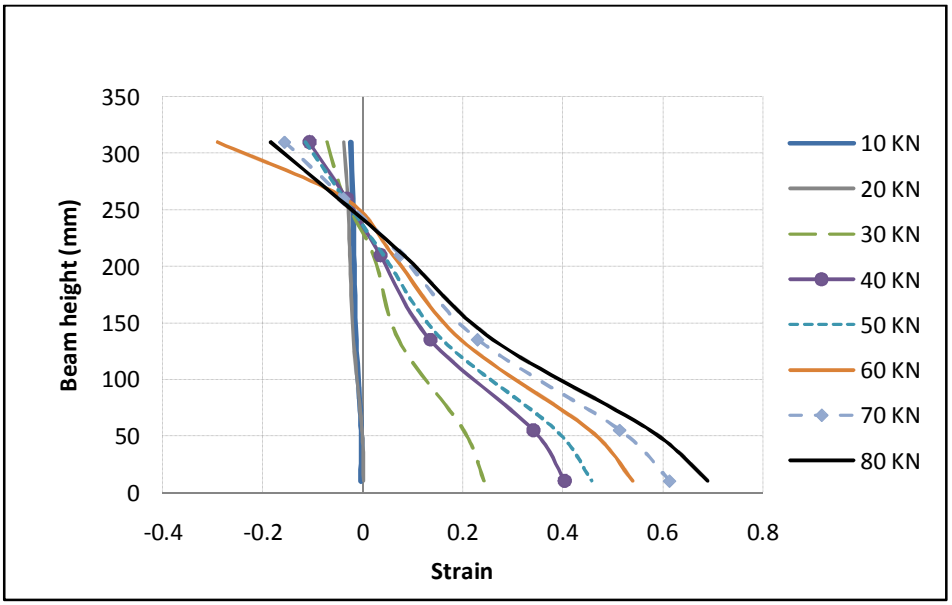

Figure B.2 Strain variation of beam B1

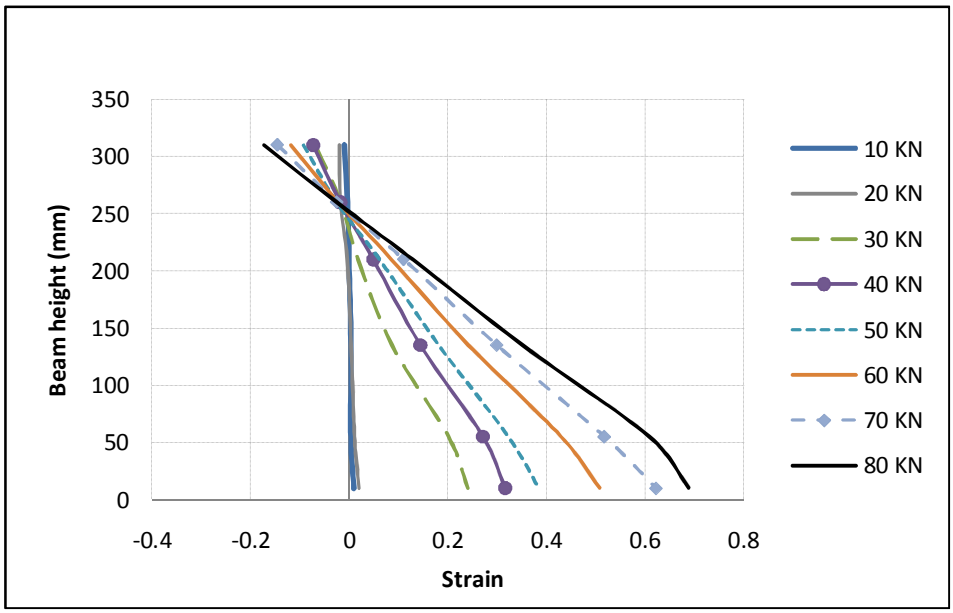

Figure B.3 Strain variation of beam B2

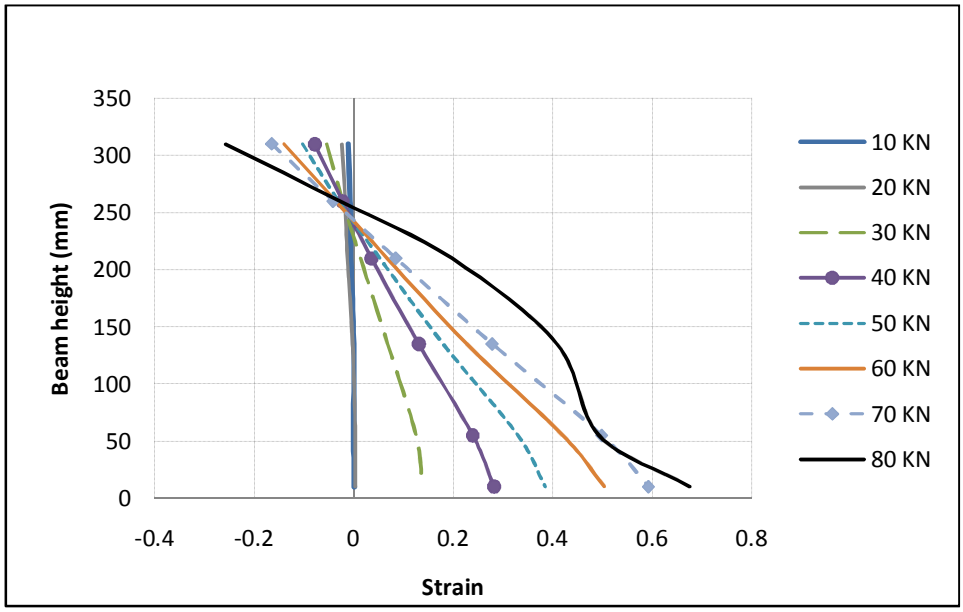

Figure B.4 Strain variation of beam B3

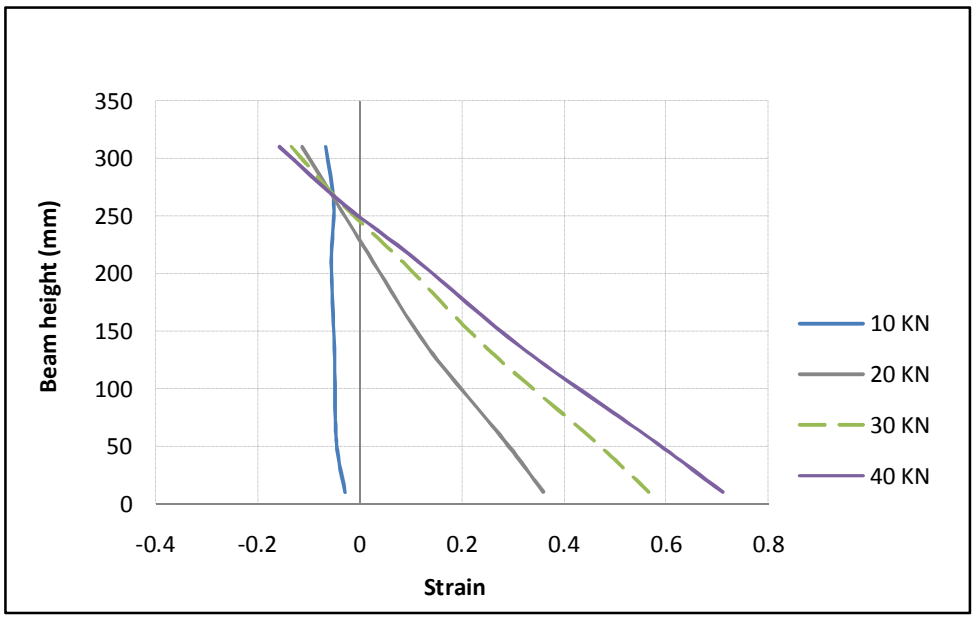

Figure B.5 Strain variation of beam B4

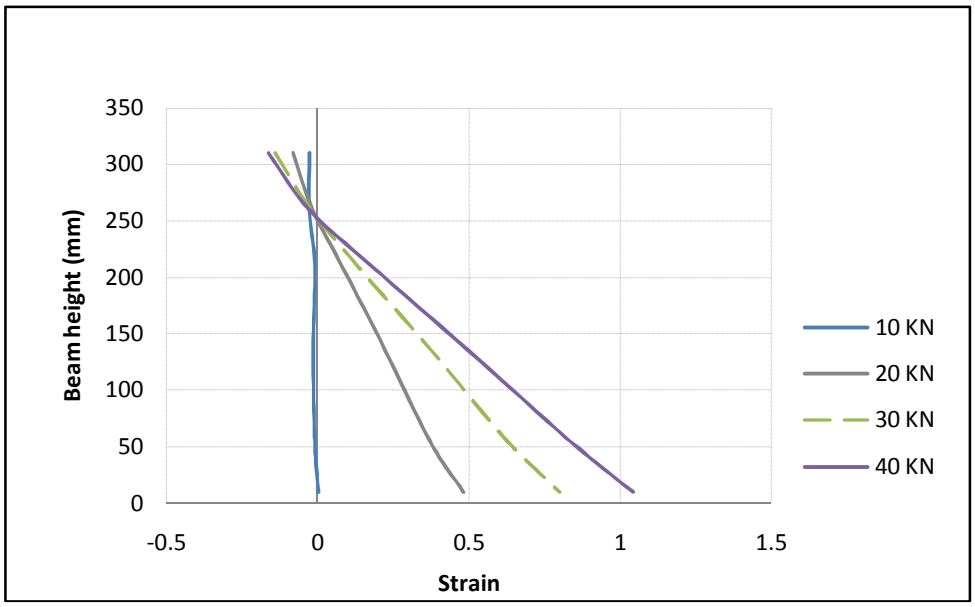

Figure B.6 Strain variation of beam B5

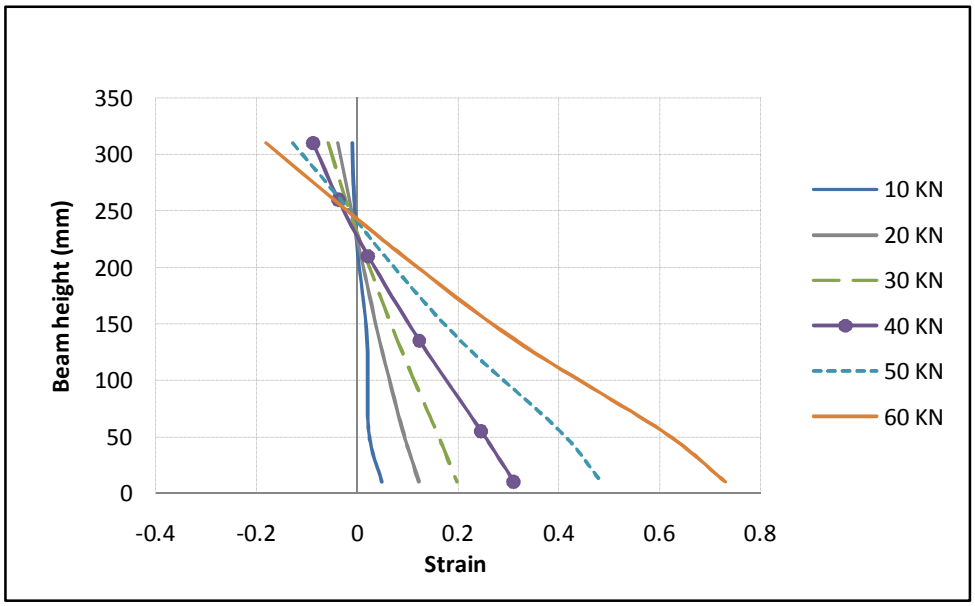

Figure B.7 Strain variation of beam B6

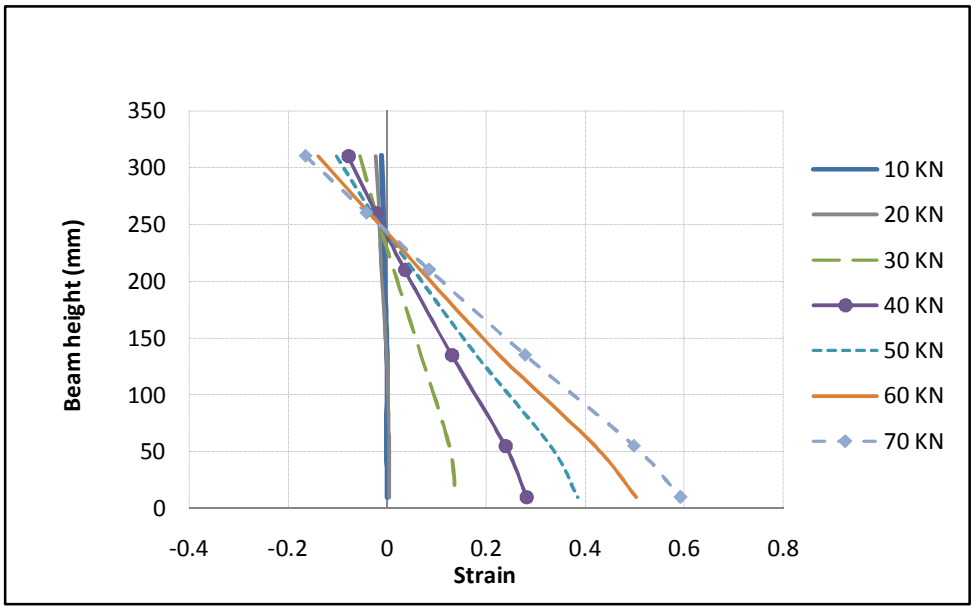

Figure B.8 Strain variation of beam B7

APPENDIX C

C.1 Bar Strain

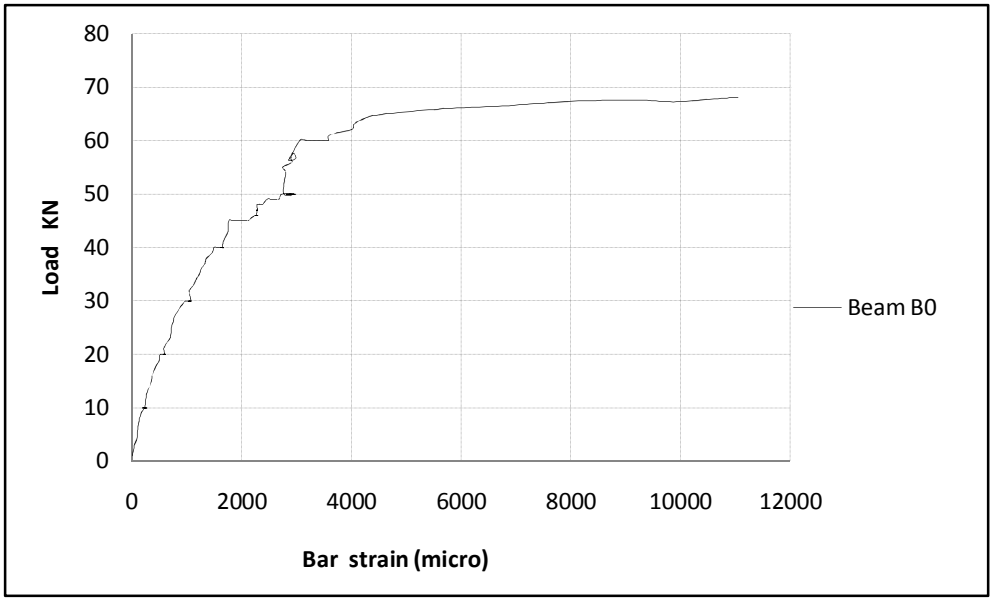

Figure C.1 Load versus bar strain of Beam B0

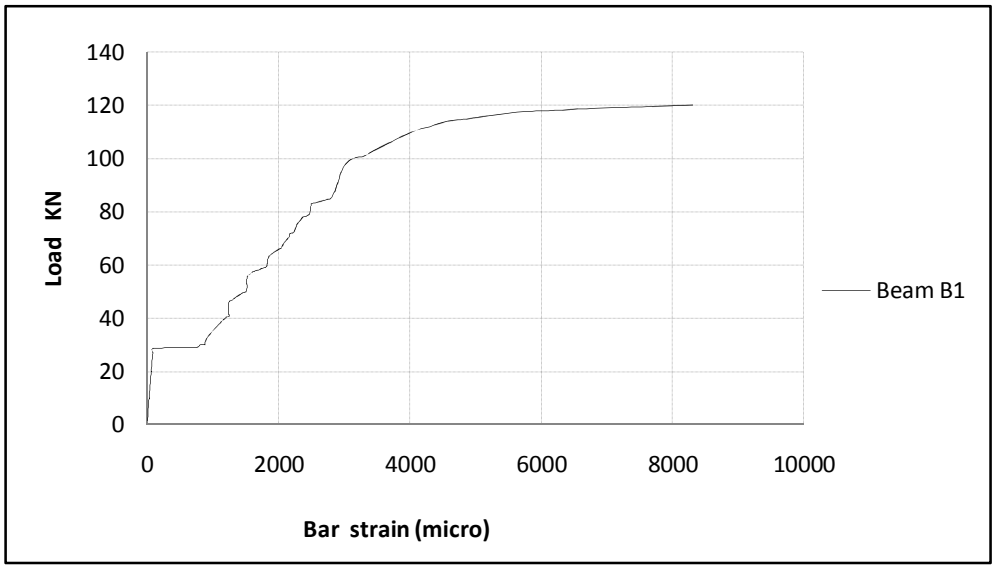

Figure C.2 Load versus bar strain of Beam B1

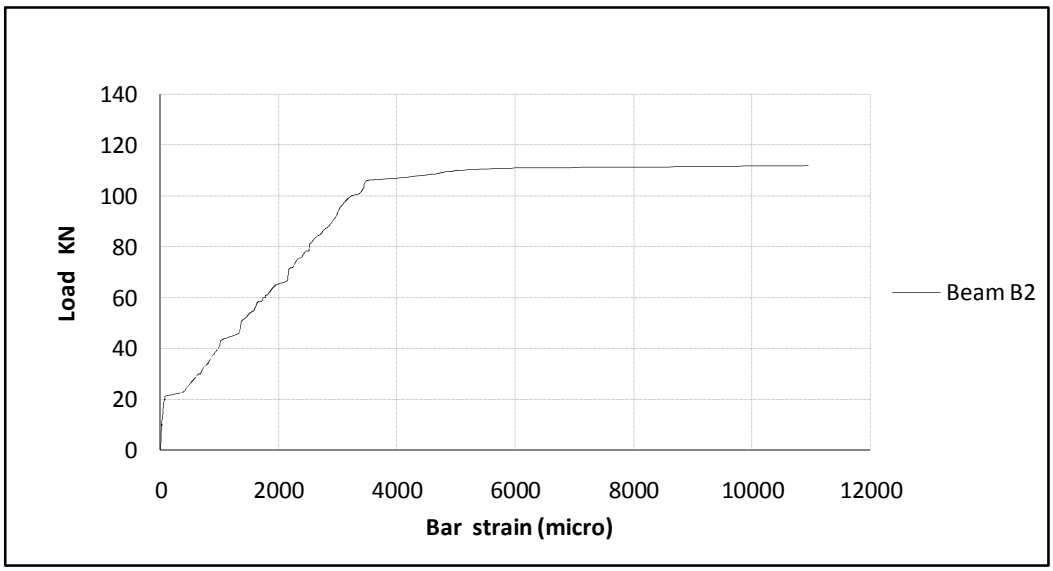

Figure C.3 Load versus bar strain of Beam B2

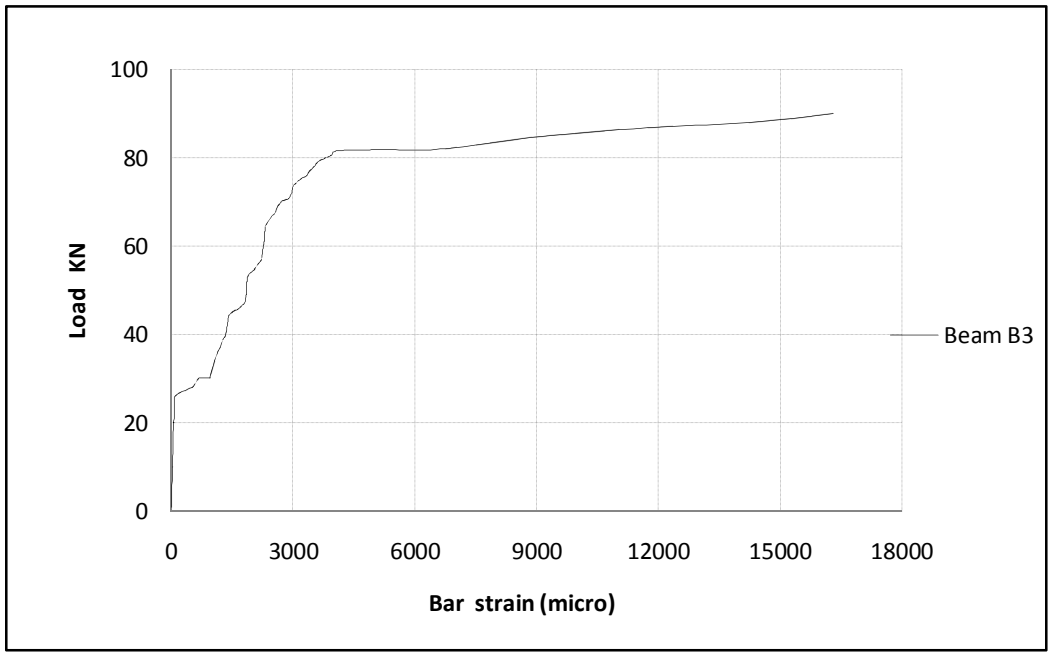

Figure C.4 Load versus bar strain of Beam B3

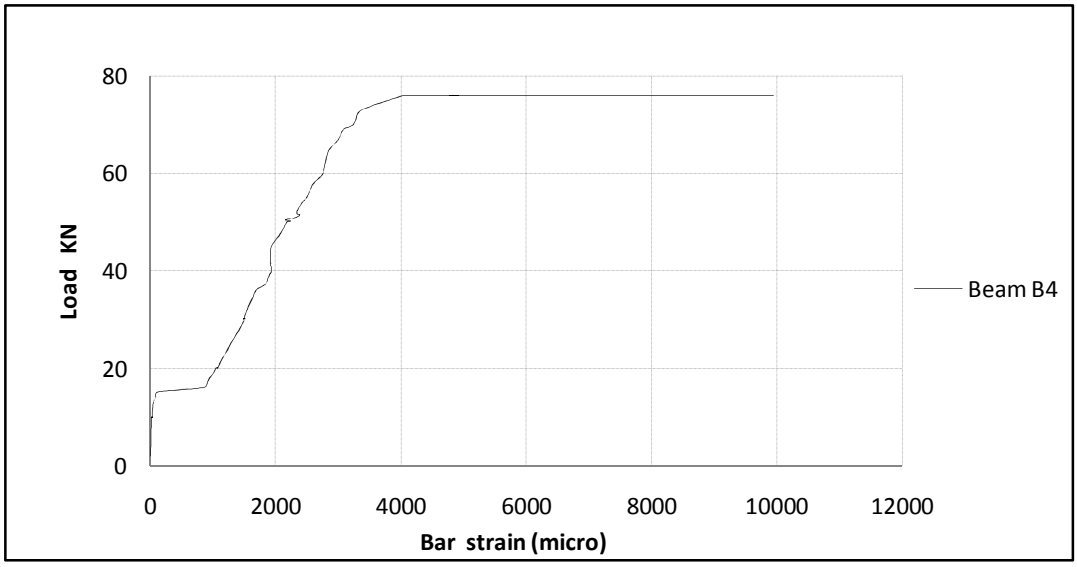

Figure C.5 Load versus bar strain of Beam B4

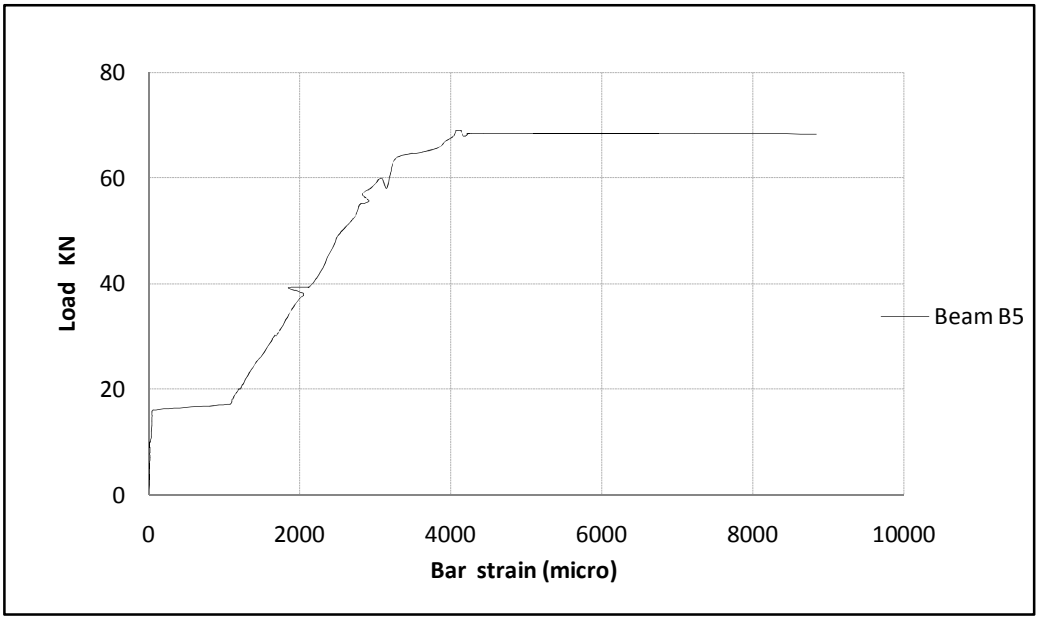

Figure C.6 Load versus bar strain of Beam B5

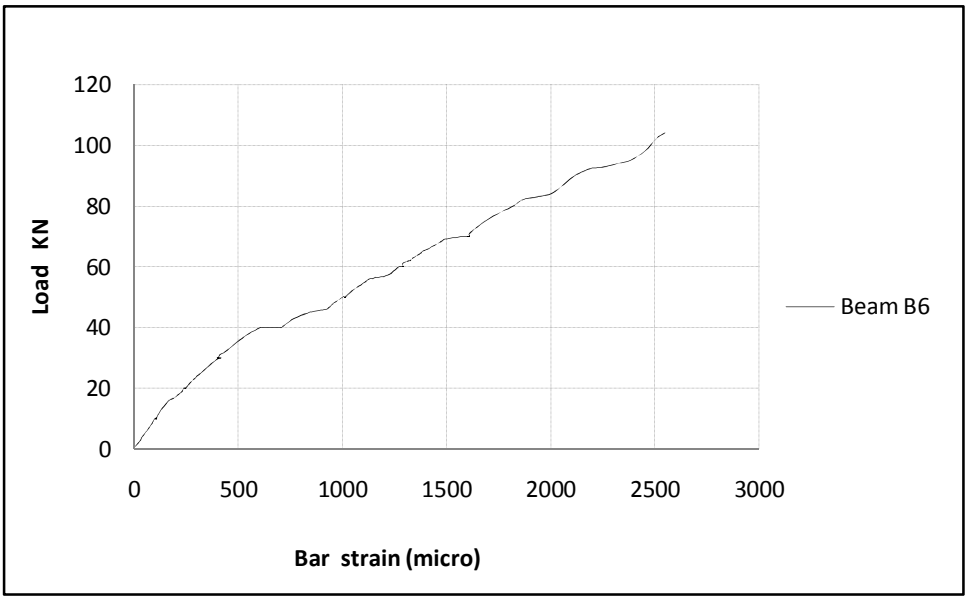

Figure C.7 Load versus bar strain of Beam B6

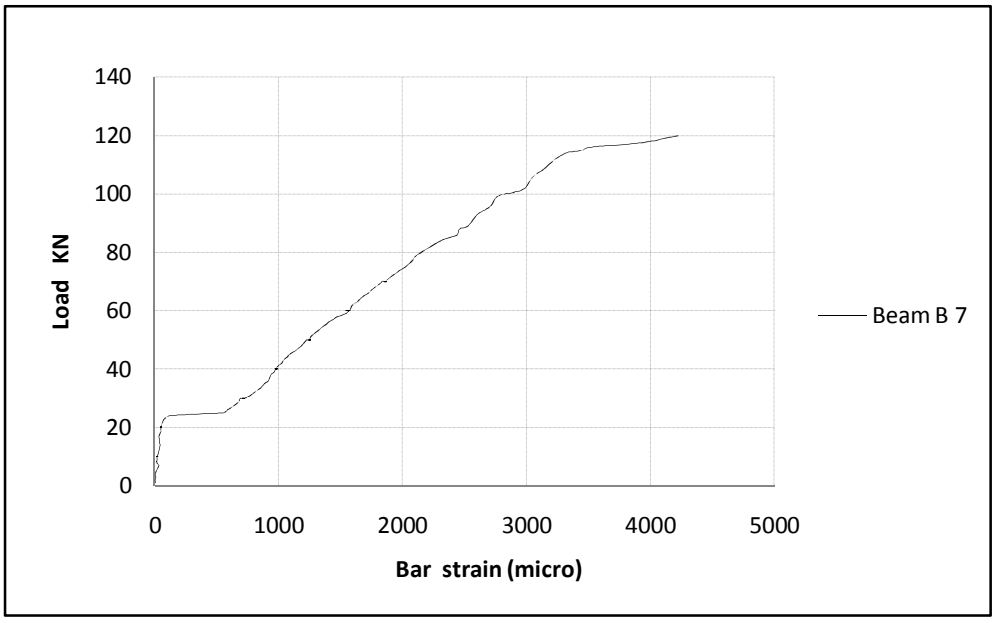

Figure C.8 Load versus bar strain of Beam B7

C.2 Concrete Compression Strain

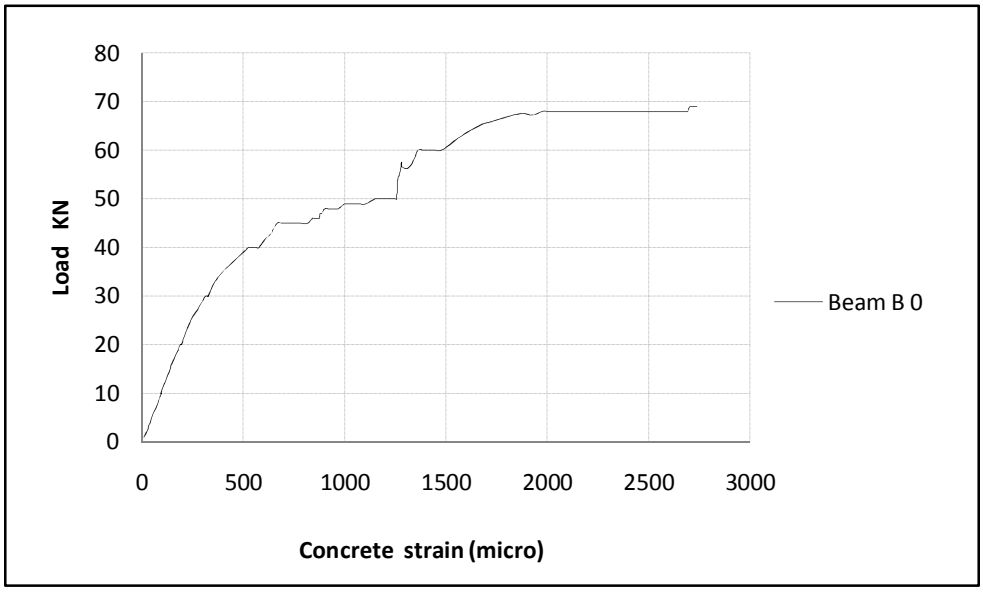

Figure C.9 Load versus concrete strain of beam B0

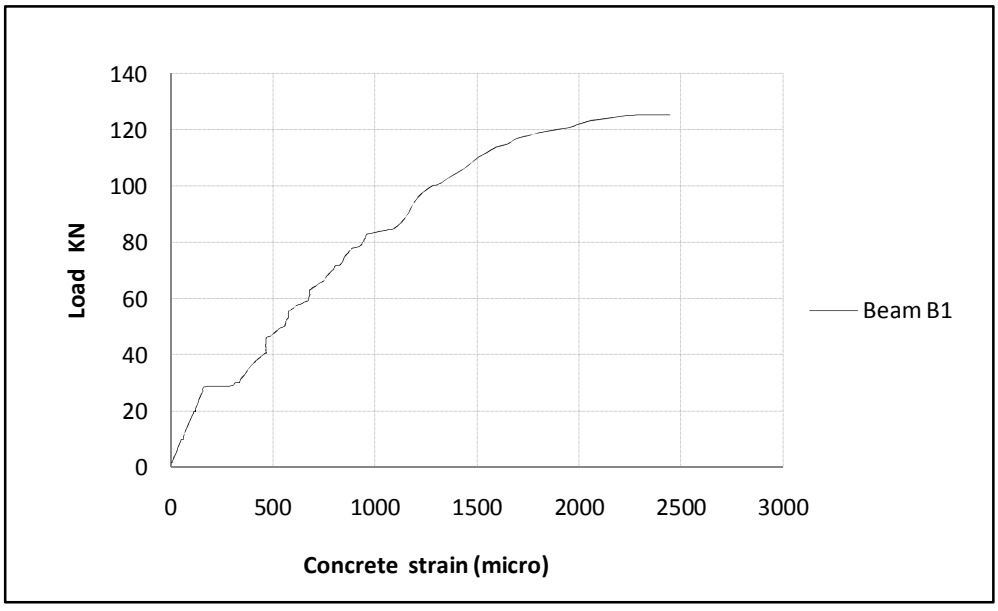

Figure C.10 Load versus concrete strain of beam B1

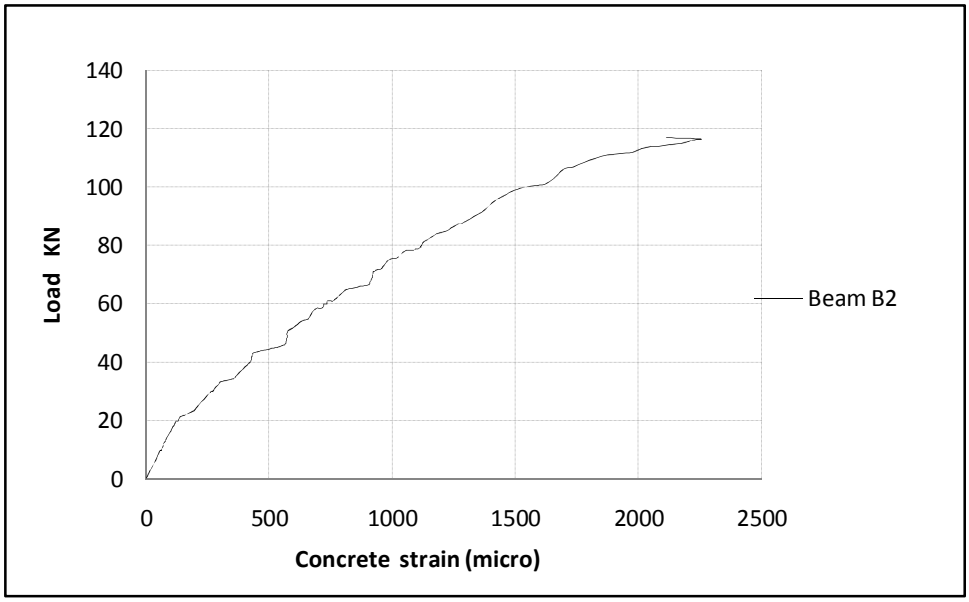

Figure C.11 Load versus concrete strain of beam B2

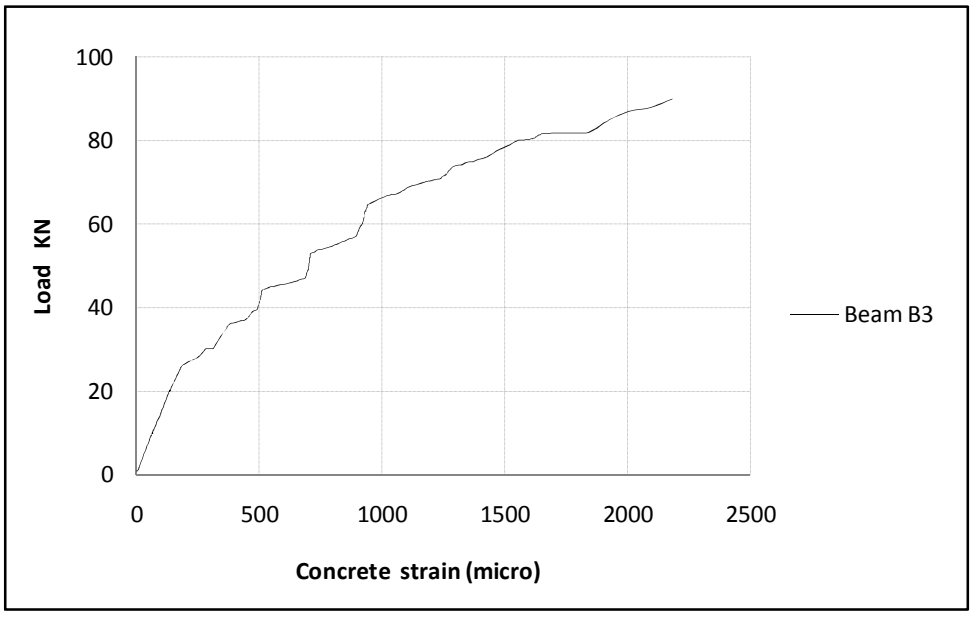

Figure C.12 Load versus concrete strain of beam B3

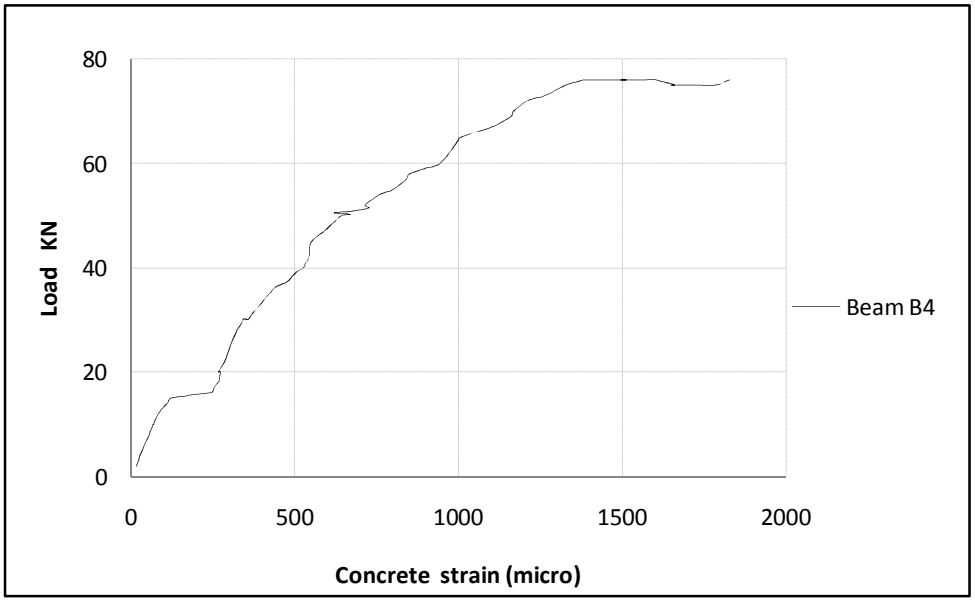

Figure C.13 Load versus concrete strain of beam B4

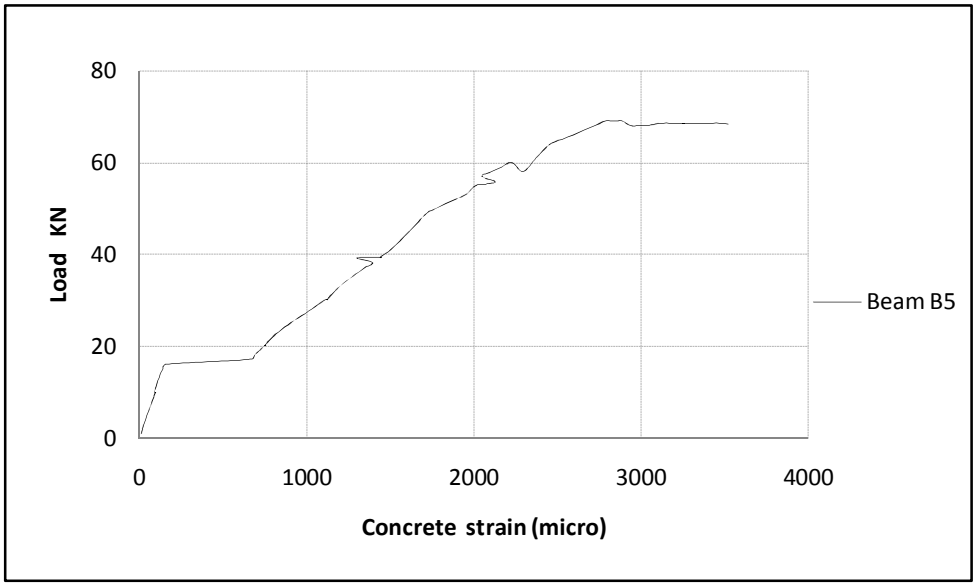

Figure C.14 Load versus concrete strain of beam B5

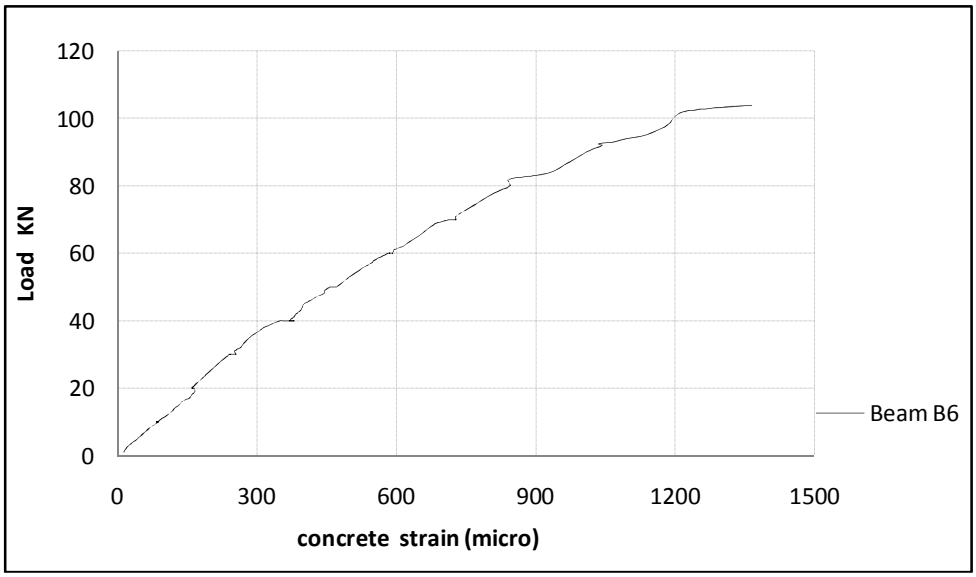

Figure C.15 Load versus concrete strain of beam B6

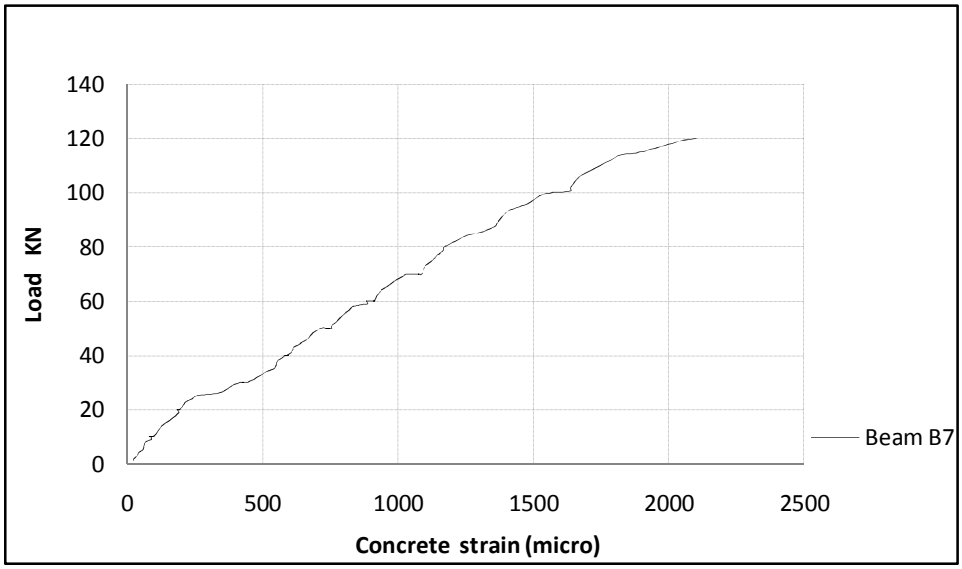

Figure C.16 Load versus concrete strain of beam B7

C.3 CFRP Strain

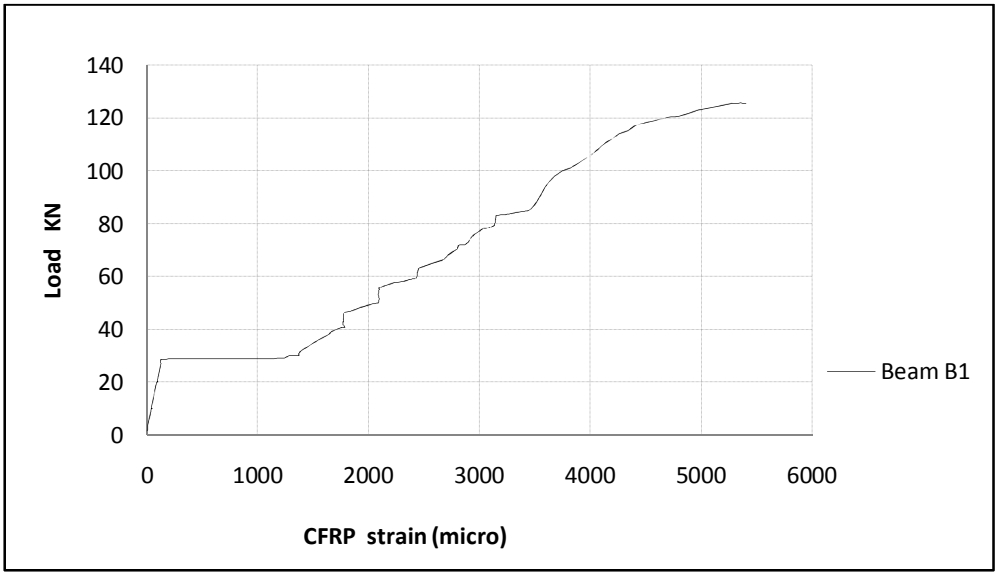

Figure C.17 Load versus CFRP strain of beam B1

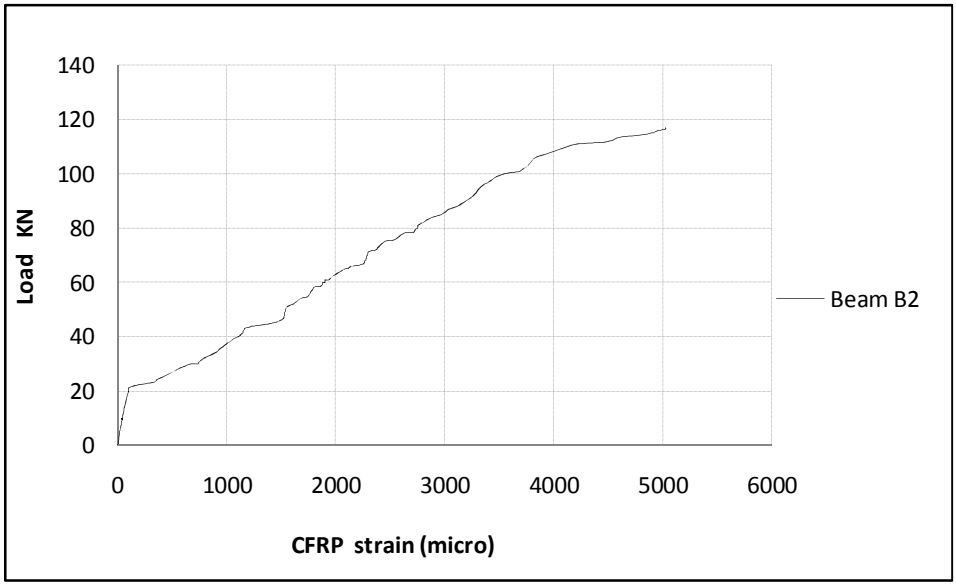

Figure C.18 Load versus CFRP strain of beam B2

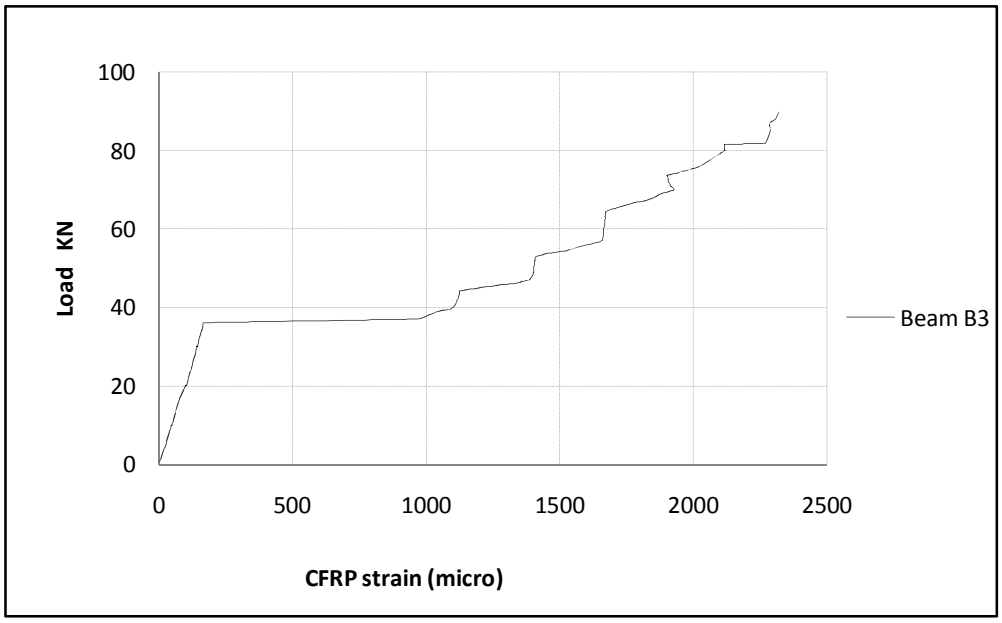

Figure C.19 Load versus CFRP strain of beam B3

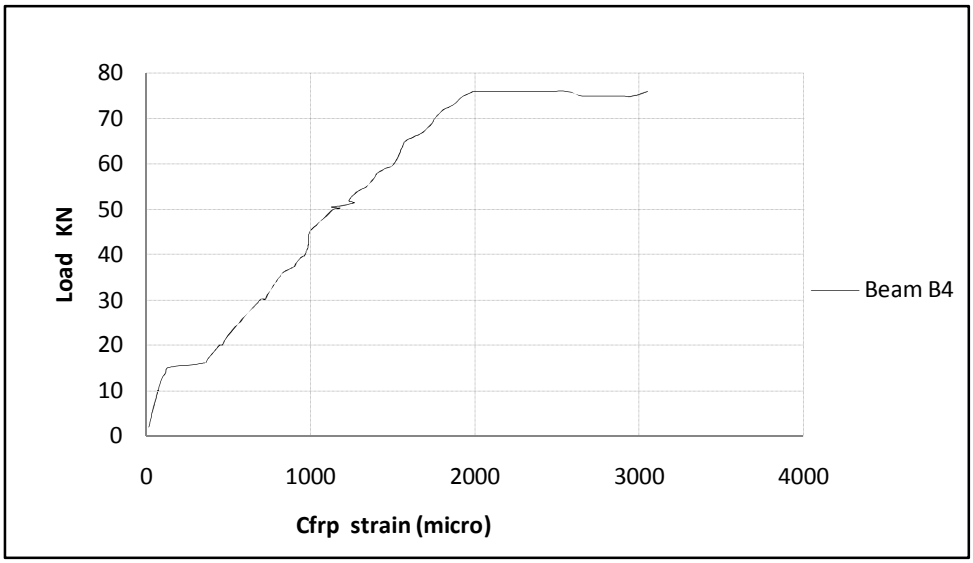

Figure C.20 Load versus compression CFRP strain of beam B4

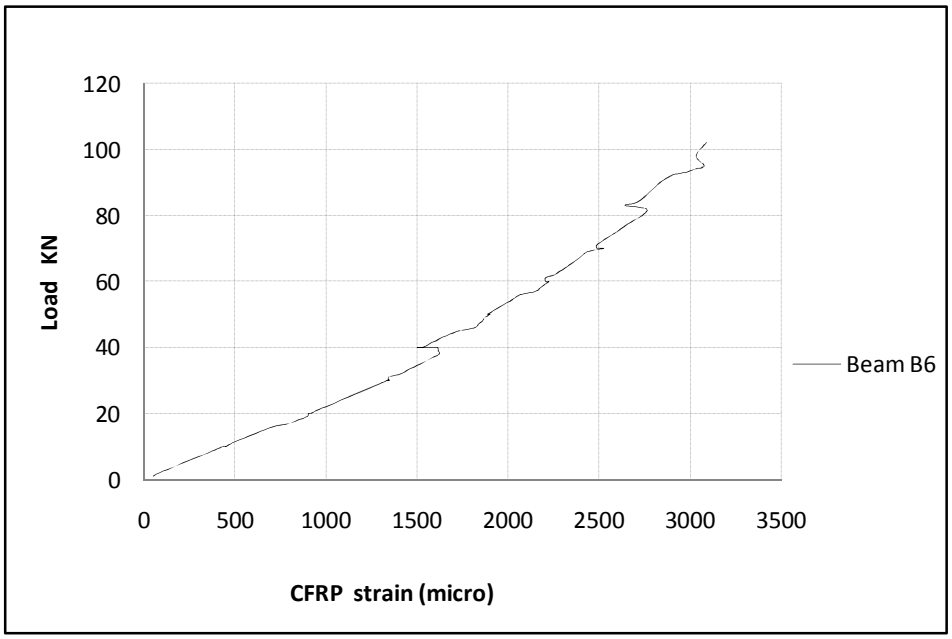

Figure C.21 Load versus tension CFRP strain of beam B6

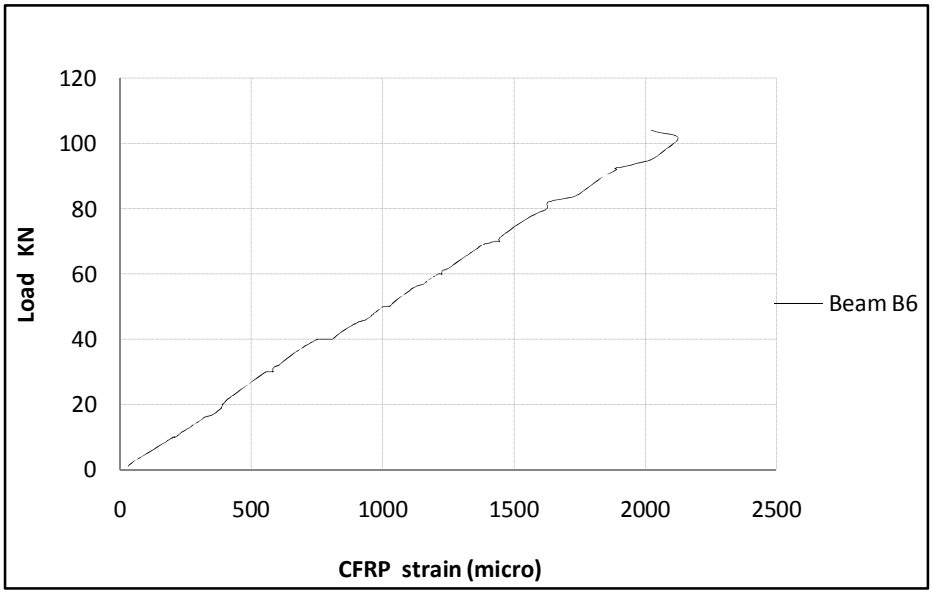

Figure C.22 Load versus compression CFRP strain of beam B6

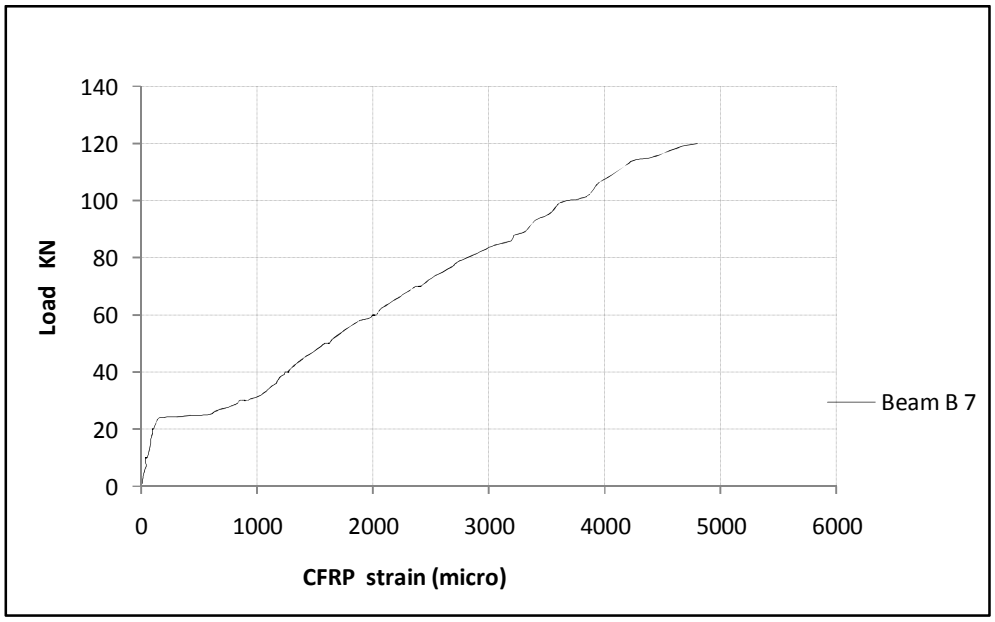

Figure C.23 Load versus tension CFRP strain of beam B7

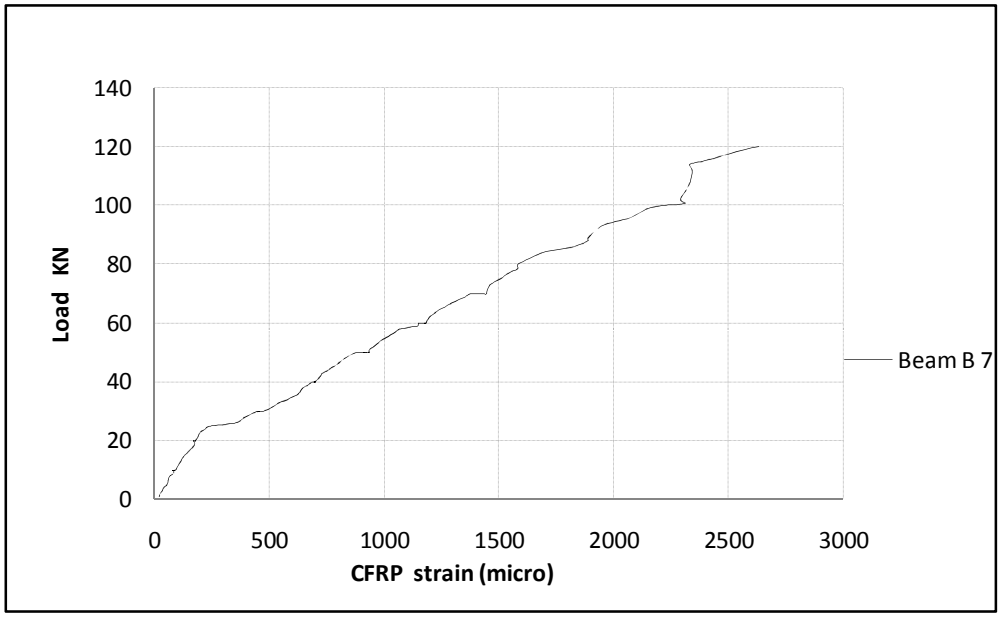

Figure C.24 Load versus compression CFRP strain of beam B7

C.4 Deflection of Beam

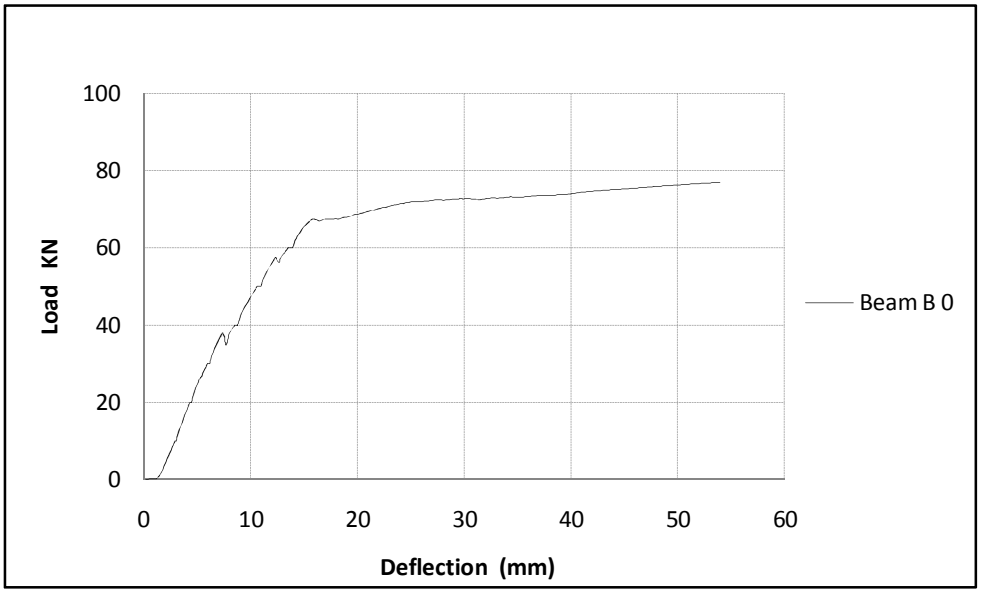

Figure C.25 Load versus deflection of beam B0

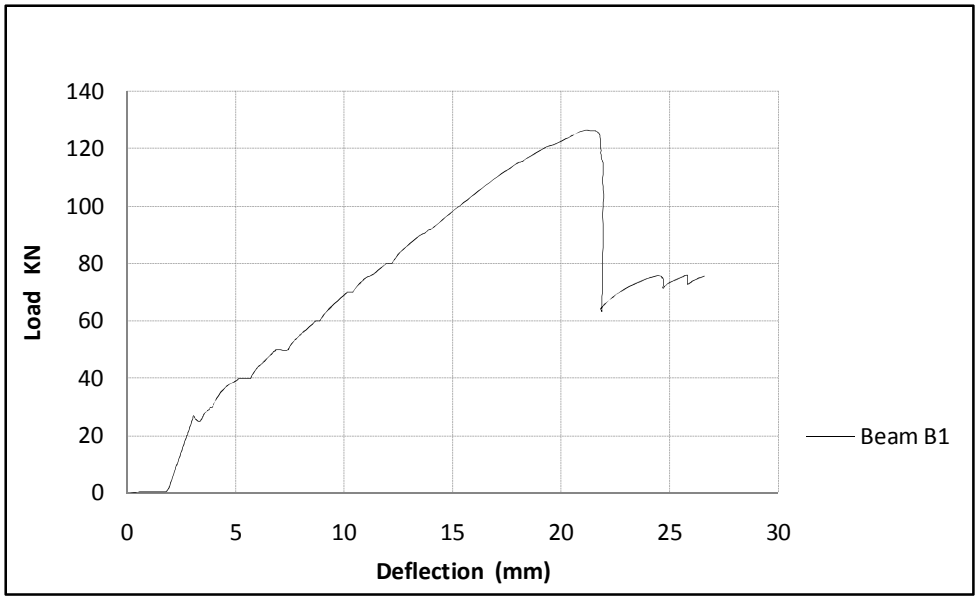

Figure C.26 Load versus deflection of beam B1

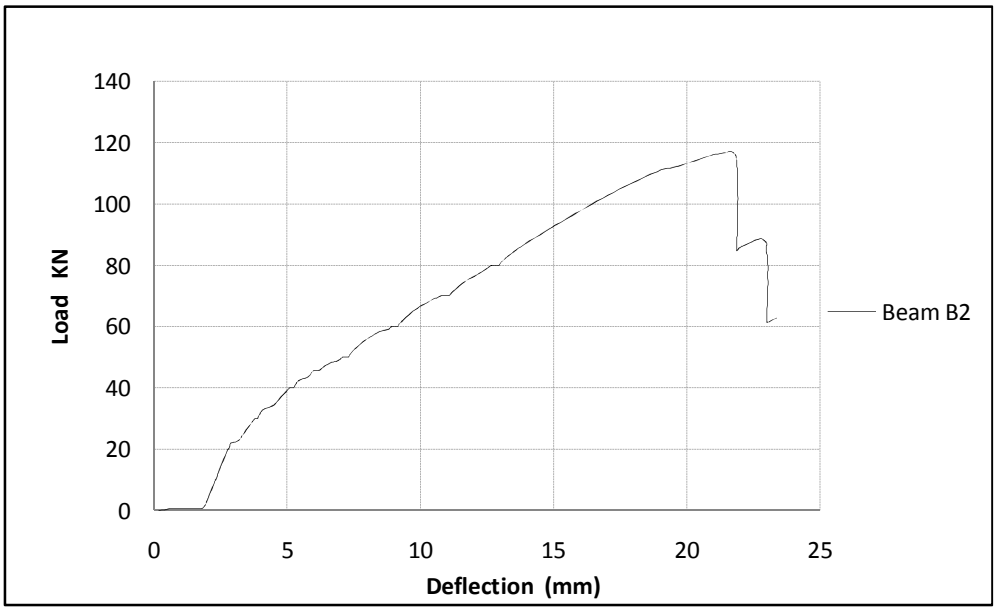

Figure C.27 Load versus deflection of beam B2

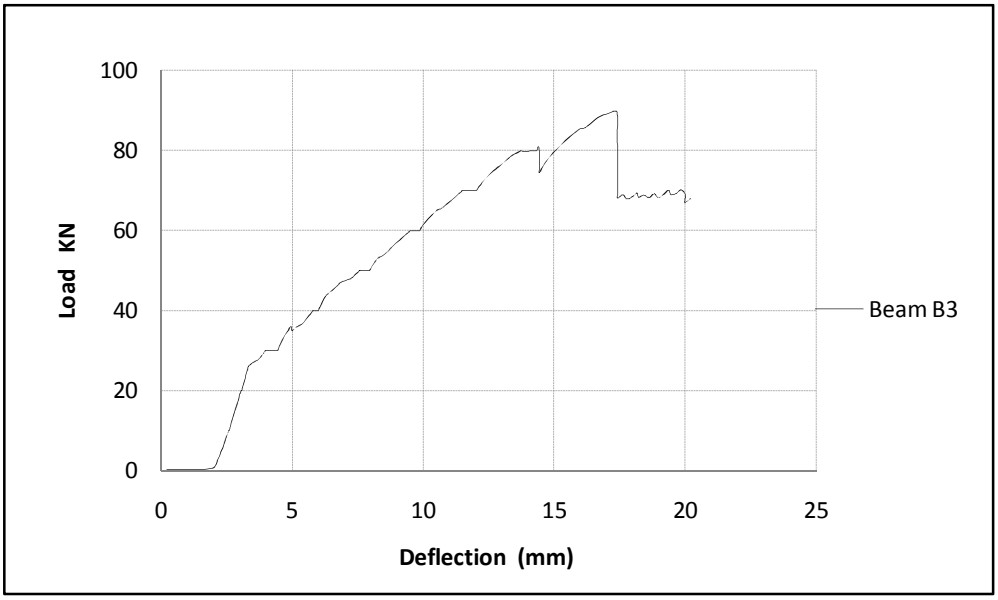

Figure C.28 Load versus deflection of beam B3

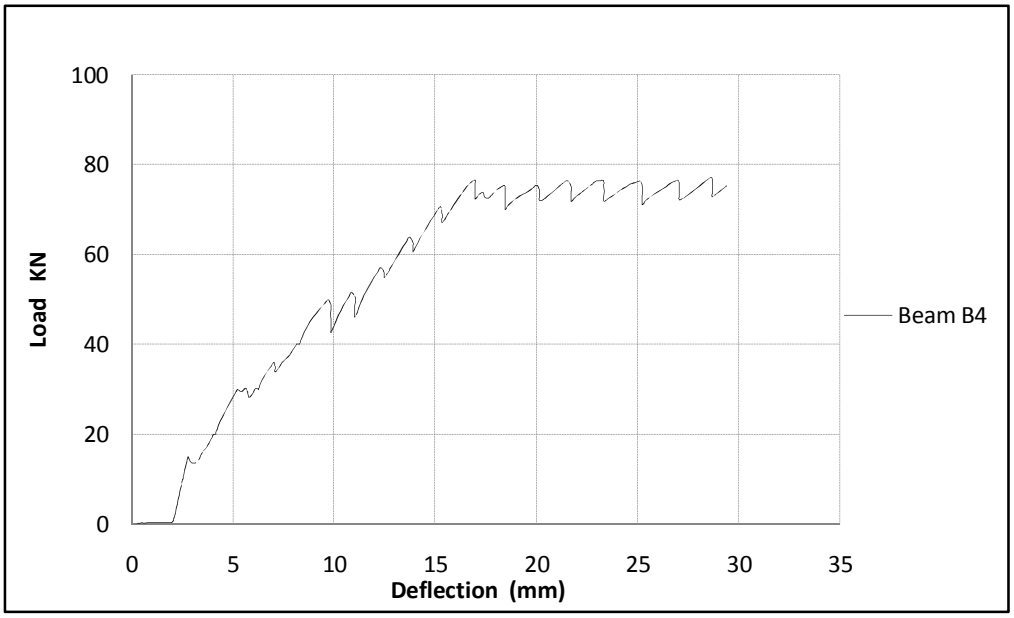

Figure C.29 Load versus deflection of beam B4

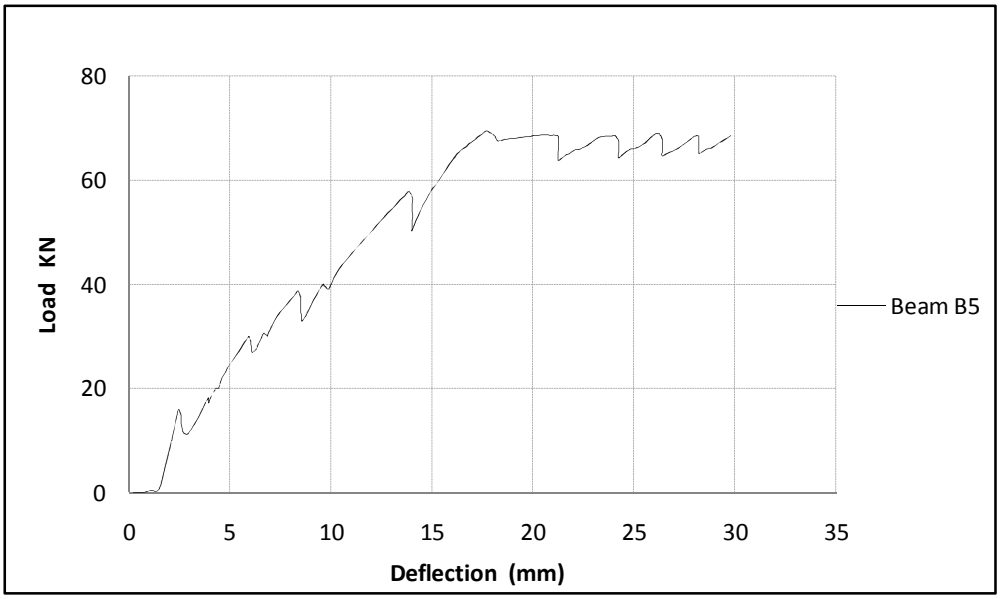

Figure C.30 Load versus deflection of beam B5

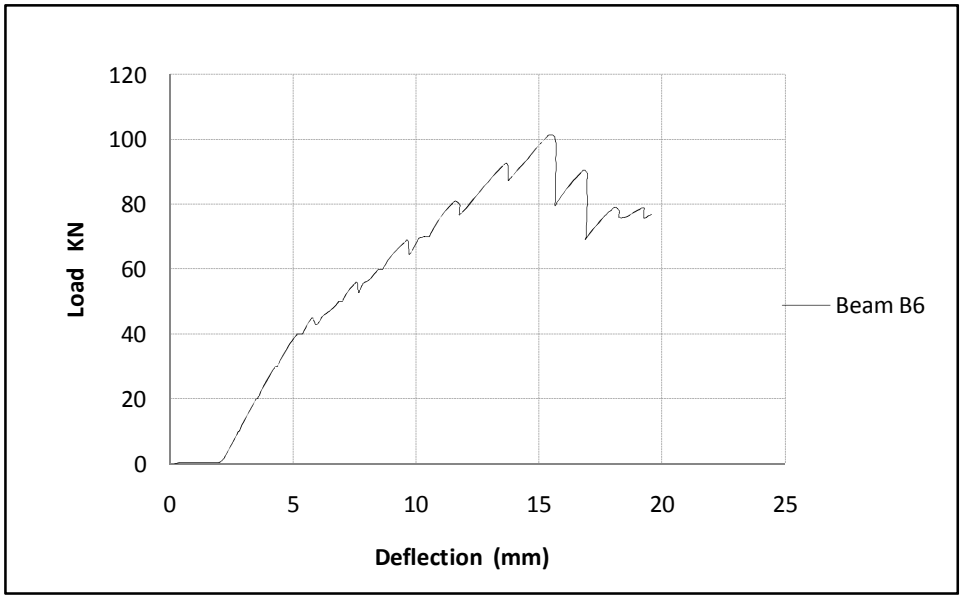

Figure C.31 Load versus deflection of beam B6

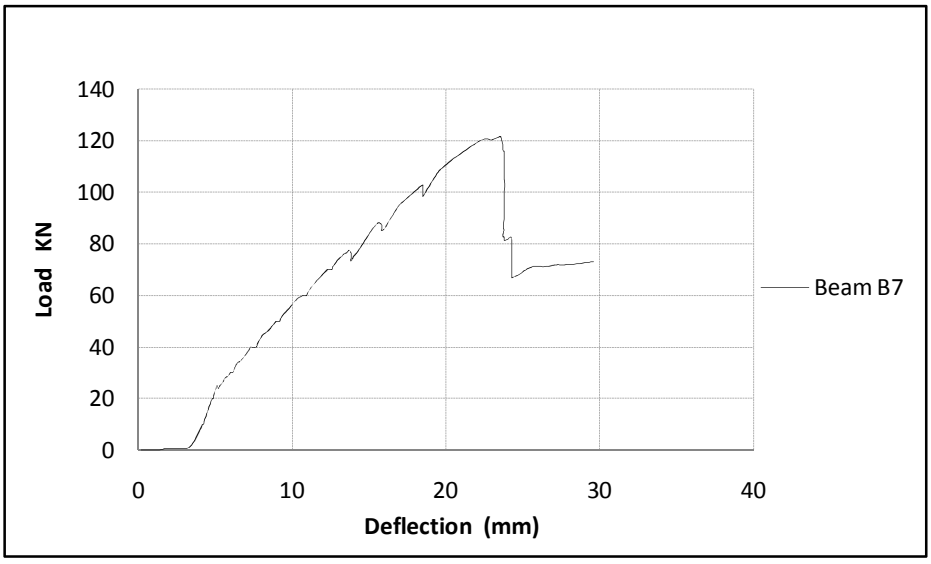

Figure C.32 Load versus deflection of beam B7

APPENDIX D

List of Author Publications

Jumaat M.Z., **Rahman M. M.** and Rahman M. A. (2011), "Review on bonding techniques of CFRP in strengthening concrete structures", *International Journal of the Physical Sciences*, (ISI Expanded), vol. 6(15), pp. 3567-3575.

Jumaat M. Z., **Rahman M. M.** and Alam M. A. (2010), "Flexural strengthening of RC continuous T beam using CFRP laminate: A review", *International Journal of the Physical Sciences*, (ISI Expanded) vol. 5(6), pp. 619-625.

Jumaat M.Z., Rahman M. A., Alam M.A. and **Rahman M. M.** (2010), "Premature failures in plate bonded strengthened RC beams with an emphasis on premature shear: A review", *International Journal of the Physical Sciences*, (ISI Expanded) vol. 6(2), pp. 156 – 168.

Jumaat M.Z., **Rahman M. M.** and Rahman M. A. (2011), "Experimental and nonlinear finite element studies of RC T-beams strengthened with FRP Laminate in presence of column", *Engineering Structures*, (ISI Expanded), (Peer Review).

List of Author Conference Proceedings

Jumaat M.Z., **Rahman M.M.**, Rahman M.A. (2011) "Appraisal of research progress on flexural strengthening of RC continuous T- beam in the negative moment region by means of CFRP laminate", *United Kingdom-Malaysia-Ireland Engineering Science Conference*, Kuala Lumpur, Malaysia.

Rahman M.A , Jumaat M.Z., **Rahman M.M.** (2011) "Design recommendation for eliminating premature shear failure of CFRP laminate flexurally strengthened RC beams", *United Kingdom-Malaysia-Ireland Engineering Science Conference,* Kuala Lumpur, Malaysia.